Production-consumption system coordination by hybrid predictive approaches : application to a solar cooling system for buildings

Eunice Herrera Santisbon

CentraleSupélec

N° d'ordre : 2015-06-TH

CentraleSupélec

Ecole Doctorale MATISSE

Ecole doctorale "Mathématiques, Télécommunications, Informatique, Signal, Systèmes Electroniques"

THÈSE DE DOCTORAT

DOMAINE : STIC

Spécialité : Automatique

Soutenue le 20 mars 2015

par:

Eunice Beatriz HERRERA SANTISBON

Coordination Producteur-Consommateur par des approches prédictives hybrides : application au rafraîchissement solaire des bâtiments

Directeur de thèse :	Hervé GUÉGUEN	Professeur (CentraleSupélec)
Co-encadrant de thèse :	Romain BOURDAIS	Professeur adjoint (CentraleSupélec)

Composition du jury :

Président du jury :	Jean BUISSON	Professeur (CentraleSupélec)
Rapporteurs :	Christian GHIAUS	Professeur (INSA de Lyon)
	Stéphane GRIEU	Professeur (Université de Perpignan)
Examinateur :	Rudy NEGENBORN	Associate Professor (TU Delft)

A mi querida familia: mi fortaleza y alegría

Acknowledgments

First of all, my sincere and deepest gratitude to my thesis supervisor, Hervé Guéguen, for giving me the opportunity to be part of the ASH team, for his guidance and persistent support in the development of this thesis. My great gratitude to my co-advisor Romain Bourdais, for his enthusiasm, cooperation and help during these three years.

My special and warm gratitude to my reviewers, Christian Ghiaus and Stéphane Grieu, for the dedicated time to carefully read my research work and because each of their comments and advices have significantly enriched this dissertation. Thanks to Jean Buisson and Rudy Negenborn, for having accepted the invitation to be part of my jury and for their contribution to the improvement of this dissertation.

My gratitude to all the members of the ASH team, because in these three years I learnt something rewarding from each of them. Thanks for their professional and non-professional support. To the CentraleSupélec personnel for its administrative support.

Thanks to my friends in Rennes, for the extraordinary moments, joy and support. My stay would not have been so pleasant without their company.

My very special thanks to my boyfriend Elfrich for his unconditional support, love and for always kindly encouraged me in the most difficult moments.

To my wonderful and inspiring family, for being my pillar of strength, shelter and source of love and for making me feel that distance is not a barrier between us.

Finally, to my sponsors CONACYT and Fundación Pablo García for their financial support to carry out my research project. My gratitude to CentraleSupélec for its financial support to culminate this dissertation.

Abstract

To guarantee thermal comfort in buildings is directly related to energy consumption. In tropical climates, cooling systems for buildings represent one of the largest energy consumers. Therefore, as energy consumption is a major concern around the world, it is important to improve the systems efficiency or seeking new methods of cooling production. A solar cooling installation based on the absorption cycle is an alternative to mitigate greenhouse gas emissions and electricity consumption. In contrast to conventional vapor-compression based cooling systems, the absorption cooling production involves a complex system composed of several components as collector panel, storage tank, cooling tower and absorption chiller. Besides the sizing of the components, this complex system requires control actions to be efficient as a coordination between hot water storage, cooling water production and consumption is necessary.

The aim of this research is to propose a management approach for a production-consumption energy system based on Model Predictive Control (MPC). The solar absorption cooling system is seen as part of this production-consumption energy system where the hot water storage system is the producer and the chiller-building system is one of the consumers. In order to provide modularity to the control structure, the coordination between the subsystems is achieved by using a partitioning approach where local predictive controllers are developed for each of the subsystems. The consumer controllers compute a set of energy demand profiles sent to the producer controller which selects the profile that better minimize the global optimization cost.

In a first part, the proposed approach is tested on a simplified linear model composed of one producer and several consumers. In a second part, a more complex case is studied. A simplified model of an absorption cooling system is evaluated using the simulation tool TRNSYS. The producer model is no longer linear, instead it is described by a nonlinear hybrid model which increases the complexity of the optimization problem. The simulations results show that the suboptimality induced by the method is low and the control strategy fulfills the objectives and constraints while giving good performances.

Resumé

Garantir le confort thermique des bâtiments est directement lié à la consommation d'énergie. Dans les zones tropicales, les systèmes de refroidissement représentent l'un des postes les plus gourmands en énergie. Afin de réduire la consommation d'énergie mondiale, il est primordial d'améliorer l'efficacité de ces systèmes ou bien de développer de nouvelles méthodes de production de froid. Une installation de refroidissement solaire basée sur le cycle à absorption est une alternative pour réduire les émissions de gaz à effet de serre et la consommation d'électricité. Contrairement aux systèmes classiques de refroidissement à compression mécanique, la production de froid par absorption est un système complexe composé de plusieurs composants comme des panneaux solaires, un ballon de stockage, une tour de refroidissement et une machine à absorption. Outre le dimensionnement des composants, ce système complexe nécessite des actions de contrôle pour être efficace parce que la coordination entre le stockage d'eau chaude, la production et la consommation du froid est nécessaire.

Le but de cette thèse est de proposer une structure producteur-consommateur d'énergie basée sur la commande prédictive (MPC). Le système de refroidissement par absorption solaire est considéré comme faisant partie de ce système de production-consommation d'énergie, le système de stockage d'eau chaude est le producteur et la machine à absorption qui distribue de l'eau froide au bâtiment est l'un des consommateurs. Pour que la structure de commande soit modulaire, la coordination entre les sous-systèmes est réalisée en utilisant une approche de partitionnement où des contrôleurs prédictifs locaux sont conçus pour chacun des sous-systèmes. Les contrôleurs des consommateurs calculent un ensemble de profils de demande d'énergie. Ces profils sont ensuite envoyés au contrôleur du producteur qui sélectionne le profil qui minimise le coût global.

Dans une première partie, l'approche proposée est testée sur un modèle linéaire simplifié composé d'un producteur et de plusieurs consommateurs. Dans une deuxième partie, un cas plus complexe est étudié. Un modèle simplifié d'un système de refroidissement à absorption est évaluée en utilisant l'outil de simulation TRNSYS. Le modèle de production n'est plus linéaire, il est décrit par un modèle non linéaire hybride qui augmente la complexité du problème

d'optimisation. Les résultats des simulations montrent que la sous-optimalité induite par la méthode est faible. De plus, la performance de l'approche atteint les objectifs de commande tout en respectant les contraintes.

List of Symbols and Abbreviations

Symbols

A	Total collector array gross area $[m^2]$
a_0	Solar collector intercept efficiency $[-]$
a_1	Solar collector efficiency slope $[kJ\,hr^{-1}m^{-2}K^{-1}\,]$
a_2	Solar collector efficiency curvature $[kJ\,hr^{-1}m^{-2}K\,]$
b	Number of energy profiles sent to the producer $[-]$
c	Specific heat of the fluid $[kJ\,kg^{-1}K^{-1}]$
$ctrl$	Binary control signal $[-]$
C_{min}	Minimum capacity rate of the fluids entering the heat exchanger $[kJ\,K^{-1}hr^{-1}]$
D_1	Producer subsystem disturbances vector $[-]$
D_2	Consumer subsystem disturbances vector $[-]$
E	Energy stored $[kWhr]$
$g_{,max}$	Maximum value of the g variable $[-]$
$g_{,min}$	Minimum value of the g variable $[-]$
$g_{,nominal}$	Nominal value of the g variable $[-]$
I_T	Total radiation on collector tilted surface $[kJ\,hr^{-1}m^{-2}]$
I_{Ts}	Total radiation on building's wall oriented to the south $[kJ\,hr^{-1}m^{-2}]$
$I_{\int U_1}$	Index to quantify the auxiliary energy use $[kWh]$
$I_{\int P_{csm}}$	Index to quantify the total energy consumption $[kWh]$
$I_{\triangle U_2^{(i)}}$	Index to quantify the number of switch on/off changes $[-]$
$I_{U_2^{(i)}}$	Index to quantify the switch on events $[-]$
$I_{Y_2^{(i)}}$	Index to quantify the average of the building temperature deviation $[^\circ C]$
I_{time}	Index to quantify the simulation time $[min]$
$\bar{J}_2$	Set of b consumer optimization costs $[-]$
J_1	Producer subsystem optimization cost $[-]$
J_2	Consumer subsystem optimization cost $[-]$
J_G	Global optimization cost $[-]$

Symbols

J_g	Calculated optimization cost using b lower than the centralized case [−]
J_g^{opt}	Calculated optimization cost of the centralized case [−]
J_t	Set of chiller-building optimization costs [−]
J_{t_h}	One element of the set J_t [−]
m	Number of consumers [−]
$\max(x)$	Maximum value of vector x [−]
$\dot{m}_1$	Diverter outlet fluid mass flow rate to the tank cold side $[kg\,hr^{-1}]$
$\dot{m}_2$	Diverter outlet fluid mass flow rate to the mixing valve $[kg\,hr^{-1}]$
$\dot{m}_{ch}$	Fluid mass flow rate in the chiller evaporator circuit $[kg\,hr^{-1}]$
$\dot{m}_h$	Fluid mass flow rate of the heat exchanger-tank loop $[kg\,hr^{-1}]$
$\dot{m}_l$	Fluid mass flow rate in the chiller generator circuit$[kg\,hr^{-1}]$
$\dot{m}_s$	Fluid mass flow rate of the heat exchanger-collector loop $[kg\,hr^{-1}]$
N_h	Prediction horizon [−]
ON	Set of b chiller optimal control inputs [−]
On	Switch control variable of the building cooling system[−]
Q	Weighting coefficient [−]
$\dot{Q}_{aux}$	Rate of energy input by the heating element $[kJ\,hr^{-1}]$
$\dot{Q}_{cool}$	Cooling power of the solar absorption cooling system $[kJ\,hr^{-1}]$
$\dot{Q}_{hot}$	Heating power of the solar absorption cooling system $[kJ\,hr^{-1}]$
$\dot{Q}_s$	Rate of energy transfer in the collector $[kJ\,hr^{-1}]$
P_{coo}	Consumption power of simplified model $[kJ\,hr^{-1}]$
P_{csm}	Cooling power of simplified model$[kJ\,hr^{-1}]$
P_{elc}	Auxiliary electric power of simplified model$[kJ\,hr^{-1}]$
P_{ese}	Storage power of simplified model $[kJ\,hr^{-1}]$
P_{sol}	Solar gains of simplified model$[kJ\,hr^{-1}]$
T_{chr}	Temperature of the fluid entering the chiller evaporator circuit $[^\circ C]$
T_{chs}	Temperature of the fluid entering the cooling ceiling of the building $[^\circ C]$
T_{ext}	Exterior temperature $[^\circ C]$
T_h	Temperature of the fluid entering the storage tank from the heat source $[^\circ C]$
T_i	Collector inlet temperature $[^\circ C]$
T_k	Temperature of the kth tank segment $[^\circ C]$
T_l	Outlet water temperature of the chiller generator $[^\circ C]$
T_o	Mixing valve outlet temperature $[^\circ C]$
T_{op}	Building operative temperature $[^\circ C]$

Symbols

T_s	Collector outlet temperature $[^\circ C]$
T_{sbg}	Set-point temperature of the building $[^\circ C]$
T_{set}	Set-point temperature demanded by the chiller generator circuit $[^\circ C]$
T_{wbp}	Water boiling point temperature $[^\circ C]$
t_k	Solar cooling plant sampling time $[hr]$
$\bar{U}_2$	Set of b optimal control inputs $[-]$
U_1	Producer subsystem controlled variables vector $[-]$
U_2	Consumer subsystem controlled variables vector $[-]$
V	Volume of the stratified storage tank$[m^3]$
W_{21}	Interacting variable between subsystems $[-]$
X_1	Producer subsystem state vector $[-]$
X_2	Consumer subsystem state vector $[-]$
x	State vector of the building state-space model $[-]$
$\hat{x}$	Estimated vector of the building state-space model $[-]$
$\bar{x}$	Average of vector x $[-]$
Y_r	Temperature set-point variable $[^\circ C]$
α	Optimized variable associated with the additional flow rate $[-]$
δ	Occupancy profile $[-]$
γ	Diverter control function $[-]$
$\triangle \dot{m}_l$	Additional flow rate sent to the chiller $[kJ\, hr^{-1}]$
$\triangle t$	Prediction model sample time $[hr]$
ε	Heat exchanger effectiveness $[-]$
η	Solar collector efficiency $[-]$
Π	Set of consumers energy demand profiles $[-]$
π_h	One element of the set Π $[-]$
ρ	Water density $[kg\, m^{-3}]$
ϱ	Solar absorption cooling power constant effectiveness $[-]$
σ	Switching mode $[-]$
σ_{sd}	Standard deviation $[-]$
ς	Consumption power constant effectiveness $[-]$
$\%_{subopt}$	Suboptimality percentage $[-]$

Abreviations

ANN	Artificial neural network
BLR	Based logic rules
CCS	Cooling consumption system
CFCs	Chlorofluorocarbons
COP	Coefficient of performance
CPS	Cooling production system
DMPC	Distributed Model Predictive Control
ESE	Energy storage element
EPA	Environmental Protection Agency
GA	Genetic algorithm
GPC	Generalized Predictive Control
HCFCs	Hydrochlorofluorocarbons
HMPC	Hierarchical Model Predictive Control
HVAC	Heating, ventilation, and air conditioning
MINLP	Mixed Integer Nonlinear Problem
MPC	Model Predictive Control
NLMPC	Non-linear Model Predictive Control
OECD	Organization for Economic Cooperation and Development
PMV	Predicted mean vote
SHWS	Solar powered hot water storage
SMPC	Stochastic Model Predictive Control
TES	Thermal energy storage

Contents

Chapter 1

Commande prédictive des systèmes de production-consommation d'énergie

1.1 Contexte

Dans les zones tropicales, les systèmes de rafraîchissement des bâtiments sont indispensables afin de maintenir le confort thermique des occupants. La manque de confort thermique peut perturber la productivité et la santé des occupants. Une faible productivité se manifeste par la manque de concentration, la somnolence, et l'absentéisme du travailleur (Kreith and West, 1997). De plus, les systèmes de rafraîchissement sont également utilisés pour le rendement et l'efficacité d'un processus de fabrication ou pour maintenir la qualité et le cycle de vie d'un produit stocké (Ameen, 2006).

De nos jours, les machines de climatisation à compression mécanique sont les systèmes les plus fréquemment utilisés mondialement. Ces systèmes fonctionnent avec l'électricité et donc émettent des gaz à effet de serre. Comme la consommation électrique devient de plus en plus élevée, il est nécessaire d'optimiser leur utilisation ou bien les remplacer par des systèmes alternatifs de climatisation.

Malgré leur faible coefficient de performance (COP), l'utilisation des machines frigorifiques à absorption solaire est une solution attractive pour réduire la consommation électrique des bâtiments lorsque la source d'énergie est gratuite (énergie solaire, chaleur résiduelle). D'autre part, le cycle à absorption solaire est particulièrement intéressant car les charges de refroidissement coïncident avec la puissance solaire disponible (Li and Sumathy, 2001).

Contrairement au système de climatisation à compression mécanique, une installation de rafraîchissement solaire nécessite généralement plusieurs composants pour fonctionner (panneau solaire, échangeur de chaleur, ballon de stockage, tour de refroidissement). En effet, la machine à absorption requiert trois sources d'énergie à différentes températures. Afin de maximiser le rendement global de l'installation, il est nécessaire de coordonner le fonctionnement

des composants. De plus, la production d'énergie doit être synchronisée avec le besoin de climatisation du bâtiment.

L'objectif de cette thèse est de proposer une méthode de coordination entre un producteur d'énergie et un ou plusieurs consommateurs qui permette de maximiser l'utilisation de la source solaire tout en assurant le confort thermique des occupants. Cette méthode est basée sur des contrôleurs prédictifs pour le producteur et les consommateurs. Dans cette approche décentralisée, une interaction entre le contrôleur du producteur et les contrôleurs des consommateurs est mise en œuvre afin de s'approcher de la solution optimale globale.

1.2 Le rafraîchissement solaire des bâtiments

1.2.1 Description générale

La figure 1.1 représente une installation de rafraîchissement solaire typique composée principalement d'un panneau solaire, d'un ballon de stockage d'eau chaude, d'un échangeur de chaleur, d'une machine à absorption et d'une tour de refroidissement. La chaleur captée par le panneau solaire est transférée au ballon de stockage à travers l'échangeur de chaleur. Le ballon de stockage fournit l'eau chaude nécessaire pour le fonctionnement de la machine frigorifique à absorption. Le chauffage auxiliaire est utilisé lorsque la source solaire est faible.

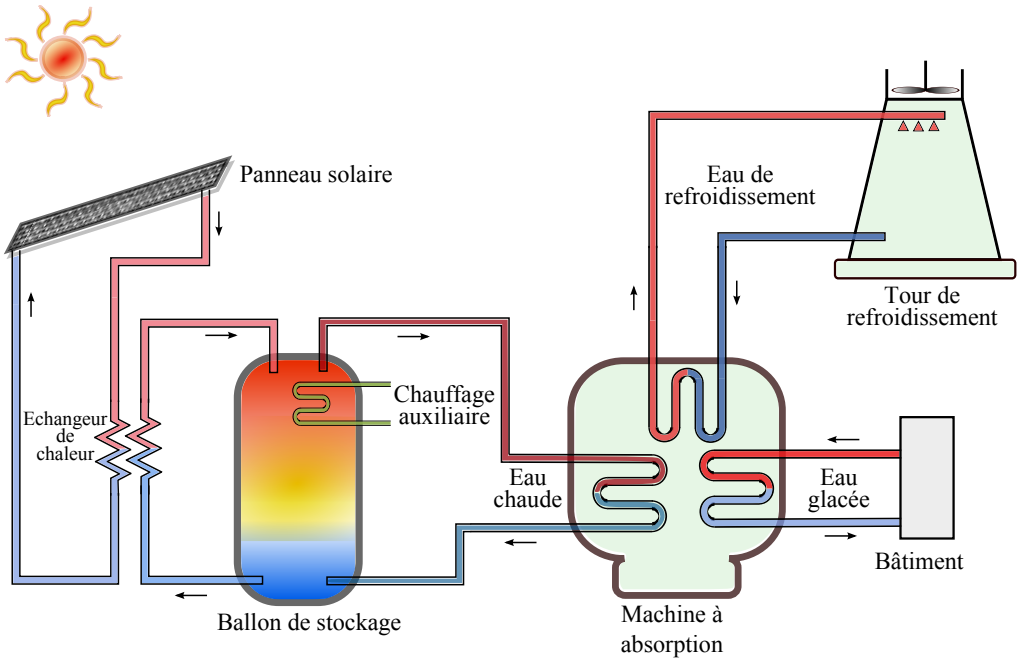

Figure 1.1: Une installation de rafraîchissement solaire typique.

La machine à absorption produit de l'eau glacée qui est distribuée à l'espace climatisé par

un plafond rafraichissant. L'eau glacée est produite à partir du cycle à absorption qui est composé de quatre éléments : l'absorbeur, le concentrateur, le condenseur et l'évaporateur. Une solution saline qui circule parmi les éléments est soumise à différentes températures et pressions ce qui entraîne des changements de concentration. La tour de refroidissement a pour fonction d'évacuer la chaleur extraite dans l'évaporateur et le condensateur.

1.2.2 Conditions d'exploitation

Pour faire fonctionner la machine à absorption et respecter les conditions de sécurité de l'installation, une série de conditions sont requises:

- La température de sortie du panneau solaire doit être supérieure à une valeur de consigne de température qui dépend soit de la température de l'eau fournie à la machine à absorption, soit de la température de l'eau qui circule du ballon de stockage vers le panneau solaire.
- Il est nécessaire de surveiller la température de sortie du panneau solaire lorsque le rayonnement solaire est important et qu'il n'y a pas de demande, car le fluide caloporteur peut monter jusqu'à la température de stagnation. Celle-ci est la température du fluide caloporteur au repos dans le panneau solaire qui continue à se chauffer par l'ensoleillement incident (Jabbour, 2011).
- La machine à absorption doit être arrêtée si la source de chaleur ne fournit pas la température requise par le circuit du concentrateur afin d'éviter un fonctionnement en dehors des conditions nominales.
- La source d'appoint électrique peut être activée lorsque le rayonnement solaire est faible.
- Comme le stockage d'eau glacée ne fait pas partie de l'installation considérée, une synchronisation est nécessaire entre la disponibilité de l'eau chaude, la production d'eau glacée et la demande de climatisation.

Dans le but de respecter ces conditions, les variable suivantes sont pilotables :

- Les débits des pompes du circuit solaire, c'est-à-dire, les débits d'eau qui circulent entre le panneau solaire, échangeur de chaleur et ballon.
- La puissance du chauffage d'appoint.
- Les températures d'entrée au concentrateur, condenseur et évaporateur.
- Le débit et la température délivrés à la zone climatisée.

Il résulte de ce qui précède qu'il est indispensable de mettre en œvre un mécanisme de gestion globale afin de respecter les conditions d'exploitation en utilisant de manière optimale les ressources énergétiques (solaire et électrique).

1.2.3 Formalisation du problème

L'installation de refroidissement solaire peut être vue comme une partie d'un système de production-consommation d'énergie. La figure 1.2 représente la structure proposée de ce système. Il est composé d'un producteur qui fournit de l'eau chaude à plusieurs consommateurs connectés par le moyen d'un système de distribution d'eau. L'un de ces consommateurs est composé de la machine à absorption qui fournit de l'eau glacée à l'espace climatisé.

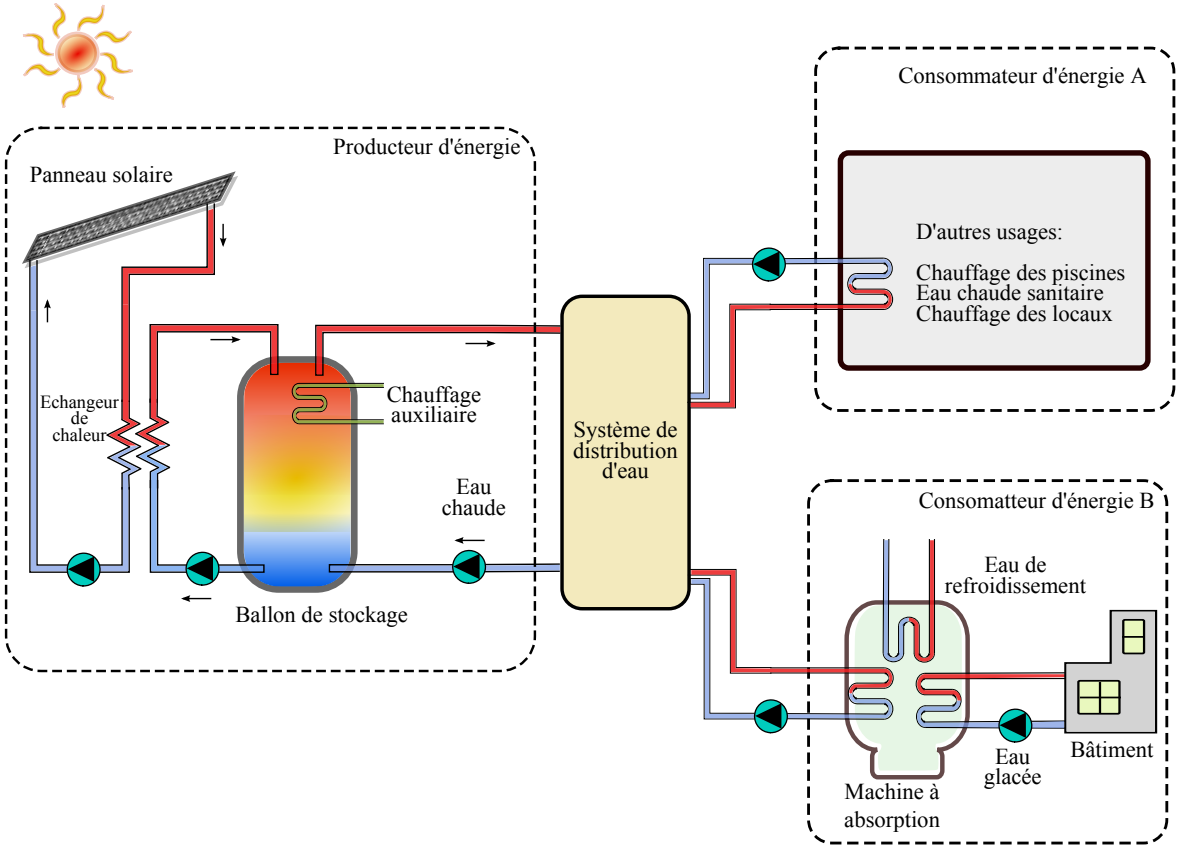

Figure 1.2: Système de production-consommation d'énergie.

Cette thèse propose une gestion globale à un niveau haut du système en considérant un contrôle modulaire, c'est-à-dire, des contrôleurs prédictifs indépendants pour le producteur et les consommateurs qui intègrent un mécanisme d'interaction. Dans cette gestion, le producteur est vu comme un fournisseur d'eau chaude à une température et débit de consigne lorsqu'une demande de consommation est requise par un ou plusieurs consommateurs.

La gestion proposée du système requiert des mécanismes d'interaction entre le producteur et les consommateurs afin de minimiser la dégradation de la solution optimale qui pourrait être obtenue en utilisant une approche centralisée. Cependant, les mécanismes d'interaction de l'approche proposée restent simples du fait que les interactions entre les consommateurs ne sont pas considérées.

1.2.3.1 Le producteur d'énergie

Ce sous-système est composé d'un panneau solaire, un échangeur de chaleur et un ballon de stockage d'eau chaude. Il doit fournir de l'eau chaude à une température et un débit fixes aux consommateurs. Les températures des composants doivent être contrôlées afin d'assurer la protection du système et de délivrer l'eau chaude à la température désirée aux consommateurs.

Le modèle du producteur est obtenu à partir des modèles des composants. Le ballon de stockage est représenté par un jeu d'équations différentielles dont l'expression change en fonction du sens du flux. Un modèle hybride associant dynamique continue et événementielle est alors utilisé. La représentation mathématique du panneau solaire et de l'échangeur de chaleur est faite par des modèles statiques proposés par l'outil de simulation thermique TRNSYS (TRNSYS17-Documentation, 2012).

1.2.3.2 Le consommateur d'énergie

Afin d'illustrer la gestion proposée du système de production-consommation d'énergie, un type de consommateur d'énergie a été choisi : une machine à absorption qui fournit de l'eau glacée à un bâtiment en utilisant un plafond rafraichissant. Un bâtiment de taille moyenne et une machine à absorption de petite puissance sont considérés pour l'étude.

Compte tenu du temps de réponse du bâtiment, la réponse transitoire de la machine à absorption n'est pas prise en compte. Par conséquent, un modèle statique est considéré et son fonctionnement est limitée aux conditions nominales. A partir de ce choix et comme la température d'entrée au concentrateur est fixe, le contrôleur peut agir uniquement sur la marche et l'arrêt de la machine.

L'objectif du contrôleur du consommateur d'énergie est de maintenir le confort thermique dans le bâtiment pendant les périodes d'occupation. La variable manipulée est un signal de commande discret qui met en marche ou à l'arrêt la machine à absorption. Le consommateur d'énergie est représenté par un modèle d'état linéaire qui décrit la dynamique du bâtiment et du plafond rafraichissant.

1.3 Approche par commande prédictive pour le management d'un système de production-consommation d'énergie

1.3.1 Modélisation

La figure 5.2 représente le système de production-consommation d'énergie. Le producteur est un sous-système décrit par une dynamique non linéaire hybride et ses variables de commande $U_1(k)$ sont les débits des pompes du circuit solaire et la puissance du chauffage auxiliaire. Le consommateur d'énergie est représenté par un système dynamique avec une entrée de commande binaire $U_2(k)$. L'entrée de commande du consommateur est la marche/arrêt de la machine à absorption.

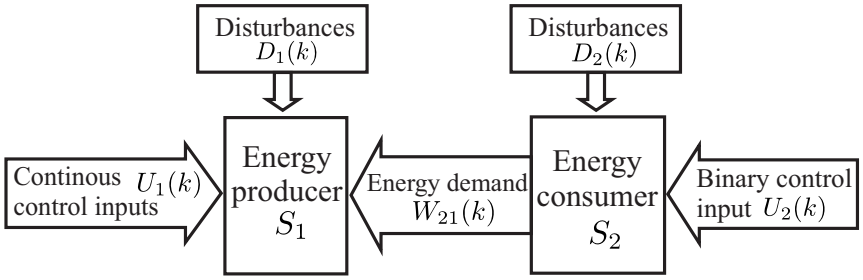

Figure 1.3: Représentation d'un système de production-consommation d'énergie.

Le producteur d'énergie S_1 est décrit par un modèle non linéaire hybride de la forme

$$X_1(k+1) \quad = \quad f_{1\sigma(k)}(\overline{U}_1(k), W_{21}(k)) \tag{1.3.1}$$

$$\sigma(k) = \sigma(\overline{U}_1(k), W_{21}(k)) \tag{1.3.2}$$

où $\overline{U}_1(k) = [X_1(k), U_1(k), D_1(k)]$. $U_1(k) \in \mathbb{R}^{m_1}$ est le vecteur de variables de commande et $D_1(k) \in \mathbb{R}^{p_1}$ est le vecteur de perturbations. $W_{21}(k) \in \mathbb{R}^{q_1}$ est le vecteur de variables de couplage entre les sous-systèmes.

Le producteur S_1 est soumis à des contraintes d'entrée et de sortie :

$$H_{1\sigma(k)}(\overline{U}_1(k), W_{21}(k)) \leq \mathbf{0} \tag{1.3.3}$$

Le consommateur S_2 est décrit comme suit :

$$X_2(k+1) = f_2(X_2(k), U_2(k), D_2(k)) \quad (1.3.4)$$

$$Y_2(k) = H_2(X_2(k)) \quad (1.3.5)$$

$$W_{21}(k) = G(X_2(k), U_2(k)) \quad (1.3.6)$$

$U_2(k) \in \{0, 1\}$ est la variable de commande discrète et $D_2(k) \in \mathbb{R}^{p_2}$ est le vecteur de perturbations. $Y_2(k) \in \mathbb{R}^{r_2}$ est le vecteur de sortie.

Le consommateur S_2 est soumis à des contraintes d'entrée et de sortie :

$$H_2(\overline{U}_2(k)) \leq \mathbf{0} \quad (1.3.7)$$

où $\overline{U}_2(k) = [X_2(k), U_2(k), D_2(k)]$.

1.3.2 Contrôle-commande

Comme le système de production-consommation d'énergie est soumis à des contraintes d'entrée et de sortie, à des perturbations et à des conditions d'exploitation, la gestion globale du système peut être effectuée en considérant une approche par commande prédictive (MPC, voir par exemple Camacho and Bordons (2004)). En effet, cette approche de contrôle-commande est caractérisée par sa capacité à gérer les contraintes, les fonctions d'optimisation multiobjectif et les dynamiques linéaires et non linéaires. Le principe du MPC est de calculer les entrées futures du système sur un horizon fixe en minimisant une fonction de coût. Un modèle de prédiction du système est nécessaire, ainsi qu'une prédiction adéquate des perturbations.

La gestion globale du système est réalisée en considérant des contrôleurs prédictifs pour le producteur et les consommateurs d'énergie. L'objectif de cette approche est de minimiser le coût de fonctionnement tout en garantissant les conditions d'exploitation et les besoins de consommation.

L'objectif de contrôle du producteur est de minimiser l'énergie électrique auxiliaire en respectant les contraintes. En ce qui concerne le consommateur, l'objectif du contrôleur est de maintenir le confort thermique du bâtiment en tenant compte des restrictions de fonctionnement de la machine à absorption. Les contrôleurs des consommateurs proposent plusieurs profils de demande d'énergie au contrôleur du producteur. Celui-ci va tester toutes ces stratégies possibles et choisir la meilleure combinaison.

La figure 1.4 représente l'architecture proposée pour la gestion globale du système de production-consommation d'énergie. Une description détaillée de l'algorithme est décrit ci-dessous.

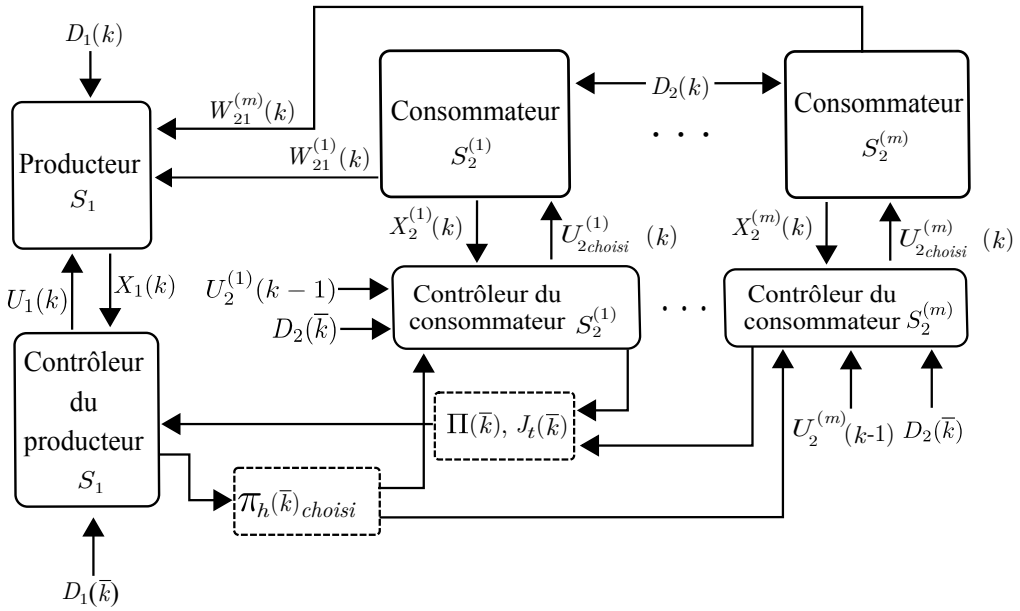

Figure 1.4: Architecture proposée pour le contrôle-commande du système de production-consommation d'énergie.

1. Les contrôleurs des consommateurs calculent la matrice $\Pi(\overline{k})$ composée par b^m profils de demande d'énergie sur l'horizon de prédiction N_h à partir du vecteur d'état de chaque consommateur $X_2^{(i)}(k)_{i=1,\ldots,m}$, les entrées de commande antérieures $U_2^{(i)}(k-1)_{i=1,\ldots,m}$, et la prédictions des perturbations $D_2(\overline{k})$ sur l'horizon de prédiction N_h. Cette matrice est envoyée au contrôleur du producteur d'énergie.

2. Le contrôleur du producteur calcule b^m optimisations linéaires selon la matrice $\Pi(\overline{k})$ et en prenant en compte le vecteur d'état du producteur $X_1(k)$ et les prédiction des perturbations $D_1(\overline{k})$ sur l'horizon de prédiction N_h.

3. Le contrôleur du producteur choisit le profil qui a le coût le plus bas.

4. Le contrôleur de producteur envoie le premier élément du vecteur de commande $U_1(k)$ au producteur et communique aux contrôleurs de consommation d'énergie quel est le profil d'énergie qui a été choisi. Les contrôleurs des consommateurs envoient le premier élément du vecteur de commande $U_2^{(i)}(k)$ qui est associé au profil choisi $\pi_h(\overline{k})$.

5. L'algorithme redémarre au pas d'échantillonnage $k+1$.

1.3.3 Résultats

La stratégie par commande prédictive est testée sur un modèle simplifié d'un système de production-consommation d'énergie. Le producteur est un modèle linéaire qui représente un

stockage d'énergie solaire et électrique et chaque consommateur est composé d'une machine à absorption et d'un espace à climatiser. Il est représenté par un modèle linéaire. Afin de comparer les résultats de la stratégie, une approche de contrôle-commandé basée sur des contrôleurs tout ou rien pour le producteur et les consommateurs est mis en œuvre. Les résultats des deux stratégies sont résumés dans le Tableau 1.1.

Table 1.1: Tableau comparatif des stratégies de contrôle-commande

Système de production-consommation d'énergie			
Caractéristiques		Difficultés	
Un producteur et plusieurs consommateurs. Des modèles linéaires pour les sous-systèmes.		Dépendance bilinéaire entre les consommateurs et producteur. Signal de commande binaire pour les consommateurs.	
Les stratégies de contrôle-commande			
	Caractéristiques	Avantages	Inconvénients
Stratégie basée sur des algorithmes tout ou rien	Contrôleurs d'hystérésis pour le producteur et les consommateurs.	Optimisation non nécessaire. Mise en œuvre facile.	Nombreux marche/arrêt de la machine à absorption. Energie auxiliaire consommée élevée.
Approche MPC: Profils optimaux	Approche MPC linéaire et hybride. La matrice de demande d'énergie envoyée au producteur est composée des profils minimisant le coût d'optimisation.	La marche/arrêt de la machine à absorption est minimisé. L'usage de l'énergie auxiliaire est adapté à la consommation. Les contraintes du producteur et des consommateurs sont respectées.	La complexité de calcul augmente de façon exponentielle avec le nombre de consommateurs. La solution obtenue est sous-optimale en comparaison avec le cas centralisé.

1.4 Commande prédictive appliquée à un modèle TRNSYS

1.4.1 Cas d'étude

La stratégie de contrôle-commande proposée est testée sur un modèle plus complexe développé dans l'outil de simulation TRNSYS. L'objectif de cette étude est d'évaluer la performance de la stratégie lorsque la complexité du système à commander augmente. Plus précisément, le

producteur n'est plus représenté par un modèle linéaire. Ce sous-système est un producteur d'eau chaude qui intègre les éléments suivants : panneau solaire, échangeur de chaleur et ballon de stockage d'eau chaude. Comme la complexité du producteur augmente, le modèle de prédiction n'est plus linéaire, il est représenté par un modèle non linéaire hybride. Par conséquent, la résolution du problème d'optimisation est bien plus difficile.

Les objectifs de la stratégie en ce qui concerne le contrôleur du producteur sont le respect des conditions d'exploitation du système et la minimisation de l'usage du chauffage d'appoint. Les températures de sortie des éléments doivent rester en dessous de la température d'ébullition de l'eau et lorsque la machine à absorption marche, la température de l'eau qui circule du ballon à la charge doit être au dessus de la température nominale de la machine à absorption. Les variables de commande de ce sous-système sont les débits des pompes.

Comme dans la Section 1.3, le consommateur d'énergie s'agit d'une machine à absorption qui délivre de l'eau glacé à un bâtiment par le moyen d'un plafond rafraichissant. Les objectifs du contrôleur sont de garantir le confort thermique des occupants en minimisant le nombre de marche/arrêt de la machine à absorption et son usage.

Dans cette étude, les modèles de prédiction et de simulation sont différents. Le modèle de prédiction du consommateur d'énergie reste inchangé, c'est-à-dire, une représentation linéaire est utilisé. Le modèle de simulation est développé sur l'outil de simulation thermique TRNSYS. Le modèle thermique du bâtiment considéré pour l'étude est composé de deux zones avec une surface globale de 192 m^2. La surface exposée au sud (120 m^2) est la zone à climatiser. Comme l'algorithme de contrôle-commande est développé sur MATLAB, un interaction entre les deux outils de simulation est mise en place en utilisant un élément spécifique de la librairie TRNSYS.

1.4.2 Résultats

Afin de comparer les résultats de la stratégie par commande prédictive, deux algorithmes de contrôle-commande ont été développés. La première stratégie utilise des contrôleurs tout ou rien tant pour le producteur que pour le consommateur. Les débits des pompes du producteur sont à débit constant lorsque la température de sortie du panneau solaire est plus grande que celle qui circule du ballon à l'échangeur de chaleur. De la même manière, le chauffage d'appoint est activé à puissance constante si le rayonnement solaire est faible et s'il y a une demande d'eau chaude par la machine à absorption. En ce qui concerne le consommateur, la température intérieure du bâtiment est contrôlée par hystérésis en mettant en marche ou à l'arrêt la machine à absorption. La seconde stratégie correspond à un contrôleur prédictif pour le producteur qui optimise l'usage du chauffage d'appoint et les débits de pompes. Le contrôleur du producteur reste inchangé par rapport à la stratégie précédent, c'est-à-dire, la

machine à absorption est contrôlée par hystérésis. Cependant, un prédicteur de consommation d'eau chaude est intégré à la stratégie. Le tableau 1.2 résume les résultats des trois stratégies de contrôle-commande.

Table 1.2: Tableau comparatif des stratégies de contrôle-commande

Système de production-consommation d'énergie: Système de rafraîchissement solaire d'un bâtiment			
Caractéristiques		Difficultés	
Système de production d'eau chaude pour le rafraîchissement par absorption d'un bâtiment		Dynamique non linéaire hybride pour le producteur. Consommateur avec entrée de commande discrète.	
Les stratégies de contrôle-commande			
	Caractéristiques	Avantages	Inconvénients
Stratégie par contrôleurs d'hystérésis	Contrôleurs d'hystérésis tant pour le producteur que pour le consommateur.	Optimisation non nécessaire. Implémentation facile.	Un nombre important de marche/arrêt de la machine à absorption. Les conditions d'exploitation du producteur ne sont pas respectées.
Stratégie prédictive-hystérésis	Contrôleur d'hystérésis pour le consommateur avec prédicteur de consommation. Commande prédictive non linéaire pour le producteur.	Pas d'optimisation dans la stratégie de commande du consommateur.	Des erreurs de modèle de prédiction provoquent des violations de contraintes de température.
Stratégie par commande prédictive	Optimisation discrète pour le consommateur. Optimisation non linéaire pour le producteur.	Les contraintes tant pour le producteur que pour le consommateur sont respectées.	Complexité de calcul augmente de façon exponentielle avec le nombre de consommateurs.

1.5 Conclusions et perspectives

L'objectif de cette thèse a été de proposer une stratégie pour la gestion globale d'un système de production-consommation d'énergie afin d'optimiser l'usage de l'énergie et de trouver un compromis entre la production et la consommation. Le cas d'étude est basé sur une installation pour le rafraîchissement solaire d'un bâtiment.

Afin d'offrir des attributs de modularité à la stratégie, le problème de contrôle-commande est traité de manière décentralisée mais avec un échange minimal d'information. La stratégie est basée sur des contrôleurs prédictifs indépendants pour les sous-systèmes avec une interaction entre les contrôleurs du producteur et des consommateurs.

Dans une première phase, l'approche de contrôle-commande est testée sur un modèle simplifié qui intègre des modèles linéaires et prend en compte plusieurs consommateurs. Les résultats de simulation montrent qu'en proposant un nombre réduit de profils de demande d'énergie, la performance de la solution obtenue ne s'éloigne pas significativement de celle de la solution obtenue à partir du cas de contrôle-commande centralisé. Dans un deuxième phase, la stratégie est testée sur un cas plus complexe où le modèle du producteur devient non linéaire hybride et par conséquence la complexité de problème d'optimisation augmente. Les résultats de simulation montrent une performance acceptable et supérieure à celles des deux autres stratégies étudiées.

Ces travaux ouvrent des perspectives telles que:

- Intégrer des approches de contrôle-commande qui garantissent l'optimalité de la solution globale comme des approches prédictives distribuées ou hiérarchiques afin d'améliorer le compromis entre la production et la consommation d'énergie.
- Implémenter un mécanisme de filtrage de profils de demande d'énergie générés par les consommateurs afin de diminuer le nombre d'optimisations du contrôleur du producteur.
- Intégrer un modèle dynamique de la machine à absorption dans le but d'étudier les enjeux liés aux perturbations qui influencent l'efficacité de la machine.
- Tester la stratégie proposée sur un cas plus complexe qui intègre des modèles du bâtiment et de l'installation de production d'eau chaude plus proches des installations réelles afin d'étudier l'adaptation et la performance de la stratégie lorsque l'inertie et la complexité des systèmes augmentent.

Chapter 2

Introduction

2.1 Motivation of the thesis

Nowadays, worldwide electricity consumption is a major concern. Besides, most of the electricity production is based on fossil fuels and generates the major greenhouse gas emissions. Only a minor percentage of electricity is produced using renewable energy. As the commercial and residential building sector is one of the largest energy consumers, it is also responsible for the largest greenhouse gas emissions.

The French Government has adopted several regulations and projects in order to make an effort to combat climate change and environmental pollution, to manage energy consumption and to reduce greenhouse gas emissions. The buildings sector (whose energy consumption in both residential and commercial sectors is mainly distributed for heating, cooling and lighting) is the most strongly affected by these measures. Indeed, it consumes around 44% of the national energy (well above transports 32,1 %, industry 21,1 % and agriculture 2,7 %) and accounts for 25% of greenhouse gas emissions (Molle and Patry, 2013).

As energy demand is rapidly growing worldwide, it is imperative to search for ways to minimize electricity consumption and greenhouse gas emissions. One possibility is to consider an efficient and eco-friendly energy production for heating and cooling in buildings.

Currently, the vapor-compression cycle based cooling system is the most used in buildings. Nevertheless, some issues regarding environmental and economical aspects come with the use of this conventional way of cooling production as the use of ozone-depleting refrigerants and electricity consumption. Besides, other disadvantages of this kind of systems are noise, vibrations and leakage of the refrigerant.

Absorption cycle based units for cooling in buildings can mitigate electricity use and greenhouse gas emissions. Despite these systems have a coefficient of performance (COP) lower than vapor-compression cycle based cooling units, they are attractive when the heating source is at low cost, for example: solar energy or waste heat. In addition, this kind of system uses

ozone friendly refrigerants as water or ammonia.

Three main actors of an absorption cooling installation driven by solar energy can be identified: the heat source (whose main components are a collector panel and a storage tank), an absorption chiller and the building to be cooled. As the cooling unit is mainly driven by solar radiation which, in turn, has frequent fluctuations, auxiliary energy is required. Furthermore, the sizing of the components contributes to the global efficiency of the installation and consequently a significant study is required in this area.

The low level control of the chiller and its complex process is also very important to improve the efficiency of the system. The coordination of heat production, absorption chiller and building cooling is fundamental as the energy production cannot be optimized without interactions with the energy demand part.

The objective of this thesis is to develop a control structure where a coordination between an energy producer and several consumers is achieved in a straightforward manner with minimal information exchange. Applied to solar absorption cooling systems, the energy producer is represented by the heat source composed of a collector panel, a storage tank and a heat exchanger. The energy consumer is composed of an absorption chiller which provides cooling to a building. The control objectives are to minimize auxiliary energy, to guarantee building thermal comfort and to respect operating conditions of the solar cooling system.

In order to provide modularity to the control structure, the energy production-consumption problem is decomposed and at the same time, interactions between the subsystems are established to adapt the energy production to consumption. Taking into account that the studied system is characterized by nonlinear and hybrid dynamics (the term "hybrid" is applied when both discrete and continuous variables, dynamics or conditions, are required in order to fully characterize the behavior of interest (Labinaz and Guay, 2011)), the proposed control approach decreases the complexity of the control problem compared to a centralized control one.

2.2 Contributions of the thesis

The contributions of this thesis are the following:

- **Interactive hybrid MPC structure**: An energy producer-consumer control problem is solved by implementing a straightforward and interactive predictive control strategy where local predictive controllers with information exchange are involved. The proposed control strategy fulfills the systems constraints and can be extended to other complex energy producer-consumer structures.

- **Proposed control approach assessment considering a solar cooling system as a case study**: The proposed control approach is evaluated by controlling a model of a solar cooling system for thermal comfort in buildings. Simulations tests are carried out with the purpose of assessing the performance of the proposed control approach.

2.3 Thesis outline

This thesis is organized as follows:

Chapter 3 contains the fundamentals of solar cooling systems and thermal building control. First, the operating principles of absorption cycle based cooling systems are presented and later the operating conditions and control requirements are detailed. In addition, a review of control approaches for solar cooling systems and thermal building control is introduced. This study gives the elements to define the energy production-consumption control problem.

Chapter 4 states the energy production-consumption control problem. This stage is crucial for the development of the control strategy.

In Chapter 5, the formalization of the energy production-consumption control problem is introduced. First, a generalized model of the energy consumer-producer is presented which has nonlinear dynamics with both continuous and discrete inputs. Later, the MPC proposed structure is applied to a representation of the generalized model which involves linear models in both producer and consumers. Finally, simulations results are presented to assess the performance of the proposed control structure in terms of constraints fulfillment, prediction horizon impact and suboptimality studies.

In Chapter 6, the proposed control structure developed in Chapter 5 is tested on a simplified model of a solar absorption cooling system for indoor temperature control implemented in the thermal simulation tool TRNSYS. This simplified model allows to assess the potential of the control structure. The results achieved by applying the proposed control strategy to the TRNSYS model are presented and compared with those of two other strategies.

Finally, Chapter 7 provides the conclusions and perspectives of the proposed investigation.

Chapter 3

Background

Air conditioning systems in tropical climates become indispensable in order to ensure thermal comfort in buildings. At the same time, as electricity consumption increases worldwide, a proper management of these systems is crucial. Furthermore, air conditioning systems driven by renewable sources as solar absorption cooling systems are encouraged as they can contribute to the mitigation of electricity consumption. However, in order to maximize the air conditioning system efficiency, optimized control strategies are required taking into account a coordination between the cooling production part and the conditioned space.

The aim of this chapter is to introduce the case study of this research. It provides a literature review about how the problem of solar absorption cooling systems management for thermal comfort in building has been treated. Furthermore, it lays the foundation for the problem statement presented in the next chapter.

The first part of this chapter focuses on the fundamentals about conventional air conditioning systems and other alternative technologies, more precisely, environmentally friendly solar absorption systems. Latter, the advantages, disadvantages and operating conditions of this kind of systems are introduced. Finally, logic rule-based and advanced control approaches reported in the literature are presented for solar cooling systems and for thermal comfort in buildings.

3.1 Cooling systems in buildings

Thermal comfort is that condition of mind which expresses satisfaction with the thermal environment (Hall, 2010). Maintaining thermal comfort in buildings is necessary since upon this depends several factors like occupant's productivity and health. Poor indoor environments can be generally described in three categories: inadequate thermal comfort, unhealthy environments, and poor lighting. Manifestations of poor productivity can be characterized by worker illness, absenteeism, distractions to concentration, and drowsiness or lethargy at work as well as by defects and mistakes in manufacturing and routine office work, and so forth

(Kreith and West, 1997).

One of the main purposes of an air-conditioning system is to provide and maintain an artificial and comfortable environment for the occupants within a building or an enclosed premise. Besides human comfort, air conditioning is also widely used for the efficiency and effectiveness of a manufacturing process, or to maintain the quality and life of a stored product (Ameen, 2006). At the same time, ensuring thermal comfort involves energy consumption. Designed strategies to maintain desired thermal conditions must have a proper management in order to minimize the energy use. A well-designed building should be able to provide good thermal comfort, while simultaneously having low energy consumption (Taylor et al., 2008).

For several decades now, the vapor-compression cycle based cooling system is the most widely used for thermal comfort control in both residential and commercial buildings. The high COP, compactness and simplicity are some of the main factors that contribute to the permanency of this technology.

3.1.1 The vapor-compression based cooling unit

Figure 3.1 depicts the components of an air conditioning system for cooling based on a conventional vapor-compression cycle. A refrigerant circulates among the components of the unit changing its phase from liquid to gas and vice versa. The low pressure liquid refrigerant passes through the cooling coils and boils (due to a pressure drop as it leaves an expansion valve) causing the heat rejection from the coils surroundings and producing the cooling effect. Then, the low pressure refrigerant in gas phase is directed towards a mechanical compressor which increases its pressure and temperature. The hot, high pressure gas is conveyed to the condenser where cold air blown by a fan is passing through the pipes. As the hot, high pressure gas circulates through the condenser coils, its heat is removed and transferred to outside air. Due to the heat removal, the gas refrigerant condenses. The high pressure liquid circulates towards the filter-dryer which absorbs any contaminants from the refrigerant and removes or holds the moisture to avoid its circulation through the system. Then, the expansion valve reduces the liquid pressure which is sent to the evaporator to begin the cycle again.

3.1.2 Economical and environmental aspects of the vapor-compression cooling unit

One of the major problems concerning vapor-compression based cooling units is the use of ozone-depleting refrigerants (HCFCs, hydrochlorofluorocarbons). The HCFC-22 (also called R-22) is the most common refrigerant used in air conditioning equipments. Important changes are being done in terms of regulation of emissions to the atmosphere, several amendments to the Montreal Protocol from 1987 include the phase out of the HCFCs in both developed and

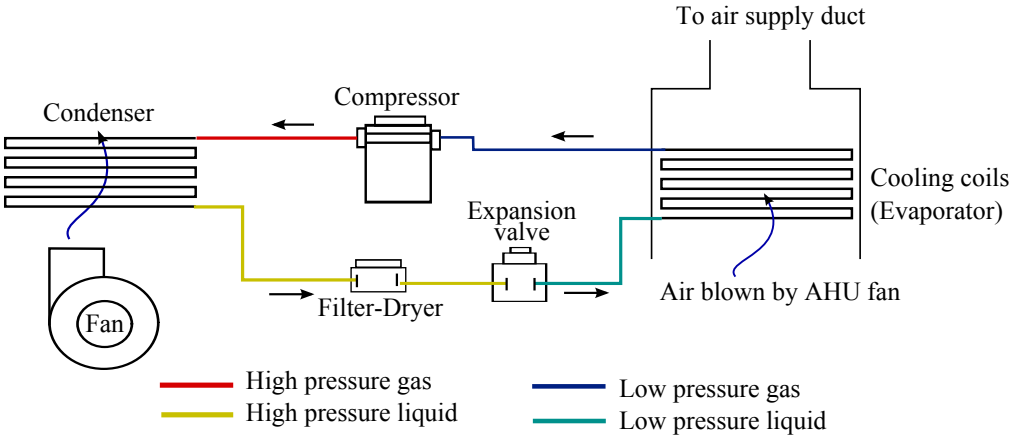

Figure 3.1: The vapor-compression cooling unit.

developing countries. Consequently, the HCFCs must be replaced by ozone-friendly chlorofluorocarbons (CFCs). The Environmental Protection Agency (EPA) of the United States has compiled a list of several alternatives to R-22 for household and light commercial air conditioning. One of these substitutes is R-410A which is touted as an environmentally friendly refrigerant that does not contribute to ozone depletion; however, it potentially contributes to global warming (Binggeli and Greichen, 2011).

As the motor compressor operates at high speed, noise and vibrations are other inconveniences of this type of systems. Strong foundations are needed to maintain the system stable when it is operating. The compressor also requires maintenance as it is composed of several moving mechanical parts. Moreover, the wear or malfunctioning of the components can cause the leakage of the refrigerant which has to be recharged.

The main problem related to the vapor-compression based refrigeration units is the use of electricity: the compressor requires large quantities of electrical power for its operation. It is well known that electricity consumption around the world is continuously rising which leads to the rise of its price. This increase is largely due to more electrical appliances, the development of electrical heating in several developed countries and rural electrification programs in developing countries (OECD, 2014). A study of the Organization for Economic Cooperation and Development (OECD) reveals that from 1971 to 2011, the share of electricity production from coal remained stable at 40-41%, the use of natural gas increased from 13% to 22% and the share of hydro-electricity decreased from 23% to 16%. Even if the use of renewable energies such as solar, wind, geothermal, biofuels and waste for electricity production is increased, the share remains of limited importance: in 2011, they accounted for only around 4.5% of the world total electricity production (OECD, 2014). As the electricity production comes mainly from fossil fuels, the CO_2 emissions to the atmosphere are increasingly important.

Furthermore, in hot climate zones, air conditioning can significantly use large amounts of electrical power during higher-temperature periods of the day. This can then require utilities to supply expensive electricity, either from old and inefficient plants or from costly purchased grid power (Boehm, 2012). For this reason, air conditioning loads are a major contributor to cause peak load on the power grid. Due to the heavy air conditioning demand, the cost for power generation is not only increased but also overall grid efficiency is reduced (Yoon et al., 2014).

3.1.3 The absorption cooling unit

It is not surprising that new environmental-friendly cooling technologies are growing up in order to reduce the global electricity demand. Despite the low COP, absorption cooling systems are an alternative to reduce this demand as they are driven by free-cost energy: instead of using electricity, the absorption cycle uses waste heat or solar energy to operate. Furthermore, solar-powered absorption cycles are particularly attractive because of the near coincidence of peak cooling loads with the available solar power (Li and Sumathy, 2001). The use of ozone-friendly refrigerants as water or ammonia is one of the incentives to use this technology: they do not deplete the ozone layer and do not contribute to global warming.

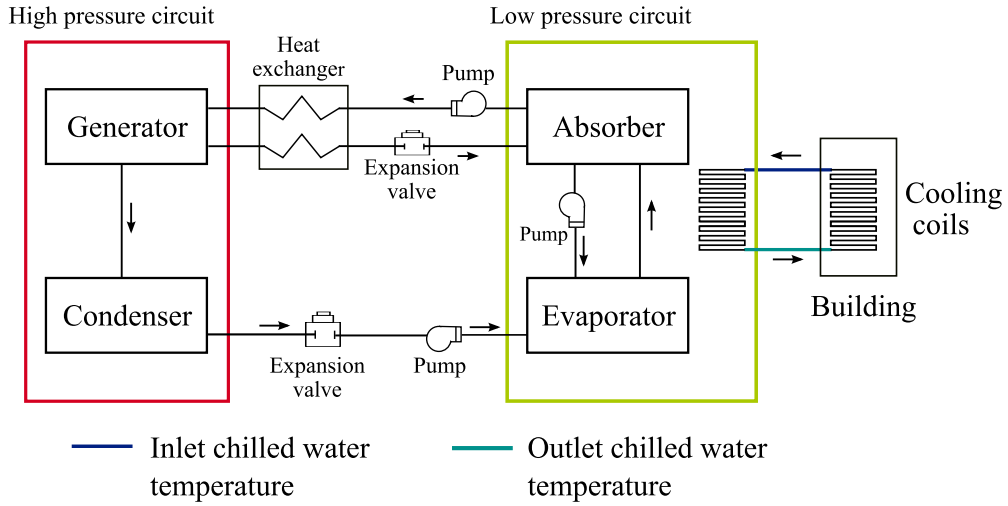

Figure 3.2: The absorption cooling unit.

Figure 3.2 depicts the schematic diagram of the absorption cooling unit. Four components can be easily identified: the generator and condenser in the high pressure circuit and the absorber and evaporator in the low pressure circuit. Instead of using a mechanical compressor, the absorption cooling unit uses a "thermo-chemical compressor" composed of the generator and the absorber to achieve the cooling effect. Consequently, the electricity consumption due to the vapor-compression is eliminated. Electricity in the absorption cycle is only used to

circulate a chemical solution through the elements of the unit using pumps. The main source of energy is thermal. Although the COP is lower than that of the vapor-compression cycle, if this energy is "free" (i.e. coming from solar or waste energy), then a large amount of energy is saved from the fact that, pumping a solution is easier and cheaper than compressing a vapor. Besides, the operation of absorption cooling units is smooth as moving parts are only present in the pumps. However, while maintenance is important for the proper operation of vapor-compression cooling systems, it is critical to the operation of absorption chillers. Two particular maintenance concerns are maintaining the proper vacuum within the shellside of the absorber and controlling corrosion within the chiller (Piper, 1999).

Unlike the vapor-compression cycle, the absorption unit uses two fluids: the refrigerant and the absorbent. The most common solution is lithium bromide-water, where the lithium bromide compound is the absorbent and water is the refrigerant. It is worth noting that these components are nontoxic and environmentally friendly. Another common solution used in absorption cycles is the pair water-ammonia where ammonia is the refrigerant and water the absorbent. The main function of the absorbent is to carry the refrigerant from the absorber to the generator passing from a low to a high pressure environment. For this reason, the absorbent should have two characteristics: strong affinity for the refrigerant and a boiling point higher than that of the refrigerant. The refrigerant and absorber are mixed in the various processes of the absorption cycle in different quantities which leads to: diluted, concentrated and partially concentrated solutions. In the diluted solution, the quantity of refrigerant is higher than that of the absorbent. In the concentrated solution, the quantity of absorbent is higher than that of the refrigerant. The partially concentrated solution is a mixture of diluted and concentrated solution.

Figure 3.3 represents the phases of the absorption cycle where four stages are carried out:

Generator: The cycle starts in this component, where the refrigerant is separated from the absorbent using a heat source. A diluted solution (e.g. lithium bromide-water) in pumped out from the absorber to the generator. Afterwards, the chemical solution is heated using hot water or steam that circulates in tubes submerged in the solution. As the generator is located in the high pressure circuit and as the absorbent boiling point is higher than that of the refrigerant, this latter boils and it is separated from the solution. Consequently, the diluted solution becomes a concentrated solution. Then, the refrigerant circulates towards the condenser and the concentrated solution returns to the absorber.

Condenser: In this component, cooling water circulates through coils and the temperature of the cooling water is smaller than the temperature of the refrigerant vapor. As heat always flows from the warmer to the cooler environment, the heat from the refrigerant vapor is

transfered to the cooling water causing the condensation of the refrigerant on the surface of the coils. Normally, as the condenser temperature is hotter than the ambient temperature, the heat absorbed from the refrigerant vapor through the coils is transfered to the ambient air. The liquid refrigerant accumulates in the bottom of the condenser before passing to the evaporator.

Evaporator: The accumulated condensed refrigerant in the condenser circulates towards the evaporator through an expansion valve which reduces its pressure. Besides, a chilled water circuit circulates through coils in the evaporator. This water is responsible for rejecting the heat from the surroundings of the conditioned space. A pump located in the bottom of the evaporator pumps out the liquid refrigerant coming from the condenser spraying it over the coils surface. As the liquid refrigerant now has a lower pressure, its boiling point temperature is also lower. For this reason, the liquid refrigerant boils causing the cooling effect and removing heat from the chilled water. The refrigerant vapor is attracted to the absorber.

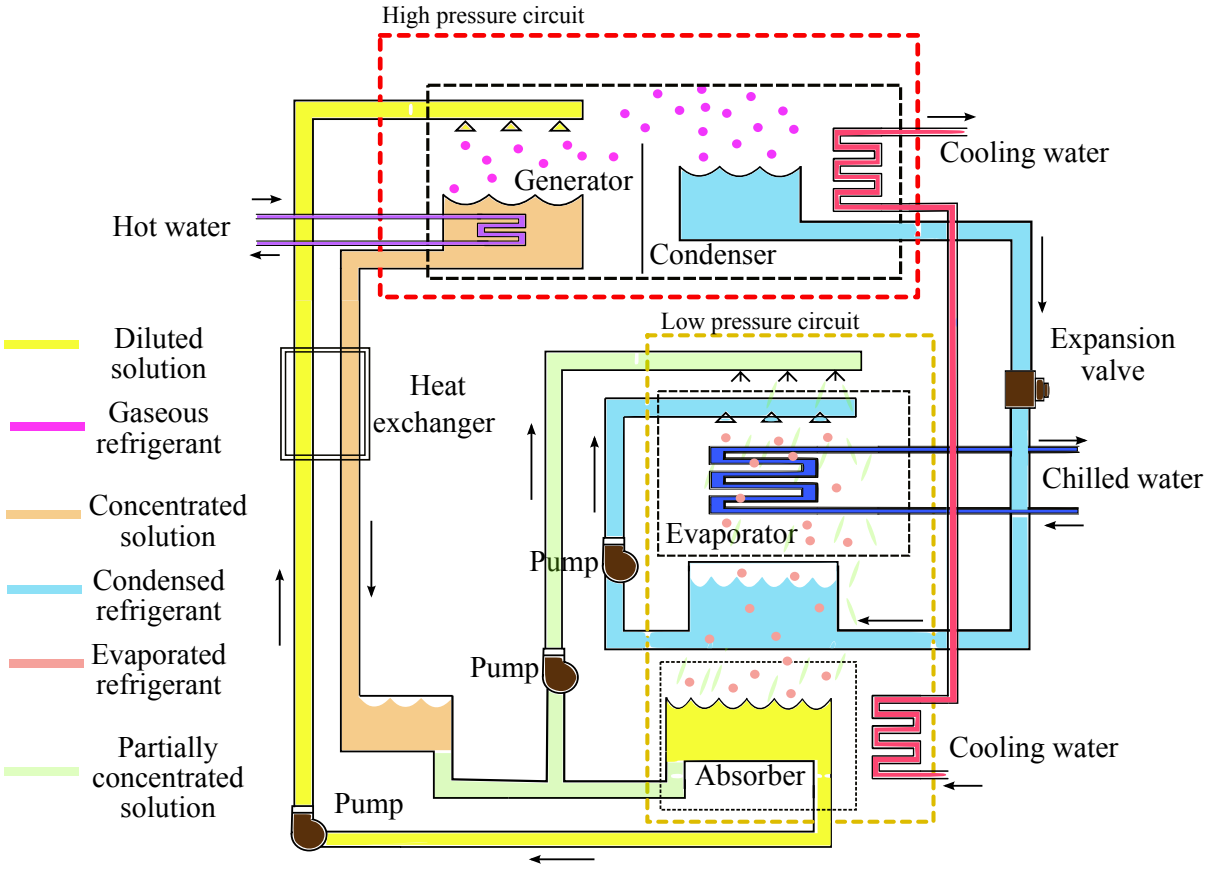

Figure 3.3: The absorption cycle.

Absorber: A mixture of concentrated and diluted solution (the partially concentrated solution) is pumped out from the bottom of the absorber to the absorber sprays which leads to a better

heat transfer between chilled water and refrigerant/absorbent. At this stage, the refrigerant vapor is pulled into the partially concentrated solution which is the absorption effect. As the refrigerant vapor is absorbed, it changes from vapor to liquid state and it transfers heat to the cooling water that circulates through the coils. In addition, the mixture of concentrated and diluted solution is required to avoid the crystallization of the lithium-bromide compound. After the refrigerant is absorbed in the partially concentrated solution, this becomes again a diluted solution. Finally, the absorption cycle restarts pumping out the diluted solution to the generator.

A heat exchanger is used between the high and low pressure circuit. The concentrated solution coming from the generator towards the absorber transfers heat to the diluted solution coming from the absorber towards the generator. This energy exchange preheats the diluted solution before entering into the generator saving the heat required to separate the refrigerant from the solution. On the other hand, the heat exchanger precools the concentrated solution flowing to the absorber which leads to a lower cooling water flow rate required to reject the heat produced in the absorption process.

3.2 The solar absorption cooling installation

3.2.1 Presentation

Figure 3.4 depicts one of the most common structures of solar absorption cooling systems (see e.g. Zhai et al. (2011); Yin et al. (2012); Lecuona et al. (2009)). The main components of the installation are: solar collector panel, heat exchanger, storage tank, absorption chiller, cooling tower and the conditioned building. This structure only provides cooling energy to the building. Other solar installations (see e.g. (ASHRAE, 2007)) are designed to distribute both heating and cooling to the building.

Flat-plate and evacuated-tube collector panels are used to concentrate solar energy which is transfered to a fluid (water or an antifreeze such as propylene glycol) that circulates in the tubes of the panel. The heat is then transfered to a water storage tank directly or using a heat exchanger as in Figure 3.4.

A stratified storage tank is used to provide the suitable hot water temperature value to the absorption chiller high pressure circuit. In a naturally stratified storage tank, buoyancy forces created by temperature dependent density differences maintain the separation between warm and cool volumes of liquid across a thin thermal transition region (thermocline). Flow into and out of a stratified tank occurs through diffusers at the top and bottom of the tank (Bahnfleth and Song, 2005). Hot water coming from the heat exchanger enters at the top of the tank and circulates towards the chiller. Return chiller hot water enters at the bottom of the tank

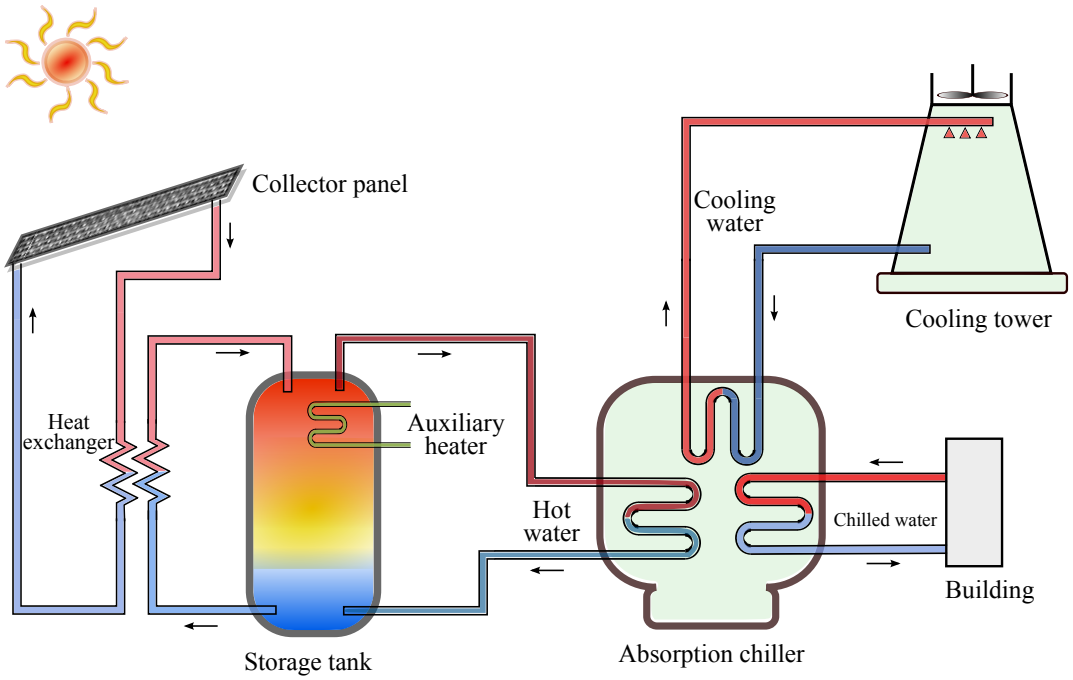

Figure 3.4: Solar cooling system.

and circulates towards the heat exchanger. An auxiliary electric heater is located at the top of the storage tank in order to provide the required hot water to the absorption chiller when the solar radiation is low.

The process of heating the top layer of the stratified storage tank by using the water coming from the heat exchanger is referred as the loading state. At this stage, cold water is taken out of the very bottom layer of the tank, pumped through the heat exchanger and introduced back up, into the very top layer of the tank. A second operational mode is the tapping state where the heated water is taken from the top fluid layer, while an equal amount of cold water (coming from the chiller) is introduced at the bottom part of the tank. Thus, the vessel is always entirely filled with water. During the idle state where there is no loading and tapping, the hot water in the storage vessel gradually cools down due to losses through the wall. These operational modes reflect the discrete event dynamics of the storage tank where the transition from one discrete state to another is caused by a tapping event or by respective control actions, i.e. switching the electric heater on or off (Kreuzinger et al., 2008). According to Eynard et al. (2012), the tank dynamics can also be described using two modes: energy storage and energy release modes.

As it can be seen in Figure 3.4, the absorption chiller has three water sources: hot water to separate the refrigerant from the solution in the generator, cooling water to reject heat from the condenser and absorber, and chilled water to distribute it to the conditioned space.

Commonly, a cooling tower is used to circulate the water for heat rejection. The cooling water coming from the chiller, which already has absorbed the heat from the absorption cycle, enters the cooling tower and it is distributed over the unit. By circulating air through the unit, a small portion of the cooling water is evaporated causing the heat rejection from the remaining water. The cooler water is collected in a basin located at the bottom of the tower and it is sent back to the chiller.

The chilled water that has absorbed the heat from the conditioned space is sent back to the chiller evaporator. Because of the pressure change in the evaporator, the circulating refrigerant absorbs the heat from the returned chilled water which causes a temperature drop. The cooler water is then recirculated to the building.

3.2.2 Impact of the sizing of components on the absorption cooling system performance and efficiency

Compared with the vapor-compression cycle based cooling system, absorption cooling systems have lower efficiency and high initial cost. In addition, to improve energy efficiency, they need a thermodynamic analysis as well as subsequent optimization of the parameters (Moreno et al., 2010). According to several studies reported in the literature, the efficiency improvement of solar cooling installations can be carried out by experimental tests analysis. For instance, Ali et al. (2008) reported the performance assessment of an integrated cooling plant with combined free cooling and solar powered single-effect lithium bromide-water absorption chiller based on experimental tests during five years of operation of the cooling installation which is fully automated, controlled and monitored. The plant has been additionally operated in connection to a building heating system in order to use excess solar heat for heating purposes and to utilize the available hot water of the building heating system as a supplementary source when the solar collector supply heat is not high enough to drive the chiller during cooling season.

Through these experimental tests, it is observed that one of the factors that affects the installation efficiency is the sizing of the components (collector field size, collector angle orientation, storage tank volume, etc.). A method to select the optimal key parameters for a solar installation (volume of the storage tank, slope and area of the collector panel) is investigated by Hang et al. (2013). The authors proposed a strategy that involves a central composite design (CCD) that is used to select the significant experimental data generated by energy system simulation and life cycle analysis. Besides, linear regression models are used to predict the functional relationship between system performance and the key system parameters using data sets. A multi-objective optimization model is solved based on the weighted Tchebycheff metric approach. The authors claimed that the proposed strategy simplified the design pro-

cess and it provided a fast and convenient design tool to assist in the design of solar absorption cooling and heating systems. Similar studies are investigated by Kulkarni et al. (2007) and Zhao et al. (2011).

Other analysis strategies have been considered in order to assess the size impact of the solar cooling system components. Several studies in the literature (de Guadalfajara et al., 2012; Assilzadeh et al., 2005; Monné et al., 2011; Tsoutsos et al., 2010; Palacín et al., 2011) have considered simulation tools like the TRNSYS thermal simulation program (TRNSYS17-Documentation, 2012) to evaluate the performance of solar cooling installations. Florides et al. (2002) investigated the modeling, simulation and warming impact assessment of a domestic-size absorption cooling system. A thermostat is used in order to control the flow to the solar collectors allowing the fluid to circulate only when the temperature of the fluid that circulates from the collectors to the storage tank is higher than that of the fluid delivered to the load. Another thermostat controls a back-up boiler in order to maintain the temperature of the fluid delivered to the load above a given set-point value. The optimization of the system is done by adjusting the various factors affecting the performance of the system: the collector slope angle, storage tank size and collector area. Eicker and Pietruschka (2009) and Martínez et al. (2012) also reported the use of TRNSYS to evaluate the energetic and economic performances of the solar cooling system and to carry out statistical studies about the influence of the design parameters in the performance of the entire cooling system.

Two main influential components are identified: collector panel area and storage tank volume. Jabbour (2011) investigated the conception and parameter optimization of a multi-source multi-function solar system for heating, cooling and production of domestic hot water. Two optimization algorithms for the sizing of the parameters are tested: the first one is based on the design of experiments (OptDOE) and the second one is a hybrid optimization algorithm. The author concluded that the OptDOE algorithm has shown good results as the optimal values calculated are close to the parametric runs carried out. Another study is presented Hang et al. (2011) where the same parameters are varied in order to optimize the installation based on a decision-making process according to the TRNSYS simulations results. Solar fraction, cost savings, and life cycle carbon dioxide reduction are the three indicators taken into account for the energetic, economic, and environmental performances, respectively. Similar studies are presented by Sayadi et al. (2013), Rosiek and Batlles (2009), Rosiek and Batlles (2012) and Praene et al. (2011).

3.2.3 Operating conditions of the solar absorption cooling system

Besides the need for an adequate sizing of the parameters, the studies previously reported agree that it is necessary to maintain a fixed set-point temperature in the collector panel in order

to operate the absorption cooling unit. Another condition is necessary: the circulating fluid temperature from the collectors to the storage tank must be higher than the fluid temperature delivered to the load. Other control strategies consider the tank bottom water temperature as the lower bound of the collector outlet temperature. For instance, a solar-assisted heating and cooling system based on evacuated solar collectors and a single-stage absorption chiller has been studied (Calise, 2010; Calise et al., 2010, 2011). Auxiliary energy for both heating and cooling is supplied by an electric-driven reversible heat pump. The control strategy of the system consists of shutting down the pump in the solar loop when the solar collector field outlet temperature is lower than the tank bottom water temperature. When the solar collector outlet temperature is higher than the water temperature at the bottom of tank, the controller varies the pump speed in the solar loop in order to achieve the fixed set point temperature at the solar collector outlet. In case of scarce irradiation, the pump flow rate is reduced; when solar irradiation is high, the pump flow is increased up to its maximum value. The absorption chiller is controlled by on/off hysteresis controllers which monitor the tank top temperature and shut down the machine when such value falls down, in order to prevent its operation at low capacity and efficiency. The cooling tower is managed by a proportional controller which modules the fan air flow according to its water inlet temperature.

From these studies it can be noticed that absorption cooling systems need an auxiliary heat source due to the solar radiation uncertainty. For instance, Florides et al. (2002) reported the use of a boiler when the required temperature condition for the absorption unit is not satisfied. Experimental results of a solar/gas cooling plant are presented by Bermejo et al. (2010). The installation is composed of a double-effect chiller powered by linear concentrating collectors and direct-fired natural gas burner. The operating conditions of the system such as, temperature and flow rate, are not constant, due to the variation of the solar radiation throughout the day. Therefore, the thermal power used to estimate the solar collector efficiency and the COP of the chiller cannot be directly calculated. Logic rules are considered to control the system: if the temperature of the solar collector surface exceeds the maximum operating temperature, the collector tracking system is shut down for security reasons. The study reported weak points of the plant: solar collector size, heat losses in the pipeline overnight, climatic conditions and lost vacuum in the absorption chiller evaporator. Other studies (Calise, 2010; Calise et al., 2010, 2011) used an electric-driven reversible heat pump as auxiliary source.

In addition, variations in solar radiation cause efficiency loss in the absorption chiller. For instance, a study carried out by González-Gil et al. (2011) investigated a direct air-cooled single-effect LiBr-H2O absorption prototype for solar cooling applications. The authors claimed that fluctuations in the chiller COP and generator mass flow could be reduced using advanced control strategies. Other problems such as the drop in the generator inlet temperature due to a

weak solar radiation are reported. Then, an auxiliary heat source helps to maintain absorption chiller efficiency by maintaining the inlet temperature in the generator circuit within its fixed set-point values.

Even if auxiliary energy source is required, it has been found in the literature that absorption cooling technologies are an alternative to reduce electricity consumption and CO_2 emissions. For instance, Balghouthi et al. (2012) assessed the performance of an absorption solar cooling installation in Tunisia. The pilot plant was tested using water and oil separately as heat transfer mediums. The installation is operated and controlled both automatically and manually. The studies have shown that even by using an auxiliary gas burner backup heater for the chiller operation, the CO_2 emissions are minor compared with compression air conditioning systems.

However, auxiliary heat source needs a permanent surveillance and control. In solar absorption systems using electric energy as the auxiliary source, electric consumption can be higher than cooling energy produced. For this reason, absorption chillers become attractive when the auxiliary source comes from cost-free energy as waste heat. A solar cooling installation controlled by logic rules is studied by Marc et al. (2010). Only the distribution loop which corresponds to the building-chilled water circuit part, is controlled by a PID rule. The experimental results concluded that electrical consumption is high with regard to refrigerating production. The authors suggested that the functioning period of each main energy-consuming component should be optimized to reduce electrical consumption. Another proposed solution is to set up a controller on the cooling tower fan which would be driven by the outlet condenser water temperature.

Furthermore, collector panel and storage tank temperatures may result in a risk for the installation security and efficiency if they are too high. Overheating may occur during periods of high isolation and low load, all portions of the solar energy system require protection against overheating. The system can be protected from overheating by (1) stopping circulation in the collection loop until storage temperature decreases, (2) discharging overheated water from the system and replacing it with cold makeup water, or (3) using a heat exchanger coil as a means of heat rejection to ambient air (ASHRAE, 2008).

According to the literature, differential temperature controllers are used to maintain the collector outlet water temperature between its limits. It must be recalled that if this temperature is below the temperature of the water delivered to the chiller or, in some cases, below the temperature of the water coming from the tank bottom layer towards the collector, the absorption chiller cannot operate properly. The solar air-conditioning system presented by Ortiz et al. (2010) is controlled via a variable frequency drive that manipulates the pumps in the

loops between collector panel and heat exchanger. Besides, chilled water and hot water flow temperatures are controlled through a three-way bypass valve that receives input from an internal microprocessor. The simulation results have shown that in some typical days, the collector outflow temperature exceeds the fixed maximum temperature. The authors stated that it is caused by physical limitations of the equipment.

As easily seen by previous studies, the temperature conditions required for the adequate operation of the installation can be mainly respected by the control of: water temperature in the solar loop (by manipulating the pumps between collector panel and heat exchanger/storage tank) and water temperature in the absorption cooling unit circuits (generator, evaporator, condenser and absorber).

Furthermore, according to Florides et al. (2002), in order to deliver the desired chilled water temperature to the final user, the absorption unit requires a control system that guarantees:

- An adequate level of the solutions and water in the various circuits of the unit and consequently, to maintain the LiBr-water percentages within the specific limits.
- An adequate pressure level in the generator by adjusting the heat input not to exceed the designed maximum capacity.
- An adequate pressure level in the absorber by adjusting the flow of cooling water in the absorber heat exchanger.

This control requirements can be achieved by applying different control strategies: the first one is to adjust the hot water inlet temperature controlling the outlet chiller water temperature, the second one is to control the inlet cooling water temperature maintaining the hot water inlet temperature constant. The third one is to adjust hot and cooling water simultaneously and finally, to adjust the chiller flow rates if it is allowed by manufacturing design (Labus et al., 2012). For instance, different control strategies have been tested by Bujedo et al. (2011) on an experimental solar air conditioning plant. The first one concerns a conventional fixed mass flow rate control strategy where the absorption chiller is operated at full load and the mass flow rate in the solar loop pumps is constant. In the second strategy, the inlet chiller condenser temperatures are adapted according to the generator water flow rate. The third one adapts the condenser temperature and the generator mass flow rate as a function of the system loads. Some system issues have been observed: the chiller capacities and demands should be correlated, the production and demand should be coincident in time and the control of the generator mass flow rate should be done using variable flow pumps instead of three-way valves in order to maintain the stratification of storage tanks.

Recapitulation

From the previous section, it has been found that several conditions should be respected in order to maintain the adequate performance and efficiency of the absorption cooling installation. These conditions are summarized as follows:

- Solar collector outflow temperature must be greater than a fixed set-point temperature which depends on the temperature of the water delivered to the load or on the temperature of the water flowing from the storage tank towards the collector.
- Solar collector outflow temperature must not exceed a fixed limit. This limit can be determined according to local conditions as stagnation temperature or pressure levels.
- Chiller must be shut down if the heat source, that is, collector and tank components, does not provide the required inlet temperature in order to prevent its operation at low capacity.
- Auxiliary energy is activated if solar radiation is weak.
- Hot water availability and cooling demand should be coincident. In addition, chiller power capacities and energy demands should be correlated.

Logic rule-based control approaches as differential temperature controllers or variable speed controllers have been considered to respect these conditions. Nevertheless, studies have proven that solar radiation is a major disturbance that influences the solar absorption cooling system and consequently, logic rule-based control approaches cannot easily manage and maintain the required operating conditions. Another factor that control strategies should take into account is the discrete event dynamics of the stratified storage tank. Finally, the cooling demand is variable since it depends on the occupancy rate and the kind of activity that is being carried out in the cooled space (Núñez-Reyes et al., 2005). All these issues cannot be easily managed by logic rule-based control approaches, which is why advanced control strategies are required to tackle the problem.

3.2.4 Advanced control strategies for solar absorption cooling systems

As mentioned in the previous section, logic rule-based control approaches like differential temperature controllers or variable speed controllers cannot properly satisfy the absorption cooling systems operating conditions. For this reason, it is imperative to search for advanced control strategies that guarantee these requirements and even more, maximize the efficiency of the installation. Model predictive control (MPC) (see e.g. Camacho and Bordons (2004))

is proven to be a useful framework to tackle the aforementioned issues of solar cooling plants due to its ability to handle constraints, multi-objective optimization functions, linear and nonlinear dynamics. The basic principle of this approach is to calculate the system future control inputs over a fixed horizon by minimizing a cost function. A model of the system is required as well as an adequate prediction of disturbances.

From the aforementioned solar absorption cooling system requirements, it can be seen that several control objectives are involved. For example, the installations must reduce the auxiliary heat source; collector, chiller and tank temperature conditions must be respected, or electricity cost must be minimized. All these objectives can be naturally translated into a multi-objective optimization problem that can be handled using MPC approaches. For instance, Prud'homme and Gillet (2001) presented a predictive control strategy for a solar domestic hot water system composed of a collector field and a stratified storage tank with multiple auxiliary heaters. The control objective is to minimize the electricity consumption while keeping the temperature of the tank outlet water as close as possible to the desired one and the maximization of the user's comfort and solar energy storage. The manipulated variables are: the flow rate in the collector loop and the power supply of each electrical element. The flow rate can continuously vary whereas the power supplies can (depending on the configuration chosen) either take discrete values or continuously vary between bounds.

Another multi-objective MPC approach is investigated by Al-Alili et al. (2010). They studied a solar cooling installation simulated in TRNSYS optimizing its performance and cost using different MATLAB algorithms. Two separate single objective optimization problems are formulated: the first one minimizes the electrical consumption of the electrical heater and the second one minimizes the total cost (which is divided into the initial capital cost and operating cost) of the system. Different MATLAB optimization algorithms (*fminsearch*, Pattern Search (PS) and genetic algorithm (GA)) which do not require knowledge about the gradient of the objective function are tested for each of the single optimization problems. Another approach simultaneously optimizes the two single objective functions using a MATLAB genetic algorithm. The results have shown that cost savings and heater consumption reduction are achieved with respect to the baseline system. Another study is presented by Labus et al. (2012) using an artificial neural network (ANN) model based on experimental data combined with a GA. The objective of the control strategy is the minimization of the energy consumption by maximizing the chiller COP value. The results have shown that the GA/ANN approach saved around 10 % of heat compared with a conventional control scheme.

In addition, since absorption cooling systems are driven by two sources: solar radiation and at least one auxiliary source like gas or electricity, control strategies need for a coordinated decision-making process that guarantees the optimal use of the energy sources. To achieve

this, some MPC strategies have been reported. For example, Salazar et al. (2013) proposed a predictive control for a solar/gas air-conditioning system that optimizes the operational costs of the plant taking into account the costs of gas heating and electricity. The aim of the controller is to maintain the inlet temperature of the absorption machine in a desired range while minimizing the gas and electrical consumption. The study concentrates on the optimal operation of the hot water subsystem, which is composed of: a solar collector field, an on/off gas heater, and a storage tank. The MPC problem corresponds to a constrained mixed integer optimization due to the discrete and continuous decisions that have to be taken: the gas heater is switched on/off and position and speed in pumps and valves are continuously controlled.

A MPC strategy to optimize energy management in a multi-source air conditioning plant is presented by Menchinelli and Bemporad (2008). In this air conditioning plant, the cooling circuit is supplied by different sources: collector panels, storage tank, auxiliary gas heater or a combination of them. The control strategy consists of a high-level supervisor that decides the optimal operating mode of the system. Low-level controllers are considered to adjust set-points and to ensure robust set-point tracking. The objectives of the control strategy are: to maintain the desired cooled water temperature, to minimize the heater gas consumption and to maximize the heat stored in the tank (which directly contributes to the minimization of the use of auxiliary energy). Compared with fixed rules approaches, the authors claimed that on-line optimization gives more degree of freedom in selecting the best operating mode. They also affirmed that it may be interesting for this kind of systems to adaptively change the parameters of the controller according to weather changes.

Another multi-source cooling plant is investigated by Rodríguez et al. (2008). As the cooling plant studied by Menchinelli and Bemporad (2008), a discrete decision-making process is necessary in order to drive the system either by solar or gas energy. The control objective is to minimize the use of gas and to maintain various variables close to their set-points. The control strategy is based on a model predictive control that deals with the discrete-continuous nature of the system. Consequently, the optimization problem becomes a Mixed Integer Nonlinear Problem (MINLP) but as the controller is tested on an experimental plant, an alternative to solve the control problem is developed. Instead of a MINLP optimization, a combination of nonlinear MPC and a based-insight controller is proposed.

Up to now, it has been seen that a coordination between the hot water storage system and the absorption chiller operating conditions is required. That is, the thermal energy storage element must provide at least the required amount of energy demanded by the absorption chiller. Therefore, lower limit conditions in the solar loop must be respected only if the chiller operates. Then, a multi-objective criterion is laid out to guarantee the solar-absorption loop

requirements. Nevertheless, a further work should be done regarding the final user. For instance, an Economic MPC for a solar-powered heating system is developed by Halvgaard et al. (2012). Unlike the traditional MPC strategy, Economic MPC is associated to an economic-related cost function; it optimizes the process operations in a time-varying fashion rather than maintaining the process variables around a few desired steady states (Tran et al., 2014). The control objective is to balance the solar collector energy and the heat consumption in a residential house minimizing the electricity cost used in auxiliary electric heaters. The storage tank is supplied by solar energy and electric elements if necessary. The authors reported that electricity cost savings of 25-30 % were found compared with current thermostat control strategy. Other MPC strategies are reported by Garcia-Gabin et al. (2009) and Zambrano and Garcia-Gabin (2008). In these studies, the multi-objective is related to the balance between the solar loop energy and the building heat consumption.

Another study that involves a multi-objective criterion between solar absorption system and final user is reported by Núñez-Reyes et al. (2005). The authors considered a MPC approach for temperature control in a solar cooling plant in Spain. The control objective is to supply chilled water to the building at the required temperature. Consequently, the chiller must work at the desired operating point by keeping the inlet water temperature at a given set-point. The chiller is driven by both solar and gas sources. The control strategy consists of a Generalized Predictive Control (GPC) using a Smith Predictor in order to improve the robustness of the closed loop system.

The previous studies have shown that other issues must be taken into consideration in the control of solar cooling absorption systems. Besides the coordination between the heat source part (that is, collector panel and storage tank) and the cooling system (absorption chiller), it is necessary to know the cooling consumption requirements of the conditioned space. Consequently, an entire energy management should be designed considering the individual operating conditions of the elements that in turn, have an influence on each other. In addition, the hybrid dynamics of the solar cooling system due to storage tank operating modes must be considered in the control strategy.

3.2.5 Summary: objectives, controlled and manipulated variables of the solar absorption cooling installation

From the aforementioned studies reported in the literature, the main control objectives of the solar absorption cooling installation can be summarized as follows:

In the hot water subsystem (solar collector panel and storage tank),

- To maximize the heat stored in the tank in order to minimize the use of the auxiliary

heat source (if this latter does not come from free-cost sources).

- To respect collector and tank temperature operating conditions.
- To minimize cost of the installation (initial cost, operating cost).

In the cooling energy consumption subsystem (absorption chiller and building),

- To maximize user's comfort.
- To fulfill chiller temperature operating conditions.
- To maximize chiller COP value.
- To deliver the desired chilled water temperature to the final user.
- To maintain the desired pressure levels in the low and high pressures circuits of the chiller.
- To maintain an adequate level of chemical solutions and water in the various circuits of the chiller.

Furthermore a global objective is to achieve a balance between the heat production and building energy consumption.

All these control objectives can be directly or indirectly achieved by controlling the following variables:

- Collector outflow temperature flowing towards the storage tank. Upper and lower limits depend on storage tank temperatures and physical operating conditions.
- Tank outflow temperature which depends on the chiller temperature requirements in the generator circuit.
- Temperatures in the low and high pressure circuits of the chiller.
- Level of the chiller chemical solutions.
- Chiller pressure levels.
- Interior temperature in the conditioned space.

Finally, the control of the aforementioned variables can be accomplished by manipulating the following:

- Water mass flow rates in the solar collector loop (by manipulating the circulation pumps).
- Auxiliary source power.
- Water mass flow rates in the low and high pressure circuits of the chiller only if it is allowed by manufacturing design. In low-power absorption chillers, the COP of the machine can be improved by controlling the temperature of the different water circuits within the corresponding designed limits as mass flow rate remains constant.
- Water mass flow rate and temperature delivered to the conditioned space.

Once the control requirements of the solar collector loop and absorption chiller are known, it is necessary to study the conditions to be fulfilled in the conditioned space. The following section presents the various control strategies that have been studied in the literature for thermal comfort in buildings.

3.3 MPC approaches for thermal comfort in buildings

So far, control strategies for solar cooling systems applied to thermal comfort in buildings has partly been addressed. The various studies cited in previous sections lay out the control of the solar cooling energy production part. This section focuses on MPC strategies that guarantee the indoor thermal comfort in buildings considering, in most cases, the cooling energy production as an available source whose use must be minimized.

The main task of air conditioning system controllers in buildings is to maintain the user's comfort in the conditioned space. At the same time, energy consumption has to be minimized. Nevertheless, energy savings must not affect the comfort during the occupied periods because the cost of people discomfort is much higher than the operational cost of the building (Hazyuk et al., 2014).

To guarantee user's thermal comfort, the controller has to deal with intermittent disturbances as: weather, appliances and occupants; which may lead to a constrained optimization problem (Oldewurtel et al., 2012). Furthermore, conventional control strategies as PID controllers are not suited for thermal comfort in the case of intermittent disturbances as the controller must react before the set-point change in order to ensure the comfort at the beginning of the occupancy period. In addition, these strategies do not guaranty minimal energy consumption because they are not really designed for this purpose (Hazyuk et al., 2012). In contrast, model predictive control is a powerful approach to tackle this problem due to its ability to handle constraints in an optimal control environment (Morosan et al., 2011).

The advantages of MPC strategies over standard control strategies as differential temperature or hysteresis controllers to handle building indoor temperature control have been reported in the literature. For instance, a predictive control approach for HVAC systems with ice cold thermal energy storage (TES) is presented by Beghi et al. (2014). Standard control strategies are compared with a Nonlinear Model Predictive Control (NLMPC) approach. The objective of the NLMPC approach is to design efficient control strategies for TES systems and to increase the performance of HVAC systems. The simulations results have shown that the MPC strategy provides the best control solution for this kind of systems. Another study comparison between MPC and conventional control strategies is presented by Wallace et al. (2012). A cascade control structure that uses identified linear models is developed. The authors concluded that the proposed control structure demonstrated better disturbance rejection ability in the zone air temperature than a PI-based cascade structure. Besides, the MPC has significantly demonstrated better tracking control with respect to conventional approaches while reducing the vapor-compression cycle energy requirements by 16 %.

In order to measure the occupant's comfort, a thermal sensation scale called as the predicted mean vote (PMV) index has been introduced. The closer to zero the PMV value, the better the user's comfort. Freire et al. (2008) presented a MPC strategy for indoor thermal comfort control using the PMV index to assess the performance of the controller. Energy consumption, indoor temperature and relative humidity control, are the key parameters considered in the control strategy. The authors concluded that the proposed algorithms can simultaneously achieve thermal comfort and energy consumption reduction. A related work regarding the use of PMV index for thermal control is presented by Garnier et al. (2014) where low-order models based on ANN have been developed to forecast the PMV index. The ANN-based models are used as internal models of the proposed predictive control structure.

Discrete events can also be found in buildings indoor temperature control. For example, Hu and Karava (2014) proposed a control strategy to find sequences of binary decisions for motorized windows. The proposed air conditioning installation for multi-zone building considers mixed-mode cooling which is composed of free cooling (natural air ventilation) and mechanical cooling systems. The study developed a progressive refinement optimization method according to a multi-level optimization topology and branch and bound decision trimming strategy.

Moreover, the area of Stochastic Model Predictive Control (SMPC) has been considered as an alternative to improve the performance in buildings indoor temperature control due to its ability to handle uncertainties. Oldewurtel et al. (2012) studied the control of HVAC systems, blind positioning and electric lighting of a building zone. The control strategy takes into account uncertainty in weather predictions. Compared with a deterministic model predictive

control approach, simulations results have shown that SMPC has a better performance in terms of energy savings and thermal comfort. According to the authors, the main limitation of the SMPC for building control is the added computational complexity.

The aforementioned studies are carried out considering a centralized MPC approach where the optimality of the controller can be proven. In large scale problems, centralized MPC schemes find the optimal solution for the plant-wide optimization problem, but they may not provide sufficient redundancy or reliability and can require substantial computation (Shah and MacGregor, 2005). Furthermore, centralized MPC is often unsuitable for control of complex systems, mainly due to the lack of scalability and to maintenance issues of global models (Bemporad et al., 2010) and it is usually infeasible due to the requirement of a formidable amount of information exchange (Mahmoud, 2011). A decentralized control strategy can avoid this latter problem but cannot guarantee optimality. In a decentralized MPC scheme, the target calculations are independently performed by ignoring interactions among units, and as a result, it will not usually find the optimal operation. In contrast to the centralized approach, a decentralized MPC provides a high degree of redundancy with respect to the failure of an individual MPC (Shah and MacGregor, 2005).

Chandan and Alleyne (2014) studied a decentralized predictive control strategy for thermal comfort in buildings. An output-feedback model predictive strategy based on a reduced order system representation is used. The output-feedback model predictive controller consists of a robust observer which can accommodate the lost measurement and a new state feedback model predictive controller fulfilling the input and state constraints (Li and Shi, 2013). Simulations results comparing the performance of the decentralized and centralized approach, have shown that the decentralized strategy achieves a balanced trade-off between performance and robustness.

Better optimality results can be achieved using Distributed Model Predictive Control (DMPC). This control strategy seems to be a suitable approach for managing energy distribution in buildings, particularly so when the number of control variables and signals from sensors and actuators rapidly grow with the number of HVAC systems (Scherer et al., 2014). DMPC based on Bender's decomposition for building temperature control is investigated by Morosan et al. (2011). In order to simplify the complexity of the optimization problem of the centralized control problem, the authors proposed a strategy based on the Bender's decomposition which is applied to a multi-source multi-zone temperature control. The simulation results have shown that the distributed strategy has a better performance compared with the centralized one regarding the computational time and the convergence speed. Other DMPC strategies are investigated by Alvarez et al. (2013), Scherer et al. (2014) and Morosan et al. (2010).

Hierarchical Model Predictive Control (HMPC) is another powerful approach for thermal control in buildings. The general principle of hierarchical control is to consider that the system to be controlled is decomposed into a number of interconnected subsystems. An optimization problem is solved for each of these subsystems and if the local solutions satisfy the constraints imposed by the interconnecting variables, the procedure is concluded. Otherwise, an iterative price coordination method is used: the coordinator sets the prices which are sent to the low level local optimizers which take them as given and recompute the optimal trajectories of the state, input and output variables over the considered prediction horizon. The iterations are stopped when the interconnecting variables satisfy the required coherence conditions (Scattolini, 2009).

Castilla et al. (2011) presented a HMPC strategy to achieve a trade-off between the use of the HVAC system and the user's comfort. The high level control computes the set-points of temperature, CO_2 level and illumination; the low level control system manipulates the actuators to reach these set-points. The high level controller of the HMPC approach investigated by Castilla et al. (2014) involves a nonlinear predictive controller which maintains the thermal comfort by optimizing the use of the HVAC system and the low level controller is composed of a PID with anti-windup function and it is responsible for reaching the set-points imposed by the high level controller. Ma et al. (2012) studied a HMPC strategy for building temperature control using a compressor vapor cycle chiller for cooling production. The high level MPC controls the cooling/heating system production and the low-level MPC is the building system control. Other related HMPC architectures for building temperature control are investigated by Domahidi et al. (2014), Ma et al. (2012) and Vana et al. (2014).

Even if in terms of constraints fulfillment MPC seems to be a suitable framework for thermal comfort control in buildings and solar cooling system control, there are some issues that cannot be ignored. MPC requires the knowledge of weather and occupancy profiles predictions, otherwise, the constraints fulfillment is not achieved. Then, stochastic MPC seems to be a suitable approach to tackle this problem. However, the product between air temperatures and mass flow rates (i.e. water flow pumps in the collector loop) leads to a non-convex MPC problem which might have distinct locally optimal solutions and many optimization solvers can only provide certificates of local optimality (Ma et al., 2012). Another issue is the computational complexity to solve the optimization problem from a practical point of view. Some alternatives to solve this issue is to consider learning rule-based controllers or to build a look-up table correlating parameters and states and solving the optimization problem off-line (Ma et al., 2012).

3.4 Conclusions

This chapter addressed the understanding of solar absorption units and the advantages of this kind of system over the vapor-compression cycle based ones. Besides, it has been identified the operating conditions of solar absorption cooling system, the impact of the sizing of the components and the control approaches that have been studied in the literature. There is a strong correlation between the solar collector loop and the cooling production part: the chiller efficiency depends on collector and heat exchanger temperature levels.

In addition, solar absorption cooling systems operation is subject to discrete events which are caused by loading, tapping and idle modes in the stratified storage tank which supplies hot water to the absorption chiller. This hybrid dynamics leads to a discrete decision-making process. Finally, the hot water circuit in the chiller generator may also involve a discrete behavior as inlet hot water flow rate may be limited to operate only at nominal values.

Efficiency improvement of solar absorption cooling systems becomes complex due to the strong influence of weather, hybrid nature, nonlinear dynamics and respect of temperature constraints. To tackle this problem, advanced control strategies as MPC have been investigated. Nevertheless, the entire problem is not solved since solar absorption cooling systems require the knowledge of cooling consumption requirements. The global efficiency of the installation cannot be maximized if the hot water production part is not correlated to the consumption part, which is the chiller that provides cooling energy to the building. Moreover, consumption demands can vary due to occupancy rate and kind of activity inside the building.

The main objectives of MPC approaches for solar cooling systems reported are: to ensure the respect of temperature operating conditions in the solar collector loop and storage tank in order to provide the required set-point temperature to the chiller; and the minimization of the auxiliary heat. These studies only consider the hot water production part and absorption chiller and do not include in the control scheme the constraints fulfillment of the space to be conditioned. On the other hand, most of the cited MPC approaches for thermal comfort in buildings only address the energy consumption part and consider the cooling/heating as an available source.

Then, in order to guarantee a global constraints fulfillment while minimizing the local objectives of production and consumption energy subsystems, a multi-objective control problem can be formulated. In addition, a coordination between energy production and consumption must be established in order to balance energy efficiency among the subsystems.

In the next chapter, the energy production-consumption control problem is stated. Taking into account the literature review about the operation and control of solar absorption cool-

ing systems in buildings, it presents under which conditions and assumptions the system management proposal is studied.

Chapter 4

Energy production-consumption problem statement

In the previous chapter, it has been shown that absorption cooling systems become attractive only when the heat source is cost-free as solar energy. According to the literature review, an adequate sizing of the components of the solar hot water storage (SHWS) system (solar collector panel, heat exchanger and storage tank) is required. An undersized installation can increase electricity consumption to ensure chiller temperature requirements.

The cooling production depends on the applied chiller control strategy. The absorption unit has a complex thermodynamic cycle where mass flow rates, low and high pressures, temperatures and solutions concentrations play an important role in its efficiency. Moreover, a proper control of the installation is needed since the driving source is intermittent and the energy demand can vary as a function of building occupancy periods.

This chapter focuses on the energy production-consumption problem statement. It presents how the energy production-consumption system is divided into two subsystems: the energy producer and one or more energy consumers. In this context, the SHWS system is seen as the energy producer and both the absorption chiller and the conditioned building are seen as one of the energy consumers. The proposed system partitioning allows the global control problem to be separately treated so that the control strategy design may be characterized by modularity and independence attributes and the complexity of the global control strategy may be minimized compared to the centralized control problem.

4.1 Motivation

In a centralized control strategy, all computations are based on the whole information about the plant. This means that the design problem is solved for a model that describes the process as a whole. In this case, the controller receives all sensor data available for a single unit that designs and applies the controller to the plant (Mahmoud, 2011).

There are several reasons why centralized control should be extended to more involved architectures (Lunze, 2014):

- If the structure of the plant changes, for example due to the appearance and the disappearance of subsystems during operation, it is reasonable to simultaneously change the structure of the controller. Architectures have to be used to provide the corresponding flexibility.
- The plant consists of independent subsystems that have their own control equipment and have to fulfill a common control goal. Then, the natural way is to associate the control algorithms with the local computing.
- The plant may be large and geographically distributed.

Hence, if the global control problem is partitioned in such a way that a controller is designed for each subsystem and where information exchange between these controllers (called from now on local controllers) may occur, the global control architecture is adaptable and has modularity. This means that the control architecture is flexible as the local controllers can be independently designed.

4.2 The solar absorption cooling system as part of an energy production-consumption system

This section focuses on the integration of the solar absorption cooling system as part of an energy production-consumption system. Figure 4.1 depicts the proposed structure where multiple users, called from now on the consumers, are connected to a heat production subsystem via a water distribution system. One of these consumers is the absorption chiller which provides chilled water to a building.

A suitable management of the system can be done by proposing a global control structure where the amount of heat production matches with the amount of total energy demanded by the users. That is, water temperature and flow rate delivered by the producer are adapted to the requirements of the multiple consumers. Then, this production-consumption management problem can be solved either by centralized or distributed control approaches. Nevertheless, this decision entails both strong interactions between the actors of the grid and, an important optimization complexity.

This thesis proposes an alternative high level management of the system which facilitates the integration of a modular control and where interactions between the subsystems are lighten. Furthermore, the proposed management contributes to the global control problem

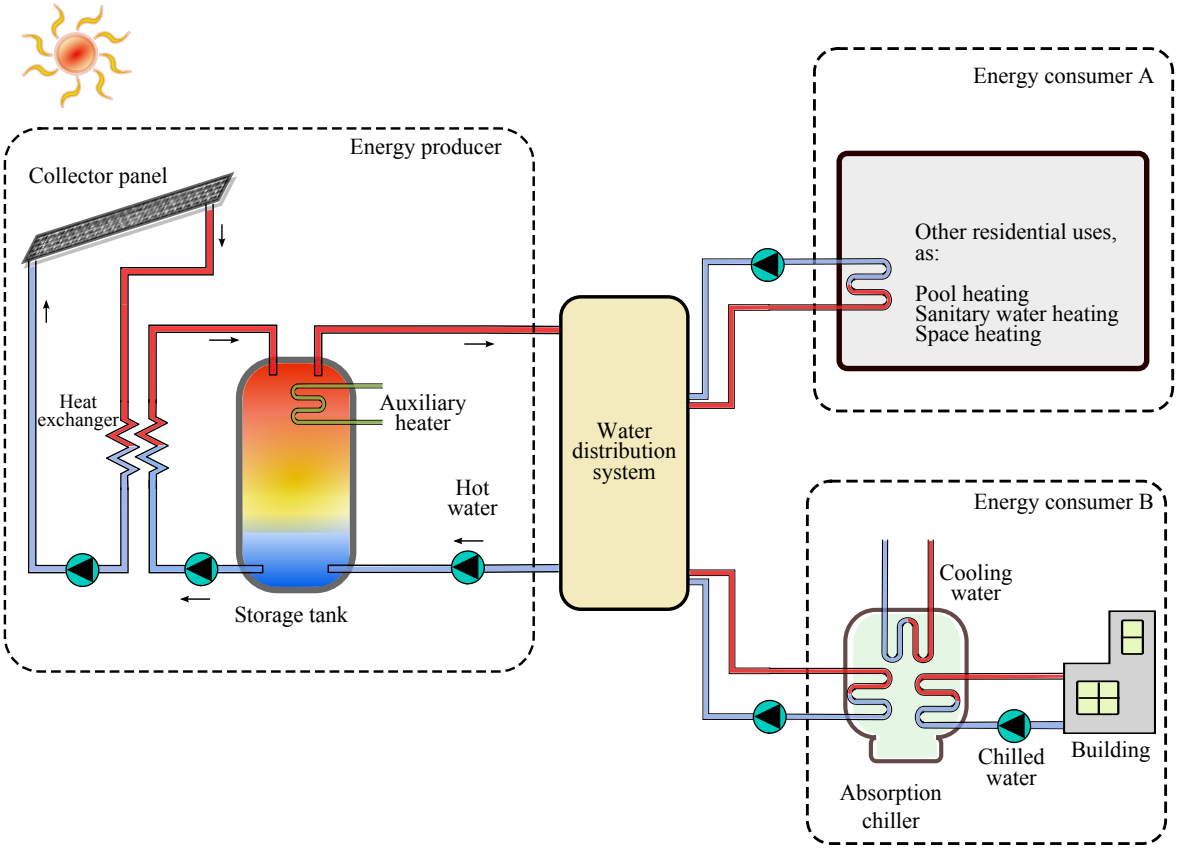

Figure 4.1: Energy production-consumption system.

simplification. In this conception, the energy producer is seen as a central source which provides hot water at a committed temperature when one or more consumers need it. This allows the producer controller to be designed regardless of the consumer controllers design. At the same time, consumer controllers design is based on the assumption that there is a hot water source available when it is required.

Moreover, the proposed system management requires interaction mechanisms between producer and consumers in order to minimize the degradation of the optimal solution which could be accomplished using a centralized approach. However, interaction mechanisms of the proposed approach remain simple as interactions between consumers are not required.

4.2.1 The energy producer

The energy producer is composed of a solar collector panel, a heat exchanger, and a stratified storage tank. An auxiliary electric source is placed at the very top layer of the storage tank in order to supply heat to the consumers in case solar energy is not strong enough. No additional task is aggregated to the solar installation (heating or domestic water use). The objective

of this subsystem is to provide hot water to the consumers taking into account the following characteristics:

- The outlet hot water flowing towards the consumers is distributed at a committed temperature in case of a consumer demand.
- Portions of the solar energy system are exposed to weather conditions, so they must be protected from freezing and from overheating caused by high isolation levels during periods of low energy demand (Kalogirou, 2004).
- Storage tank operation is characterized by a discrete decision-making process: various operation modes are established as a function of the tank inlet/outlet water direction. An example of these operating modes is presented by Kreuzinger et al. (2008).
- A proper control is required in order to maximize the solar energy use and to minimize the auxiliary electric source.

Controlled variables: Collector, heat exchanger and storage tank temperatures should be controlled in order to ensure protection to the system and to guarantee the required hot water temperature distributed to the consumers.

Manipulated variables: The maximum and minimum temperature limits can be respected by manipulating the water flow of the circulation pumps and the amount of auxiliary energy delivered by the electric heater.

Disturbances: The energy producer is subject not only to weather conditions but also to the consumers energy demand.

A mathematical representation of the energy producer can be developed from the collector panel, heat exchanger and storage tank models. The storage tank model can be represented by a time-varying nonlinear model described by differential equations and discrete events related to the operating modes. Some storage tank models are studied by Jabbour (2011), Kreuzinger et al. (2008), Li et al. (2013) and Steinert et al. (2013). As a result, the energy producer is represented by a nonlinear hybrid model. The hybrid nature is due to the tank operating modes. Furthermore, it is assumed that the pumps flow rate and the auxiliary electric heater are continuously manipulated (smooth behavior).

For the remaining components (collector panel and heat exchanger), the steady-state models presented by the simulation tool TRNSYS (TRNSYS17-Documentation, 2012) are used. The collector model developed by Duffie and Beckman (1974) assumes that thermal capacitances are neglected and a single value of collector overall heat loss coefficient is considered, which

depends on the collector characteristics (geometry, mass flow rate, efficiency itself, etc.), average plate temperature and external conditions (Tagliafico et al., 2014). This model predicts the instantaneous performance of the component based on the collector manufacturer's data (Rodríguez-Hidalgo et al., 2012). The heat exchanger is modeled considering that the maximum possible heat transfer rate is calculated based on the minimum capacity rate fluid and the cold and hot side fluid inlet temperatures (TRNSYS17-Documentation, 2012). Besides, the heat exchanger effectiveness is constant and it is provided as a model parameter.

4.2.2 The energy consumer

In order to illustrate the proposed management of the consumption-production system, one type of energy consumer has been chosen within the possible users: an absorption chiller that supplies chilled water to a building using a radiant ceiling. Then, the studied system can account for one or more chiller-building subsystems. These absorption cooling systems only work in summer. A small-sized building and a generic low-capacity chiller are considered for the study.

The aim of this study is not focused on the control and modeling of the absorption machine. It has been mentioned in the previous chapter that a proper control of the machine is needed in order to maximize the COP which is lower than vapor-compression cycle-based cooling units. The efficiency of the chiller is a result of the solution concentrations, water temperatures and flow rates values of the high and low pressure circuits. A control strategy that takes into account all theses variables is beyond the scope of this research.

The objective of this research is to develop a control strategy for the proper high level management of energy producer-consumer systems using MPC approaches as it is shown in the following chapters. For this reason, the computational time required for the optimization algorithms should be taken into account. Working with small sampling times (typically lower than five minutes) may give accurate control results but at the same time may lead to a significantly computational burden. The time constant for the case study allows to work with bigger sampling times (e.g. 0.5-1 hour) which may contribute to establish an adequate trade-off between computational burden and controller performance. From this assumption and taking into account that the absorption chiller can be characterized by a fast transient response compared to time constants in the order of 0.5-1 hour (e.g. the Rotartica chiller presented by Jabbour (2011) and Evola et al. (2013)), the transient dynamics of the machine is not included as part of the consumer model. Instead, a steady-state abstract model is used to characterize the energy transfered from the hot water source to the building.

As the dynamical model of the absorption chiller is not studied and as it has been said before, a proper control of the machine is not designed, it is supposed that the absorption chiller

operates at nominal capacity. This implies that inlet temperatures at generator, condenser and evaporator circuits are controlled at nominal values. Furthermore, another supposition is done concerning the heat rejection process. It is supposed that a well designed controller maintains the adequate water temperature to reject the heat produced in the condenser and absorber circuits.

As it has been shown by Anies (2011), Jabbour (2011) and Labus (2011), it is recommended that water flow rates in the different circuits of small capacity absorption machines be controlled at nominal values. Then, it is considered that the circulation pumps in the hot water and chiller water flow rates are manipulated at constant values.

Under these considerations, the controlled and manipulated variables of the chiller-building subsystem are:

Controlled variables: The aim of the control strategy for the chiller-building system is to maintain the indoor thermal comfort in the building during occupancy periods. The controlled variable is the building operative temperature.

Manipulated variables: Maintaining indoor thermal comfort is achieved by manipulation of the chilled water flow rate. As it is supposed that the chiller operates at nominal capacity with constant flow rates values, the only degree of freedom is the switch on/off of the chiller. Consequently, the manipulated variable is a discrete control signal that switches the chiller on/off. The water flow rates in the hot and chilled water circuits are obtained as the product of the binary control signal by the nominal flow rate values.

Disturbances: The energy consumer is subject to weather conditions (which influence the building operative temperature).

The mathematical representation of the energy consumer is an identified state-space linear model which involves the dynamics of the building and radiant ceiling. The transient response of the chiller is beyond the scope of this study. The identification procedure carried out in TRNSYS is detailed in Appendix C.

4.3 Conclusion

This chapter sets the conditions and assumptions of the problem studied in the following part of the thesis. The solar cooling system studied in the previous chapter is considered now as part of an energy production-consumption system where there is a producer which provides hot water to the consumers connected to a water distribution system.

Then, the collector panel, heat exchanger and storage tank are part of the energy producer. A mathematical representation of the system can be achieved using a nonlinear hybrid model

(as it is presented in Chapter 6). The hybrid dynamics is due to the tank operating modes. The energy producer has continuous control inputs representing the water flow rates of the circulation pumps.

The consumer studied in this thesis is an absorption chiller that supplies chilled water to a building. The mathematical representation of the system is an identified linear state-space model where the controlled variable is discrete and from which are calculated the hot and chilled water flow rates.

In the following chapter, a hybrid MPC strategy is developed for the management of an energy production-consumption system that involves three chiller-building subsystems. As the objective of the chapter is focused on the control strategy assessment, a simple linear model of the producer is used. This model is based on a power balance and represents a solar and electric energy storage unit.

Chapter 5

Predictive and interactive controllers for a producer-consumer system

The previous chapter presented the proposed energy production-consumption management which is characterized by a partitioning approach with one energy producer and several consumers. The energy producer is a solar hot water storage (SHWS) system which provides hot water at a committed temperature in case of a consumers demand. The case study for the energy consumer is composed of an absorption chiller which supplies chilled water to a building.

This chapter focuses on the development of a predictive control approach for the energy production-consumption management. It is based on predictive and interactive local controllers for both producer and consumers. First, each consumer controller solves an optimization problem (without interaction with the other consumers) and sends the best optimal solutions to the producer controller which computes an optimal solution according to the information provided by the consumers. In this approach, the control inputs applied to the consumers depend on the producer controller optimal solution. The term interactive refers to the communication mechanism established between producer and consumers.

First, this chapter presents the energy production-consumption system modeling. As the model is oriented to control, it is presented in discrete form and used for both prediction and simulation purposes. Then, the performance of a logic rule-based control approach is evaluated. Afterwards, the proposed predictive and interactive control approach is developed and compared with the logic rule-based control results. Finally, the conclusions of this chapter are provided.

5.1 The producer-consumer system

Figure 5.1 depicts the structure of the studied producer-consumer system. As mentioned earlier, the producer is a representation of the SHWS system whose control inputs $U_1(k)$

are the water flow rates in the circulation pumps and the auxiliary energy (which can be continuously controlled). The producer has a nonlinear hybrid dynamics. The nonlinear characteristic is due to the dependency between temperature and water flow rates circulating in the storage tank and the hybrid one is introduced by the tank operating modes. The energy consumer is represented by a dynamical system with a binary control input $U_2(k)$. The consumer control input represents the chiller switch on/off. Indeed, as stated in Chapter 4, the chiller is operated at nominal capacity and consequently it works at constant water flow rates and temperatures. The disturbances $D_1(k)$ and $D_2(k)$ represent the weather variables.

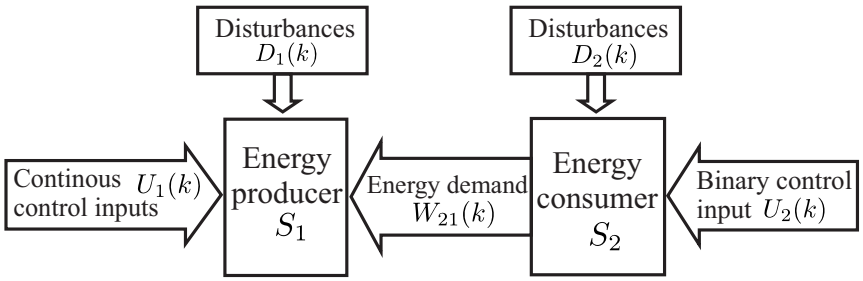

Figure 5.1: Structure of an energy producer-consumer system.

5.1.1 Generalized model

The energy producer S_1 is described by a hybrid nonlinear discrete model of the form

$$X_1(k+1) \quad = \quad f_{1\sigma(k)}(\overline{U}_1(k), W_{21}(k)) \tag{5.1.1}$$

$$\sigma(k) = \sigma(\overline{U}_1(k), W_{21}(k)) \tag{5.1.2}$$

where $\overline{U}_1(k) = [X_1(k), U_1(k), D_1(k)]$. The state vector of the system is $X_1(k) \in \mathbb{R}^{n_1}$. $U_1(k) \in \mathbb{R}^{m_1}$ is the vector of controlled variables and $D_1(k) \in \mathbb{R}^{p_1}$ is the vector of non-controlled inputs. $W_{21}(k) \in \mathbb{R}^{q_1}$ is the vector of interacting variables with the consumer S_2.

$\sigma(k)$ represents the switching mode that depends not only on the state but also on the controlled and uncontrolled variables. The number of modes is finite.

The producer S_1 is subject to output and input constraints given by

$$H_{1\sigma(k)}(\overline{U}_1(k), W_{21}(k)) \leq \mathbf{0} \tag{5.1.3}$$

Consequently, the producer S_1 is seen as a hybrid system with continuous control inputs subject to nonlinear constraints that depend on hybrid conditions.

The consumer S_2 is represented as

$$\begin{aligned} X_2(k+1) &= f_2(X_2(k), U_2(k), D_2(k)) && (5.1.4)\\ Y_2(k) &= H_2(X_2(k)) && (5.1.5)\\ W_{21}(k) &= G(X_2(k), U_2(k)) && (5.1.6) \end{aligned}$$

$X_2(k) \in \mathbb{R}^{n_2}$ is the state vector. $U_2(k) \in \{0, 1\}$ is the binary control variable and $D_2(k) \in \mathbb{R}^{p_2}$ is the vector of non-controlled inputs. $Y_2(k) \in \mathbb{R}^{r_2}$ is the output vector.

The consumer S_2 is subject input and output constraints given by

$$H_2(\overline{U}_2(k)) \leq \mathbf{0} \tag{5.1.7}$$

where $\overline{U}_2(k) = [X_2(k), U_2(k), D_2(k)]$. Then, the consumer S_2 is a hybrid system due to the discrete nature of its control input.

5.1.2 Simplified model

A representation of the system in Figure 5.1 is depicted in Figure 5.2 which is composed of one producer and a set of m consumers. In this structure, an abstraction of the SHWS system is used: a solar an electric energy storage element (ESE) whose model is based on a power balance. In addition, linear models are used for both producer and consumers. The i^{th} consumer is composed of a cooling production system (CPS) and a cooling consumption system (CCS). The i^{th} CPS and CCS represent the chiller and building respectively.

The energy stored $E(k)$ in the ESE is defined as a discrete model with continuous inputs as follows

$$E(k+1) = E(k) + \triangle t \quad (P_{sol}(k) + P_{elc}(k) - \sum_{i=1}^{m} P_{csm}^{(i)}(k)) \tag{5.1.8}$$

The storage power is given by

$$P_{ese}(k) = \frac{E(k) - E(k-1)}{t(k) - t(k-1)} \tag{5.1.9}$$

where $\triangle t = t(k) - t(k-1)$ is the sampling time period. The continuous inputs of the system are: the power related to solar gains $P_{sol}(k)$, the auxiliary electric power $P_{elc}(k)$ which is

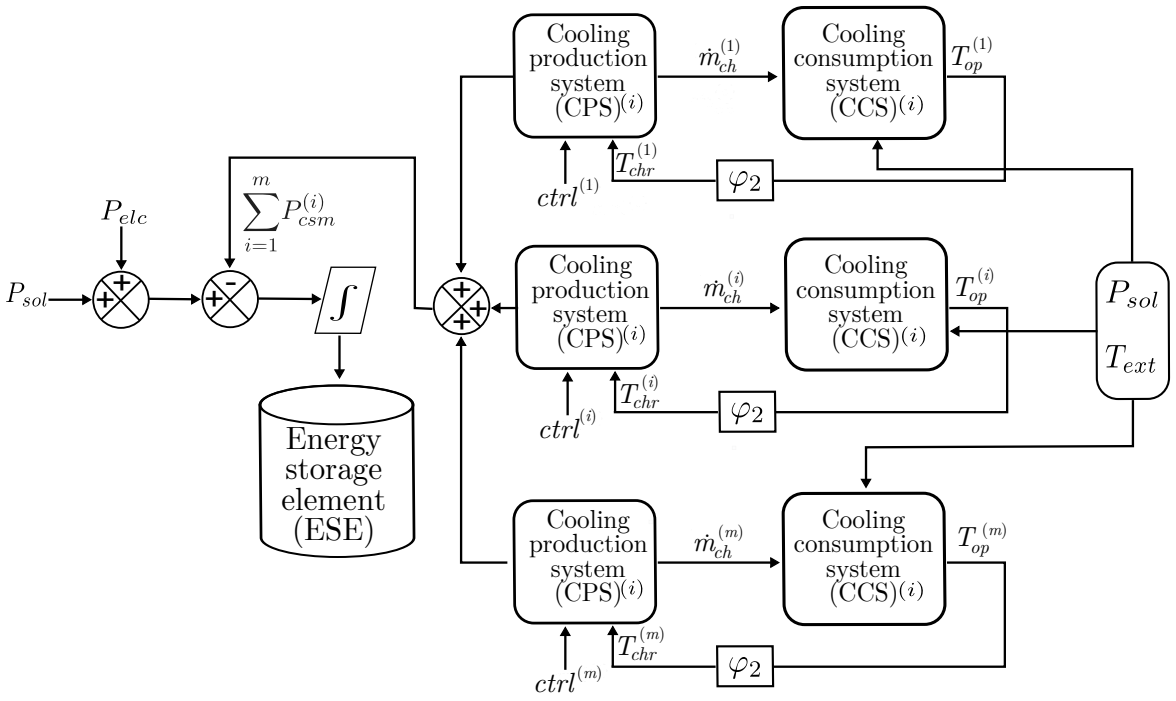

Figure 5.2: Simplified representation of an energy producer-consumer system.

necessary when there is no enough solar gains and the total power consumption of the m energy consumers $\sum_{i=1}^{m} P_{csm}^{(i)}$. Electric power $P_{elc}(k)$, energy stored $E(k)$ and storage power $P_{ese}(k)$ are subject to the following conditions

$$E(k) \geq E_{\min} \tag{5.1.10}$$

$$P_{ese,\min} \leq P_{ese}(k) \leq P_{ese,\max} \tag{5.1.11}$$

$$P_{elc,\min} \leq P_{elc}(k) \leq P_{elc,\max} \tag{5.1.12}$$

The i^{th} CPS depends on a binary control input $ctrl^{(i)}(k)$ and on the i^{th} CCS output $T_{op}^{(i)}(k)$. Consumption and cooling power are defined as follows

$$P_{coo}^{(i)}(k) = c\dot{m}_{ch}^{(i)}(k)(T_{chr}^{(i)}(k) - T_{chs}) \tag{5.1.13}$$

$$P_{csm}^{(i)}(k) = \frac{1}{\varsigma} P_{coo}^{(i)}(k) \tag{5.1.14}$$

where

$$\begin{aligned} T_{chr}^{(i)}(k) &= \varphi_2 T_{op}^{(i)}(k) && (5.1.15)\\ \dot{m}_{ch}^{(i)}(k) &= \varphi_1 ctrl^{(i)}(k) && (5.1.16)\\ ctrl^{(i)}(k) &\epsilon \{0,1\} && (5.1.17) \end{aligned}$$

where c, φ_1, φ_2 and ς are constants. c represents the chiller water specific heat. $\dot{m}_{ch}$ is the chilled water flow rate. T_{chr} is the chilled water return temperature which linearly depends on the building operative temperature $T_{op}^{(i)}(k)$. T_{chs} is the temperature of the chilled water supplied to the building which is considered constant and equal in each of the cooling production systems. A constant performance factor ς is introduced between cooling power $P_{coo}^{(i)}(k)$ and consumption power $P_{csm}^{(i)}(k)$ (Equation (5.1.14)).

Equation (5.1.14) can be rewritten as follows,

$$P_{csm}^{(i)} = (k_1 T_{op}^{(i)}(k) - k_2)\dot{m}_{ch}^{(i)}(k) \quad (5.1.18)$$

Where $k_1 = \frac{1}{\varsigma} c\varphi_2$, $k_2 = \frac{1}{\varsigma} cT_{chs}$ are constants.

The i^{th} CCS is represented by a linear state space model of the form

$$\begin{aligned} X_2^{(i)}(k+1) &= A^{(i)} X_2^{(i)}(k) + B^{(i)}\dot{m}_{ch}^{(i)}(k) + F^{(i)} D_2(k)\\ T_{op}^{(i)}(k) &= C^{(i)} X_2^{(i)}(k) && (5.1.19) \end{aligned}$$

where $X_2^{(i)}(k)$ is the state vector of the i^{th} CCS, $B^{(i)}$ is a vector, $A^{(i)}$, $C^{(i)}$ and $F^{(i)}$ are constant matrices, $\dot{m}_{ch}^{(i)}(k)$ is the discrete inlet water flow rate and $D_2(k) = [P_{sol}(k); T_{ext}(k)]$ is the vector of disturbances where $T_{ext}(k)$ is the exterior temperature. This model is identified using TRNSYS (more details are given in Appendix C).

The operative temperature of the i^{th} CCS is subject to the following constraint

$$T_{\min}^{(i)}(k) \leq T_{op}^{(i)}(k) \leq T_{\max}^{(i)}(k) \quad (5.1.20)$$

According to the notation presented in Section 5.1.1, Equations (5.1.8), (5.1.18) and (5.1.19) can be rewritten as

$$X_1(k+1) = X_1(k) + \triangle t(D_1(k) + U_1(k) - \sum_{i=1}^{m} W_{21}^{(i)}(k)) \quad (5.1.21)$$

$$X_2^{(i)}(k+1) = A^{(i)} X_2^{(i)}(k) + B^{(i)} \varphi_1 U_2^{(i)}(k) + F^{(i)} D_2(k) \quad (5.1.22)$$

$$Y_2^{(i)}(k) = C^{(i)} X_2^{(i)}(k) \quad (5.1.23)$$

$$W_{21}^{(i)}(k) = k_1 U_2^{(i)}(k) Y_2^{(i)}(k) - k_2 U_2^{(i)}(k) \quad (5.1.24)$$

subject to the following constraints

$$X_1(k) \geq X_{1\,\min} \quad (5.1.25)$$

$$U_{1\,\min} \leq U_1(k) \leq U_{1\,\max} \quad (5.1.26)$$

$$Y_{2\,\min}^{(i)}(k) \leq Y_2^{(i)}(k) \leq Y_{2\,\max}^{(i)}(k) \quad (5.1.27)$$

$$U_2^{(i)}(k)\ \epsilon\ \{0,1\} \quad (5.1.28)$$

where $X_1(k) = E(k)$, $D_1(k) = P_{sol}(k)$, $U_1(k) = P_{elc}(k)$, $W_{21}^{(i)}(k) = P_{csm}^{(i)}(k)$, $\varphi_1 U_2^{(i)}(k) = \dot{m}_{ch}^{(i)}(k)$ and $Y_2^{(i)}(k) = T_{op}^{(i)}(k)$.

The interacting variable $W_{21}^{(i)}(k)$ between the producer and consumers is related to the consumption power $P_{csm}^{(i)}(k)$ which depends on the binary water flow rate $U_2^{(i)}(k)$ and the consumer operative temperature $Y_2^{(i)}(k)$.

5.2 Logic rule-based control approach

In this section, a logic rule-based control strategy is developed for the producer-consumer system introduced in Section 5.1.2. The producer and consumers are controlled using on-off controllers.

- *Consumers hysteresis controller*: To fulfill the consumers constraint stated in Equation (5.1.27), a hysteresis controller designed for each of the consumers maintains the operative temperature $Y_2^{(i)}(k)$ as close as possible to a fixed set-point by switching the chiller on according to the following conditions:

  $U_2^{(i)}(k) = 1$ if $T_{op}^{(i)}(k) > Y_{2\,\max}^{(i)}(k)$ and $U_2^{(i)}(k-1) = 0$
  $U_2^{(i)}(k) = 1$ if $T_{op}^{(i)}(k) > Y_{2\,\min}^{(i)}(k)$ and $U_2^{(i)}(k-1) = 1$

  If these conditions are not satisfied, the chiller is switched off. The hysteresis controller computes the current control input $U_2^{(i)}(k)$ based on the past input $U_2^{(i)}(k-1)$. Then, the controller turns the chiller off when the temperature drops below the lower limit

$Y_{2\,\min}^{(i)}(k)$ and the chiller remains off until the operative temperature reaches the upper bound $Y_{2\,\max}^{(i)}(k)$.

- *Producer on-off controller*: The aim of this controller is to maintain the energy stored $X_1(k) > 0$ by switching the auxiliary electric heater on/off. At each sampling time, the controller evaluates if the future state $X_1(k+1)$ (Equation 5.1.21) is greater than zero by applying $U_1(k) = 0$ considering the current total consumers energy demand and the available solar power. If this is the case, the applied control input is $U_1(k) = 0$, otherwise the controller switches the heater on ($U_1(k) = 1$) to avoid the energy stored fall below zero.

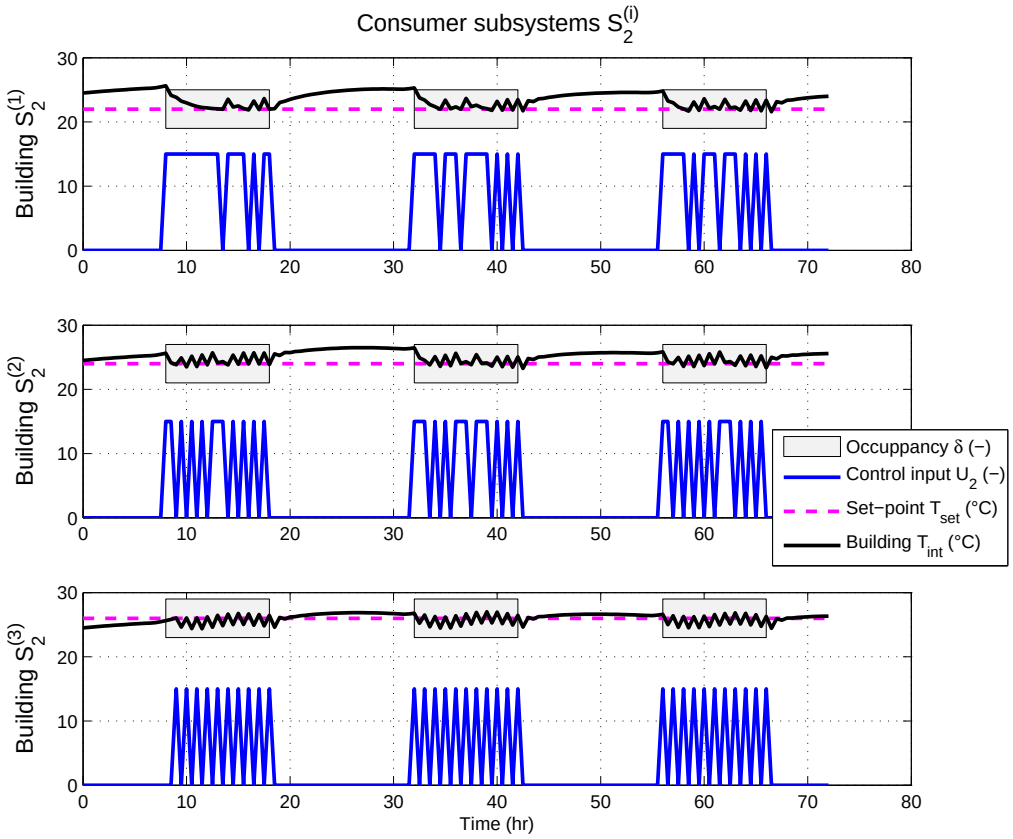

Figure 5.3: Consumer controllers performance.

Figures 5.3 and 5.4 depict the simulation results of the logic rule-based control strategy. The experiment is carried out during 72 hours with a sampling time of $t_k = 0.5$ hr. The i^{th} consumer is a simplified model of an absorption chiller which distributes chilled water to a building using a radiant ceiling (see Appendices A and C). When the auxiliary heater $U_1(k)$ is switched on, the power is delivered at 30 kW. As for the consumers control strategy, when the chiller operates, the water flow rate $\dot{m}_{ch}^{(i)}(k)$ remains constant at 700 kg/hr. The

operative temperature of buildings $S_2^{(1)}$, $S_2^{(2)}$ and $S_2^{(3)}$ are controlled at 22 °C, 24 °C and 26 °C respectively. Therefore, according to Equation (5.1.27), the upper $Y_{2\,\max}^{(i)}(k)$ and lower $Y_{2\,\min}^{(i)}(k)$ limits are equal to the corresponding set-point.

Figure 5.3 displays the operative temperature control of the buildings which is performed during the occupancy profile $\delta^i(k)$, from 8:00 up to 18:00 hrs. Outside this occupancy period, thermal comfort is no longer required. In terms of temperature control, the logic rule-based strategy ensures the requirements of each of the buildings with temperature fluctuations around the set-point lower than one degree. However, a large number of switch on/off events occur in building $S_2^{(3)}$ as lower chilled water is required to ensure the corresponding set-point temperature. From a practical point of view, switching the chiller on/off each 30 minutes is not desired. Therefore, a better control strategy can be achieved by focusing on the minimization of this behavior.

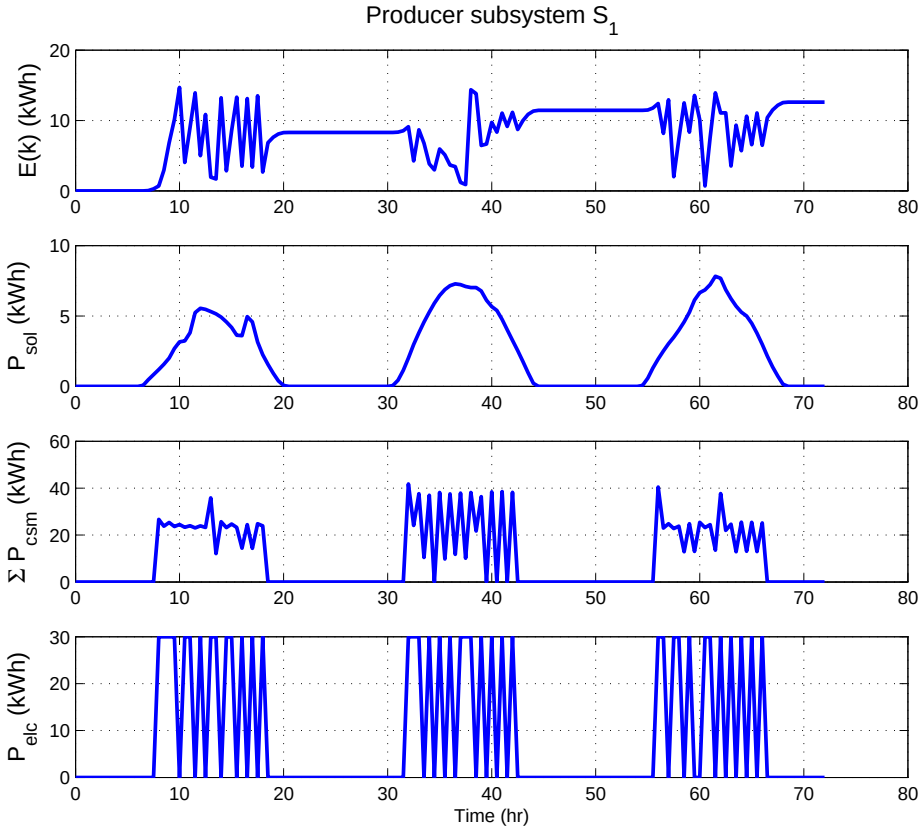

Figure 5.4: Producer performance.

As for the producer logic rule-based controller, the on/off behavior of the auxiliary energy $U_1(k)$ leads to an important energy consumption which can be avoided by implementing another control strategy based on continuous control signals that minimizes the energy consumption and at the same time, ensures the constraint fulfillment related to the stored energy.

5.3 Model predictive control approach

The logic rule-based control strategy presented in the previous section has shown an adequate performance in terms of building thermal comfort. However, some issues cannot be ignored, a large number of chiller switch on/off events and a significant auxiliary electricity consumption in the producer. This behavior can be at least minimized by seeking an alternative control strategy whose objectives are to guarantee building thermal comfort, to minimize the change of switch on/off events and to minimize the auxiliary electricity.

In this section, a model predictive control strategy for the simplified energy producer-consumer system presented in Section 5.1.2 is developed. The aim of this approach is to guarantee the aforementioned objectives using the system partitioning approach presented in Chapter 4. Then, the global control problem is solved using predictive controllers associated with each subsystem with an information exchange between producer and consumer controllers. Each of these predictive controllers is called local controller. First, the global problem of energy production-consumption is defined. Latter, the global problem is divided solving local optimization problems. To simplify the notation, given a prediction horizon N_h at step k, $x(\bar{k}) = \left[x(k)^T, \ldots, x(k+N_h-1)^T\right]^T$.

5.3.1 Global optimization problem: a multi-objective criterion

From the model stated in Equations (5.1.21-5.1.28), the control objectives are identified. The producer has two energy sources: solar and electric energy. The solar energy is considered as a disturbance since it is an external input that cannot be controlled. The other source is the auxiliary electric energy which instead can be controlled according to the availability of solar energy. As the electric energy use is translated into electric power consumption associated to a corresponding cost, it is necessary to minimize this energy as much as possible. Consequently, the control objective in the producer is to minimize the auxiliary electric energy $U_1(k)$. The objective function for this subsystem can be expressed as

$$J_1(U_1(\bar{k})) = \sum_{j=1}^{N_h} \|U_1(k+j-1)\|_d^d \tag{5.3.1}$$

where the notation $\|v\|_d^d$ refers to the ℓ^d-norm of vector v with exponent d.

As for the consumer, the control objectives are related to the energy consumption. Besides, the binary behavior of the control input $U_2^{(i)}(k)$ in Equation (5.1.28) imposes a restriction on the operating periods of the consumer. That is, during a given lapse of time, it is preferable to operate the energy consumer with as low as possible turn on/off events in order to avoid

damages in the subsystem and to improve its performance.

Thus, the objective of the consumer system can be translated into the optimization cost function as

$$J_2^{(i)}(U_2^{(i)}(\overline{k})) = \sum_{j=1}^{N_h} \Big[Q_1^{(i)} \left\| \triangle U_2^{(i)}(k+j-1) \right\|_d^d + Q_2^{(i)} \left\| U_2^{(i)}(k+j-1) \right\|_d^d + Q_3^{(i)} \delta^{(i)}(k+j) \left\| Y_2^{(i)}(k+j) - Y_r^{(i)}(k+j) \right\|_d^d \Big] \tag{5.3.2}$$

where $\triangle U_2^{(i)}(j) = U_2^{(i)}(j) - U_2^{(i)}(j-1)$ represents the change in the control input; a discrete variable is given by $\delta^{(i)}(k) \epsilon \{0,1\}$; and $Q_1^{(i)}$, $Q_2^{(i)}$ and $Q_3^{(i)}$ are weighting coefficients.

In order to minimize the complexity of the optimization problem, it can be seen from Equation (5.3.2) that the consumer constraint described in Equation (5.1.27) is introduced in the optimization criterion by adding a set-point variable $Y_r(k)^{(i)}$. The minimization of the difference between the consumer output $Y_2(k)^{(i)}$ and the desired output $Y_r(k)$ only takes place if the binary variable introduced $\delta^{(i)}$ is different from zero.

According to equations (5.3.1) and (5.3.2), the global problem of energy production-consumption can be stated as follows

$$J_G(U_1(\overline{k}), U_2^{(i)}(\overline{k})) = J_1(U_1(\overline{k})) + \sum_{i=1}^{m} J_2^{(i)}(U_2^{(i)}(\overline{k})) \tag{5.3.3}$$

Consequently, taking into account the output and input constraints stated in Equations (5.1.25-5.1.28), the global optimization problem can be formulated as follows

Optimization problem. At a time k and given the prediction horizon N_h, the current state of the subsystems ($X_1(k)$, $X_2^{(i)}(k), i = 1, ..., m$), the previous consumer control input $U_2^{(i)}(k-1), i = 1, ..., m$, and the prediction of the uncontrolled variables ($D_1(\overline{k})$, $D_2(\overline{k})$), the global optimization problem can be defined as

$$\min_{U_1(\overline{k}), U_2^{(i)}(\overline{k})} J_G(U_1(\overline{k}), U_2^{(i)}(\overline{k})) \tag{5.3.4}$$

$$s.t. \qquad \forall j = 1, \ldots, N_h, \qquad \forall i = 1, \ldots, m$$

$$\begin{gathered} X_1(k+j-1) \geq X_{1\,\min} \\ U_{1\,\min} \leq U_1(k+j-1) \leq U_{1\,\max} \\ Y_{2\,\min}^{(i)}(k+j) \leq Y_2^{(i)}(k+j) \leq Y_{2\,\max}^{(i)}(k+j) \\ U_2^{(i)}(k+j-1)\,\epsilon\,\{0,1\} \end{gathered} \tag{5.3.5}$$

The optimization problem described in Equations (5.3.4) and (5.3.5) leads to a mixed integer nonlinear optimization due to the bilinear dependency in the interacting variable stated in Equation (5.1.24). As the number of consumers m increases, this kind of optimization problem may not be easy to solve from a centralized control point of view. Instead, the problem can be solved by decomposition techniques but due to the bilinear dynamics involved and the discrete nature of the consumer control input $U_2^{(i)}(k)$, these techniques would be difficult to develop. As it is shown in the recent book Maestre and Negenborn (2014) on distributed methods, distribution in the hybrid case is still an open complex problem. Other techniques such as communication-based methods could be interesting but it would require many iterations between the controllers without any guarantee of convergence. In this thesis, the optimization problem is tackled in a straightforward manner: each consumer controller solves a local integer optimization proposing a number b of consumption profiles to the producer. The cost $J_{2_{(i)}}^{(p)}(\overline{k})$ is associated with each p consumption profile related to the i^{th} consumer. The producer system controller solves its local linear optimization problem taking into account the optimization costs of the m consumers. The local controllers interact only once, more precisely, consumers will propose various energy consumption profiles so that the producer can have more freedom to optimize its cost function. Following the proposed control structure is detailed.

5.3.2 Proposed MPC architecture

Figure (5.5) represents the proposed control structure for the energy production-consumption system. In this strategy, the difficulty level of solving the global mixed integer nonlinear problem is decreased by considering a reduced number of integer possibilities. A model predictive controller is developed for the producer S_1 which solves a linear optimization according to the information sent by the m consumer controllers which solve an integer optimization.

5.3.2.1 Consumer optimization problem

In this control structure, the control objectives for the producer and consumers are separately treated. As for the consumer optimization problem, the i^{th} consumer controller has to guarantee that the i^{th} consumer output $Y_2^{(i)}(k)$ remains as close as possible to the fixed set-point

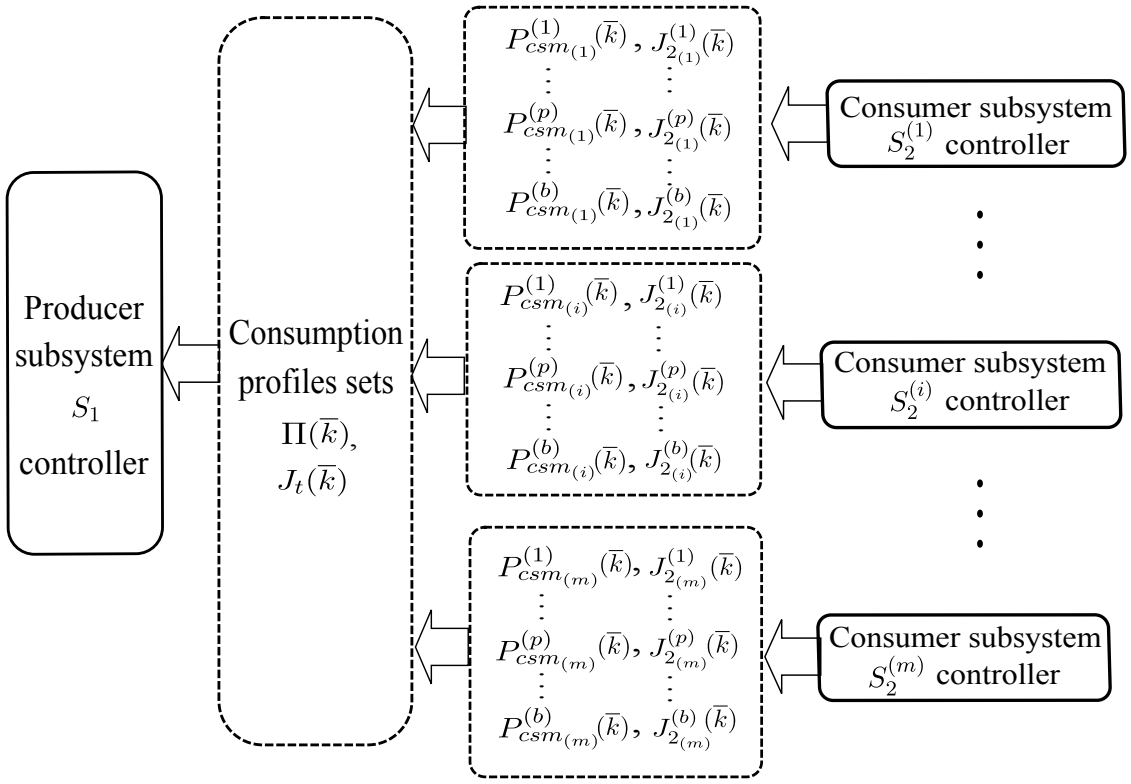

Figure 5.5: Proposed control structure for the production-consumption system.

temperature taking into account the constraints in the control input $U_2^{(i)}(k)$ as stated in Equations (5.1.27) and (5.1.28). The optimization cost function for the i^{th} consumer controller is rewritten as follows

$$\begin{aligned} J^{(p)}_{2_{(i)}}(U^{(p)}_{2_{(i)}}(\overline{k})) = \sum_{j=1}^{N_h} \Big[& Q_1^{(i)} \left\| \triangle U^{(p)}_{2_{(i)}}(k+j-1) \right\|_d^d + Q_2^{(i)} \left\| U^{(p)}_{2_{(i)}}(k+j-1) \right\|_d^d \\ & + Q_3^{(i)} \delta^{(i)}(k+j) \left\| Y_2^{(i)}(k+j) - Y_r^{(i)}(k+j) \right\|_d^d \Big] \end{aligned} \tag{5.3.6}$$

The optimization problem for each of the m consumers can be written as

Optimization problem. At a time k and given the prediction horizon N_h, the current state of the system $X_2^{(i)}(k)$, the previous control input $U_2^{(i)}(k-1)$ and the prediction of the uncontrolled variables $D_2(\overline{k})$, the optimization problem for the energy consumer predictive controller can be defined as

$$\min_{U_{2_{(i)}}^{(p)}(\overline{k})} J_{2_{(i)}}^{(p)}(U_{2_{(i)}}^{(p)}(\overline{k})) \tag{5.3.7}$$

$s.t. \quad \forall j = 1, \ldots, N_h, \quad \forall i = 1, \ldots, m \quad \forall p = 1, \ldots, b$

$$U_{2_{(i)}}^{(p)}(k+j-1)\, \epsilon\, \{0,1\} \tag{5.3.8}$$

which is a discrete optimization problem. As explained before, the aim of the consumer controller is to compute the control profile that minimizes $J_2^{(i)}(U_2^{(i)}(\overline{k}))$. However, in order to offer a degree of freedom to the energy producer controller, the i^{th} energy consumer controller computes b optimal control sequences which compose the set $\bar{U}_{2_{(i)}}(\overline{k})$ of the form

$$\bar{U}_{2_{(i)}}(\overline{k}) = \begin{bmatrix} U_{2_{(i)}}^{(1)}(\overline{k}) \\ \vdots \\ U_{2_{(i)}}^{(p)}(\overline{k}) \\ \vdots \\ U_{2_{(i)}}^{(b)}(\overline{k}) \end{bmatrix} \tag{5.3.9}$$

The associated optimization cost function of each of these control sequences form the set $\bar{J}_{2_{(i)}}(\overline{k})$ of the form

$$\bar{J}_{2_{(i)}}(\overline{k}) = \begin{bmatrix} J_{2_{(i)}}^{(1)}(\overline{k}) \\ \vdots \\ J_{2_{(i)}}^{(p)}(\overline{k}) \\ \vdots \\ J_{2_{(i)}}^{(b)}(\overline{k}) \end{bmatrix} \tag{5.3.10}$$

Where $J_{2_{(i)}}^{(1)}(\overline{k})$ is the optimization cost with the lower value. Also, the interacting variable between producer and the i^{th} energy consumer is defined as

$$W_{21_{(i)}}^{(p)}(\overline{k}) = P_{csm_{(i)}}^{(p)}(\overline{k}) \tag{5.3.11}$$

The m consumer controllers generate a set $\Pi(\overline{k})_{b^m \times N_h}$ of consumption profiles. This set is defined as follows

$$\Pi(\bar{k}) = \begin{bmatrix} P^{(1)}_{csm_{(1)}}(\bar{k}) + \ldots + \begin{Bmatrix} P^{(1)}_{csm_{(i)}}(\bar{k}) + \begin{Bmatrix} P^{(1)}_{csm_{(m)}}(\bar{k}) \\ \vdots \\ P^{(p)}_{csm_{(m)}}(\bar{k}) \\ \vdots \\ P^{(b)}_{csm_{(m)}}(\bar{k}) \end{Bmatrix} \\ \vdots \\ P^{(p)}_{csm_{(i)}}(\bar{k}) + \begin{Bmatrix} P^{(1)}_{csm_{(m)}}(\bar{k}) \\ \vdots \\ P^{(p)}_{csm_{(m)}}(\bar{k}) \\ \vdots \\ P^{(b)}_{csm_{(m)}}(\bar{k}) \end{Bmatrix} \\ \vdots \\ P^{(b)}_{csm_{(i)}}(\bar{k}) + \begin{Bmatrix} P^{(1)}_{csm_{(m)}}(\bar{k}) \\ \vdots \\ P^{(p)}_{csm_{(m)}}(\bar{k}) \\ \vdots \\ P^{(b)}_{csm_{(m)}}(\bar{k}) \end{Bmatrix} \end{Bmatrix} \\ \vdots \\ P^{(p)}_{csm_{(1)}}(\bar{k}) + \ldots + P^{(p)}_{csm_{(i)}}(\bar{k}) + \cdots + P^{(p)}_{csm_{(m)}}(\bar{k}) \\ \vdots \\ P^{(b)}_{csm_{(1)}}(\bar{k}) + \ldots + P^{(b)}_{csm_{(i)}}(\bar{k}) + \cdots + P^{(b)}_{csm_{(m)}}(\bar{k}) \end{bmatrix} = \begin{bmatrix} \pi_1\left(\bar{k}\right) \\ \vdots \\ \pi_h\left(\bar{k}\right) \\ \vdots \\ \pi_{b^m}\left(\bar{k}\right) \end{bmatrix} \tag{5.3.12}$$

where $\pi_h(\overline{k})$ is the h^{th} element of $\Pi(\overline{k})$. Likewise, the set of consumer optimization costs $J_t(\overline{k})$ is built. Each of the b^m elements is the sum of the local optimization costs of each consumer: $\sum_{i=1}^{m} J^{(p)}_{t_{(i)}}(\overline{k})$. The vector $J_{t_h}(\overline{k})_{h=1,\ldots,b^m}$ is one element of the set $J_t(\overline{k})$.

To make more explicit the notation introduced in Equation 5.3.12, considering $m = 3$ consumers where each of them proposes $b = 2$ energy profiles, the matrix $\Pi(\overline{k})$ is built as follows

$$\Pi(\bar{k}) = \begin{bmatrix} P^{(1)}_{csm_{(1)}}(\bar{k}) + P^{(1)}_{csm_{(2)}}(\bar{k}) + P^{(1)}_{csm_{(3)}}(\bar{k}) \\ P^{(1)}_{csm_{(1)}}(\bar{k}) + P^{(1)}_{csm_{(2)}}(\bar{k}) + P^{(2)}_{csm_{(3)}}(\bar{k}) \\ P^{(1)}_{csm_{(1)}}(\bar{k}) + P^{(2)}_{csm_{(2)}}(\bar{k}) + P^{(1)}_{csm_{(3)}}(\bar{k}) \\ P^{(1)}_{csm_{(1)}}(\bar{k}) + P^{(2)}_{csm_{(2)}}(\bar{k}) + P^{(2)}_{csm_{(3)}}(\bar{k}) \\ P^{(2)}_{csm_{(1)}}(\bar{k}) + P^{(1)}_{csm_{(2)}}(\bar{k}) + P^{(1)}_{csm_{(3)}}(\bar{k}) \\ P^{(2)}_{csm_{(1)}}(\bar{k}) + P^{(1)}_{csm_{(2)}}(\bar{k}) + P^{(2)}_{csm_{(3)}}(\bar{k}) \\ P^{(2)}_{csm_{(1)}}(\bar{k}) + P^{(2)}_{csm_{(2)}}(\bar{k}) + P^{(1)}_{csm_{(3)}}(\bar{k}) \\ P^{(2)}_{csm_{(1)}}(\bar{k}) + P^{(2)}_{csm_{(2)}}(\bar{k}) + P^{(2)}_{csm_{(3)}}(\bar{k}) \end{bmatrix} \tag{5.3.13}$$

Then the matrix $\Pi(\overline{k})$ which contains b^m components is sent along with the vector $J_t(\overline{k})$ to the producer controller.

5.3.2.2 Producer optimization problem

Considering that each of the consumer controllers sends more than one consumption profile, Equation (5.1.8) is rewritten as

$$E(k+1) = E(k) + \triangle t(P_{sol}(k) + P_{elc}(k) - \pi_h(k) \tag{5.3.14}$$

which in turn is equivalent to

$$X_1(k+1) = X_1(k) + \triangle t(D_1(k) + U_1(k) - W_{21_h}(k)) \tag{5.3.15}$$

According to Equations (5.3.1) and (5.3.17) and due to the interactions between the producer and consumers, the optimization problem for the energy producer can be stated as follows:

Optimization problem. At a time k and given the prediction horizon N_h, the current state of the system $X_1(k)$, the prediction of the uncontrolled variables $D_1(\overline{k})$ and the set of energy demand profiles $\Pi(\overline{k})$ where each element of the set $\pi_h(\overline{k})$ has an associated optimization cost $J_{t_h}(\overline{k})$, the optimization problem for the energy producer predictive controller is given by

$$\min_{U_1(\overline{k}),\pi_h(\overline{k})} J_1(U_1(\overline{k}), \pi_h(\overline{k})) + J_{t_h}(\overline{k}) \tag{5.3.16}$$

$s.t. \qquad \forall j = 1, \ldots, N_h, \qquad \forall h = 1, \ldots, b^m$

$$\begin{aligned} X_1(k+j-1) &\geq X_{1\min} \\ U_{1\min} \leq U_1(k+j-1) &\leq U_{1\max} \\ \pi_h(k+j-1) \quad &\epsilon \quad \Pi(k+j-1) \end{aligned} \tag{5.3.17}$$

Once the b^m linear optimizations are computed, the producer controller selects the energy demand profile $\pi_h(\overline{k})$ that better minimizes the energy of production according to its local and consumer optimization costs.

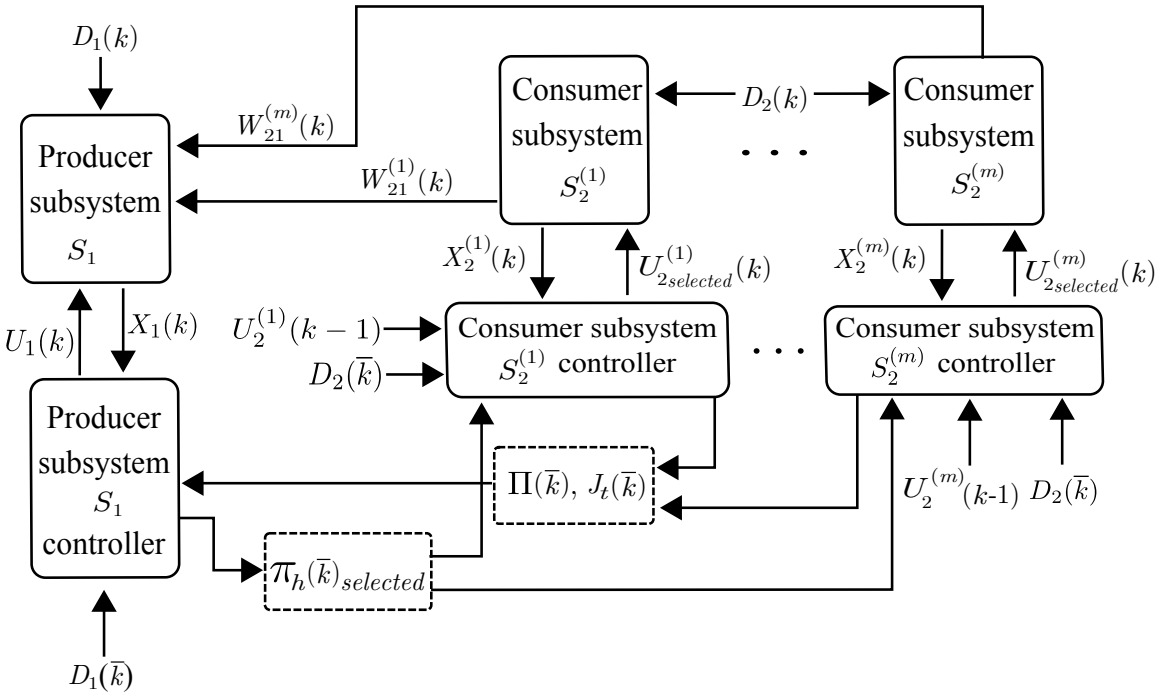

Figure 5.6: Global control architecture.

5.3.2.3 Control strategy algorithm

Figure 5.6 displays the architecture of the proposed control strategy. A detailed description of the algorithm is described below.

1. Given the consumer state vectors $X_2^{(i)}(k)_{i=1,\ldots,m}$, the previous control inputs $U_2^{(i)}(k-1)_{i=1,\ldots,m}$, and the prediction of the disturbances $D_2(\overline{k})$ over the prediction horizon N_h, the energy consumer controllers compute the set $\Pi(\overline{k})$ of b^m energy demands over the prediction horizon N_h. This set is sent to the energy producer controller.

2. Given the producer state vector $X_1(k)$, the set $\Pi(\overline{k})$ provided by the energy consumer controllers and the prediction of the disturbances $D_1(\overline{k})$ over the prediction horizon N_h, the energy producer controller computes b^m linear optimizations according to the set of energy demands $\Pi(\overline{k})$.

3. Given the set of b^m linear optimizations, the energy producer controller selects the one that has the lowest cost (described by equation (5.3.16)). The energy demand profile $\pi_h(\overline{k})$ selected associated with the producer optimization lower cost is identified.

4. The producer controller sends the first element $U_1(k)$ of the control signal vector to the producer and communicates to the energy consumer controllers the energy demand profile $\pi_h(\overline{k})$ that has been selected. The consumer controllers send the first element $U_2^{(i)}(k)$ of the control signal vectors associated with the selected energy demand profile $\pi_h(\overline{k})$.

5. The algorithm restarts at the sampling time $k+1$.

5.3.3 Performance indexes

In order to assess the performance of the proposed control strategy, the following indexes are introduced. They are calculated *a posteriori*, after the simulation tests.

For the producer controller:

- The first indicator $I_{\int U_1}$ (measured in kWh) quantifies the use of auxiliary energy $U_1(k)$ over the simulation from the initial time t_i until the final time t_f. The value of this indicator should be as small as possible. It can be formalized as follows:

$$I_{\int U_1} = \int_{t_i}^{t_f} U_1(t)dt \tag{5.3.18}$$

- The second indicator $I_{\int P_{csm}}$ (measured in kWh) is related to the total energy demand of the consumers. It is expressed as follows

$$I_{\int P_{csm}} = \int_{t_i}^{t_f} P_{csm,total}(t)dt \tag{5.3.19}$$

  Where $P_{csm,total} = \sum_{i=1}^{m} P_{csm}^{(i)}(k)$.

  For the consumers:

- Two indicators are related to the control input of each consumer. The first one (dimensionless) quantifies the number of changes of the i^{th} control input over the simulation. It can be defined as

$$I_{\triangle U_2^{(i)}} = \sum_{k=t_i}^{t_f} \left| \triangle U_2^{(i)}(k) \right| \tag{5.3.20}$$

- The second one (dimensionless) quantifies the number of switch on events of the i^{th} building:

$$I_{U_2^{(i)}} = \sum_{k=t_i}^{t_f} U_2^{(i)}(k) \tag{5.3.21}$$

- The third indicator (measured in $^\circ C$) computes the average of the i^{th} building operative temperature deviation from the corresponding set-point during occupancy profiles:

$$I_{Y_2^{(i)}} = \frac{1}{\|V\|_1} \sum_{k=t_i}^{t_f} \delta^{(i)}(k) \left| Y_2^{(i)}(k) - Y_r^{(i)}(k) \right| \tag{5.3.22}$$

  where $V = [\delta^{(i)}(t_i), \ldots, \delta^{(i)}(t_f)]$.

- The last indicator I_{time} (measured in minutes) computes the time needed to carry out the simulation. It is obtained using the MATLAB functions *tic* and *toc*. The function *tic* starts a stopwatch timer to measure performance. The function records the internal time at execution of the *tic* command (MATLAB, 2012). The elapsed time is displayed with the *toc* function.

5.3.4 Simulation results

In the following sections, the performance of the control strategy is assessed. The impact of the prediction horizon, the number of energy demand profiles and the optimality of the proposed solution are investigated. For the simulation tests, the identified model presented in Appendix A is used for both prediction and simulation.

According to Equations (5.3.1) and (5.3.2), the parameter d considered in the simulations is 1. That is, the cost functions of both producer and consumer controllers use the ℓ^1-norm with exponent 1. This choice comes from the fact that the producer cost function only quantifies the amount of auxiliary energy use. Also, the terms in the i^{th} consumer cost function involves the binary control signal and the term related to the indoor thermal comfort. This can be translated into linear cost functions.

The weighting factors of the i^{th} consumer cost function are $Q_1^{(i)} = 2$, $Q_2^{(i)} = 0.5$ and $Q_3^{(i)} = 5$. The justification of this choice is that it is a priority to guarantee the building thermal comfort. At the same time, as the cooling energy is provided by an absorption chiller, it is also necessary to seek non-intermittent operating periods by minimizing its switch on/off changes. This criterion has a higher priority than the minimization of the chiller operation as its main driving source is cost-free. In addition, these weighting factors are selected taking into account that both consumer and producer cost function values must have the same degree of impact on the global optimization cost.

The *linprog* function of the MATLAB optimization toolbox has been used to solve the producer optimization problem and the consumers optimization problem is solved using the branch and bound algorithm (see Section 5.3.4.2).

5.3.4.1 Prediction horizon N_h impact

Several studies have been carried out to analyze the impact of the prediction horizon N_h over the proposed control strategy. The results are summarized in Table 5.1. The tests evaluate from $N_h = 2$ (1 hour) up to $N_h = 20$ (10 hours). Also, $m = 3$ consumer controllers calculate $b = 3$ energy demand profiles which are sent to the producer controller. The number of linear optimizations carried out by the producer controller at each sampling time is $b^m = 27$. In order to simplify the analysis, the same state-space model detailed in Appendix A is used for all the consumers as well as the binary variable $\delta^{(i)}(k)$ which represents the period in which the operative temperature $Y_2^{(i)}(k)$ must remain as close as possible to the corresponding set-point.

The simulation parameters of the logic rule-based strategy presented in Section 5.2 are considered. That is, the experiment is carried out during 72 hours with a sampling time of $t_k = 0.5$ hr, the stored energy lower limit stated in Equation (5.1.25) is zero, the temperature set-point in each of the buildings is only defined during occupancy periods, the water flow rate delivered to the radiant ceiling is 700 kg/hr and the operative temperature of buildings $S_2^{(1)}$, $S_2^{(2)}$ and $S_2^{(3)}$ is controlled at 22 °C, 24 °C and 26 °C respectively.

It is well known that the more the size of the prediction horizon, the higher the complexity of the optimization problem and consequently the computational burden increases. This is clearly shown by the indicator I_{time} which has an exponential rise from $N_h = 2$ (lower than 1 minute) up to $N_h = 20$ (28 minutes).

As for the i^{th} consumer controller, three control objectives must be achieved: the minimization of both switch on events and switch on/off changes as well as to maintain as small as possible the distance between the consumer output $Y_2^{(i)}(k)$ and the desired set-point $Y_2^{(r)}(k)$. These objectives are evaluated using the indexes previously defined in Section 5.3.3.

As the optimization problem tackles a multi-objective criterion in both producer and consumer controllers, it is difficult to individually determine the impact of the prediction horizon over some indexes. For example, it is not obvious to observe the impact of the prediction horizon over the first indicator, $I_{\triangle U_2^{(i)}}$ (which is dimensionless) as it arbitrarily changes in each of the consumers.

The indicators $I_{Y_2^{(1)}}$, $I_{Y_2^{(2)}}$ and $I_{Y_2^{(3)}}$ relate the average of the i^{th} building operative temperature deviation from the corresponding set-point. From $N_h = 2$ up to $N_h = 8$, the decreasing trend of the index can be noticed. This means that the bigger the prediction horizon size,

Table 5.1: Performance indexes according to prediction horizon N_h

		N_h					
		2	4	8	12	16	20
Consumer $S_2^{(1)}$	$I_{\triangle U_2^{(1)}}$	16	16	22	18	18	20
	$I_{U_2^{(1)}}$	50	50	51	51	51	51
	$I_{Y_2^{(1)}}$	0.7	0.65	0.5	0.53	0.55	0.49
Consumer $S_2^{(2)}$	$I_{\triangle U_2^{(2)}}$	14	20	24	20	22	18
	$I_{U_2^{(2)}}$	35	39	40	39	40	40
	$I_{Y_2^{(2)}}$	0.85	0.6	0.56	0.59	0.55	0.59
Consumer $S_2^{(3)}$	$I_{\Delta U_2^{(3)}}$	14	24	22	18	18	20
	$I_{U_2^{(3)}}$	25	28	29	30	30	30
	$I_{Y_2^{(3)}}$	1.02	0.57	0.53	0.54	0.53	0.52
Producer S_1	$I_{\int P_{csm}}$	651.22	684.72	697.65	694.85	701.47	699.71
	$I_{\int U_1}$	496.18	529.29	540.34	539.42	546.05	547.11
I_{time}		0.65	0.71	0.85	1.33	4.13	28

the smaller the temperature deviation. However, these indicators do not significantly change from $N_h = 8$ up to $N_h = 20$. This may imply that the building temperature deviation is not significantly minimized using prediction horizon values larger than $N_h = 8$.

From $N_h = 2$ up to $N_h = 8$, it can be seen that the indicators $I_{U_2^{(1)}}$, $I_{U_2^{(2)}}$ and $I_{U_2^{(3)}}$ (representing the number of chiller switch on events) increase as the prediction horizon becomes larger. This can be easily explained observing the indicator $I_{Y_2^{(i)}}$ which has a decreasing trend. This means that the temperature deviation is minimized by increasing the use of the chiller. From $N_h = 8$ up to $N_h = 20$, the number of chiller switch on events remain almost constant. This is related to the minimal change presented in the temperature deviation.

The control objective of the producer is the minimization of the auxiliary energy $U_1(k)$ while maintaining the storage energy above the lower limit. The results show that the producer linear optimization always maintains the storage energy within the bounds. Once again, from $N_h = 2$ up to $N_h = 8$, it can be observed that the index $I_{\int P_{csm}}$ increases as the prediction horizon increases. This index refers to the total energy of consumption demanded to the producer (see Equation (5.1.13)) which increases as the buildings temperature deviation over the prediction horizon decreases. In addition, the more the total energy required by the consumers, the more the supplied auxiliary energy, as it can be seen from the index $I_{\int U_1}$

which also has an increasing behavior.

From these results, it can be seen that $N_h = 8$ is an adequate value in terms of controller performance and computational complexity. The decreasing trend of the buildings temperature deviation is notable up to this value. After $N_h = 8$, the building thermal comfort is not significantly improved. However, it must be noticed that more auxiliary electric energy is required compared to lower prediction horizon values.

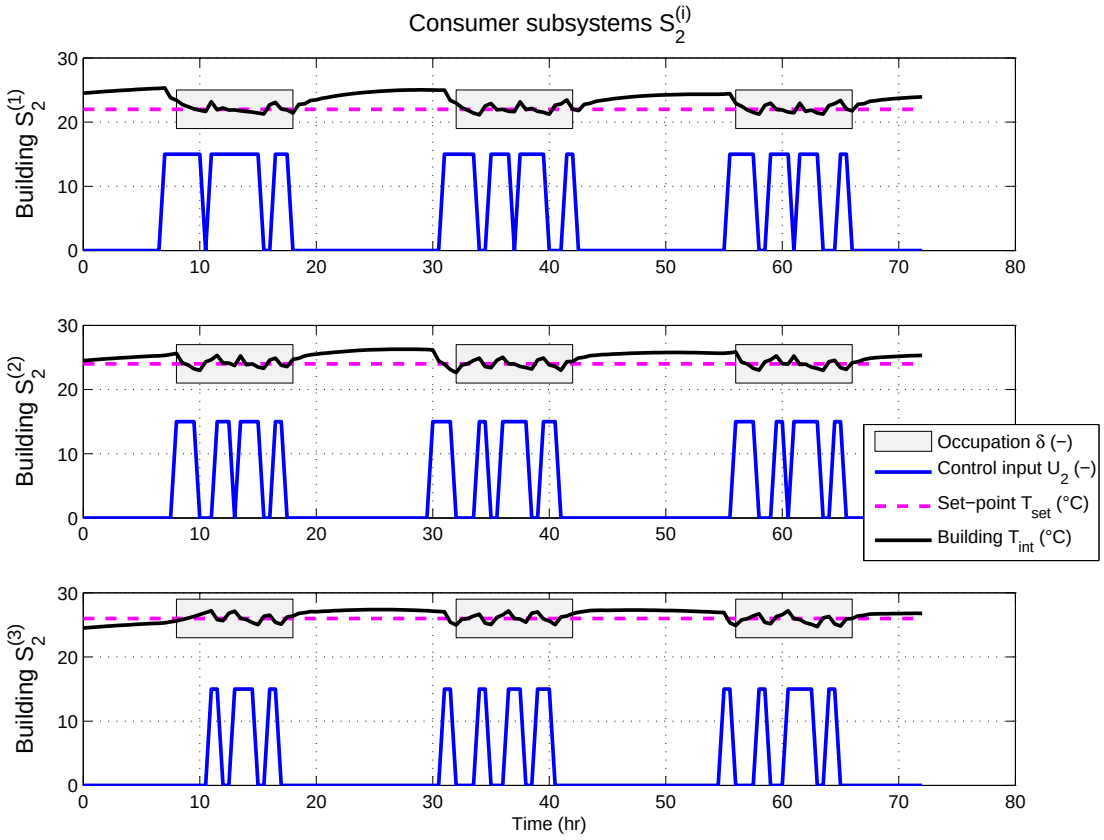

Figure 5.7: Consumer controllers behavior when $N_h = 8$ and $b = 3$.

Figure 5.7 depicts the simulation results of the consumer controllers when $N_h = 8$ and $b = 3$. For display purposes, the binary variable is multiplied by 15 in each of the buildings. The results show that the weighting factors criterion ensures that it is more important to maintain the building operative temperature close to the fixed set-point rather than to minimize the changes in the control input. In addition, it is noticeable that the higher the building set-point, the lower the chiller operation.

Figure 5.8 shows the variables behavior of the producer controller. According to Equation (5.1.8), the first curve is the energy stored $E(k)$ in the producer. The second one is the solar

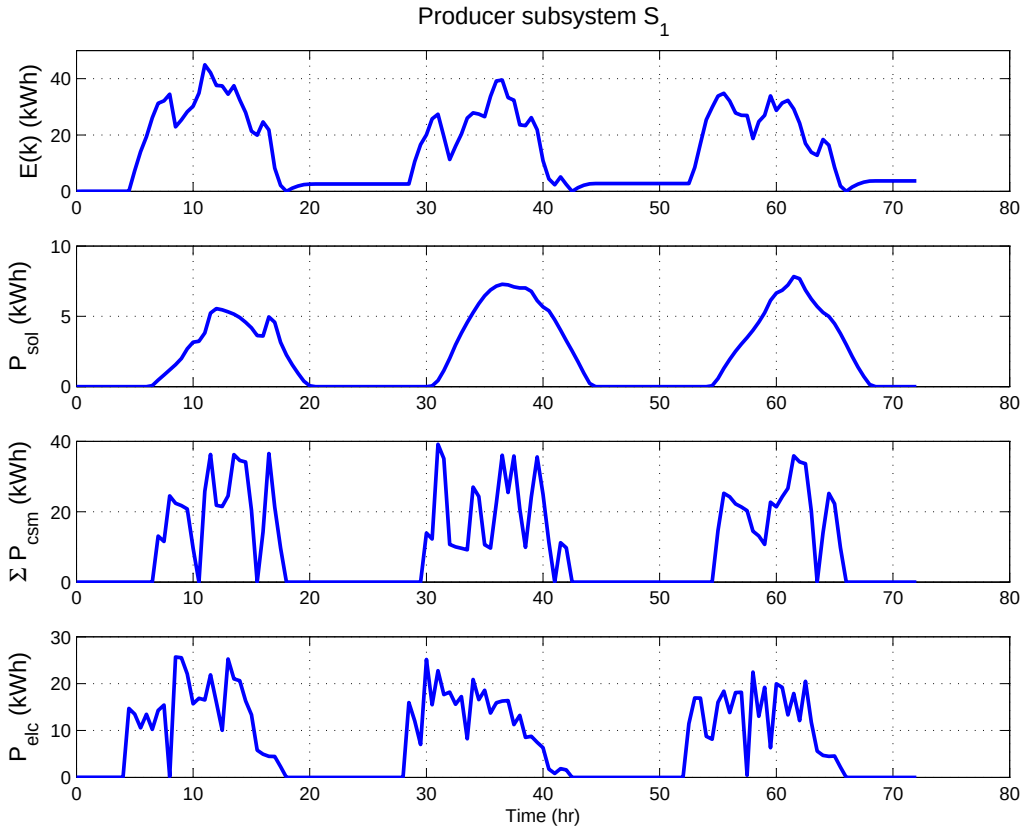

Figure 5.8: Producer controller behavior when $N_h = 8$ and $b = 3$.

radiation $P_{sol}(k)$ supplied to the producer which in turn, is the primary energy source. The third one is the total energy demanded by the consumers $\sum_{i=1}^{m} P_{csm}^{(i)}(k)$ and the last one is the auxiliary energy $P_{elc}(k)$. It can be seen that the solar gains do not provide enough energy to supply the energy demand, throughout the simulation auxiliary electric energy is required. It is visible that as solar gains are stronger, lower auxiliary energy is required. A further study should be done to adequately select the producer parameters as the size of the solar energy collectors or the storage capacity according to the energy of consumption.

Table 5.2 shows the performance indexes of the MPC and the logic rule-based control (LRBC) strategy presented in Section 5.2. The MPC strategies use the same prediction horizon value $N_h = 8$ and different number b of energy demand profiles. In the MPC strategy of the first column each consumer sends only 3 energy demand profiles while the results of the second column correspond to 32 energy profiles.

It can be noticed an important difference between the MPC and LRBC strategies: the MPC strategy is better in terms of building thermal comfort (index $I_{Y_2^{(i)}}$), switch on/off changes

Table 5.2: Performance indexes comparative between MPC and LRBC strategies

		MPC: $b = 3$, $N_h = 8$	MPC: $b = 32$, $N_h = 8$	BLRC strategy
Consumer $S_2^{(1)}$	$I_{\triangle U_2^{(1)}}$	22	24	34
	$I_{U_2^{(1)}}$	51	50	49
	$I_{Y_2^{(1)}}$	0.5	0.55	0.79
Consumer $S_2^{(2)}$	$I_{\triangle U_2^{(2)}}$	24	20	52
	$I_{U_2^{(2)}}$	40	38	38
	$I_{Y_2^{(2)}}$	0.56	0.62	0.74
Consumer $S_2^{(3)}$	$I_{\Delta U_2^{(3)}}$	22	18	64
	$I_{U_2^{(3)}}$	29	28	32
	$I_{Y_2^{(3)}}$	0.53	0.55	0.81
Producer S_1	$I_{\int P_{csm}}$	697.65	679.91	733.4
	$I_{\int U_1}$	540.34	522.6	585
I_{time}		0.85	754.76	0.22

($I_{\Delta U_2^{(i)}}$) and auxiliary energy use (index $I_{\int U_1}$). Compared with the results of the MPC strategy when $b = 3$, the index $I_{Y_2^{(i)}}$ for the buildings $S_2^{(1)}$, $S_2^{(2)}$ and $S_2^{(3)}$ is decreased 58 %, 32 % and 52 % respectively. Besides, the index $I_{\triangle U_2^{(i)}}$ for the buildings $S_2^{(1)}$, $S_2^{(2)}$ and $S_2^{(3)}$ is decreased 76 %, 69 % and 79.6 % respectively. Finally, the number of chiller switch on events is not significantly different comparing both control strategies which is related to the minimal difference in terms of auxiliary energy use: the LRBC approach consumes 8 % more electricity.

Comparing the results of the MPC strategies, it can be noticed that when the number of energy profiles is $b = 32$, the index $I_{U_2^{(i)}}$ decreases compared to the experiment when $b = 3$. In addition, the index $I_{Y_2^{(i)}}$ has a minimal increment as the number of energy demand profiles grows. The lower number of chiller switch on events measured by the index $I_{U_2^{(i)}}$ causes a lower global energy consumption $I_{\int P_{csm}}$ and naturally a lower auxiliary energy $I_{\int U_1}$ use. This results may imply that in general a better controller performance is obtained considering a large number of energy demand profiles and that the building thermal comfort is not significantly affected as the energy demand profiles number grows.

5.3.4.2 About the suboptimality of the proposed control strategy

In the proposed control strategy, each of the consumer controllers carries out an integer optimization (based on the branch and bound algorithm (Scholz, 2012)) which computes b energy demand profiles sent to the producer controller. Taking the example reported in the previous section, where the experiment considers $m = 3$ consumers which propose $b = 3$ energy demand profiles over a prediction horizon $N_h = 8$, the number of optimizations performed by the producer controller is $b^m = 27$. In a centralized approach, this number increases exponentially to $2^{(mN_h)} = 16777216$. To better explain this, consider the scenario depicted in Figure 5.9 where the number of consumers is $m = 2$ and each of them proposes $b = 3$ energy demand profiles over a prediction horizon of $N_h = 2$. If a centralized optimization is used, the number of possible integer combinations is $2^{(mN_h)} = 16$. That is, 16 linear optimizations are performed by the producer controller. Instead, the proposed control strategy only considers a given number b of combinations which generates a reduced field of possibilities, in this case, the number is $b^m = 9$. It can be noticed that the combinations $c_1 - c_4$, c_6, c_{10} and c_{14} are not explored which may lead to a suboptimality in the solution of proposed control strategy.

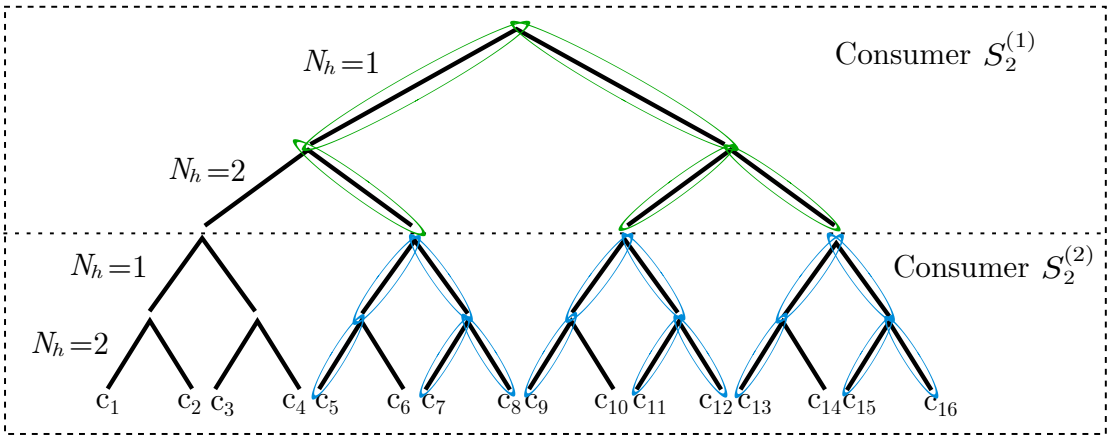

Figure 5.9: Possible integer combinations considering $N_h = 2$, $m = 2$ and $b = 3$.

Test 1: Constraints fulfillment vs number of energy profiles b

In terms of performance of the control strategy, Figure 5.10 depicts the simulation results when the number of energy demand profiles sent to the producer controller varies from $b = 1$ up to $b = 32$ over a prediction horizon $N_h = 5$ and considering the number of consumers $m = 3$. The evolution of the curves according to the number of energy demand profiles up to the optimal scenario can be observed. When $b = 32$ the number of optimizations performed by the producer controller is $2^{(mN_h)} = b^m = 32768$ which corresponds to the results obtained in a centralized control approach.

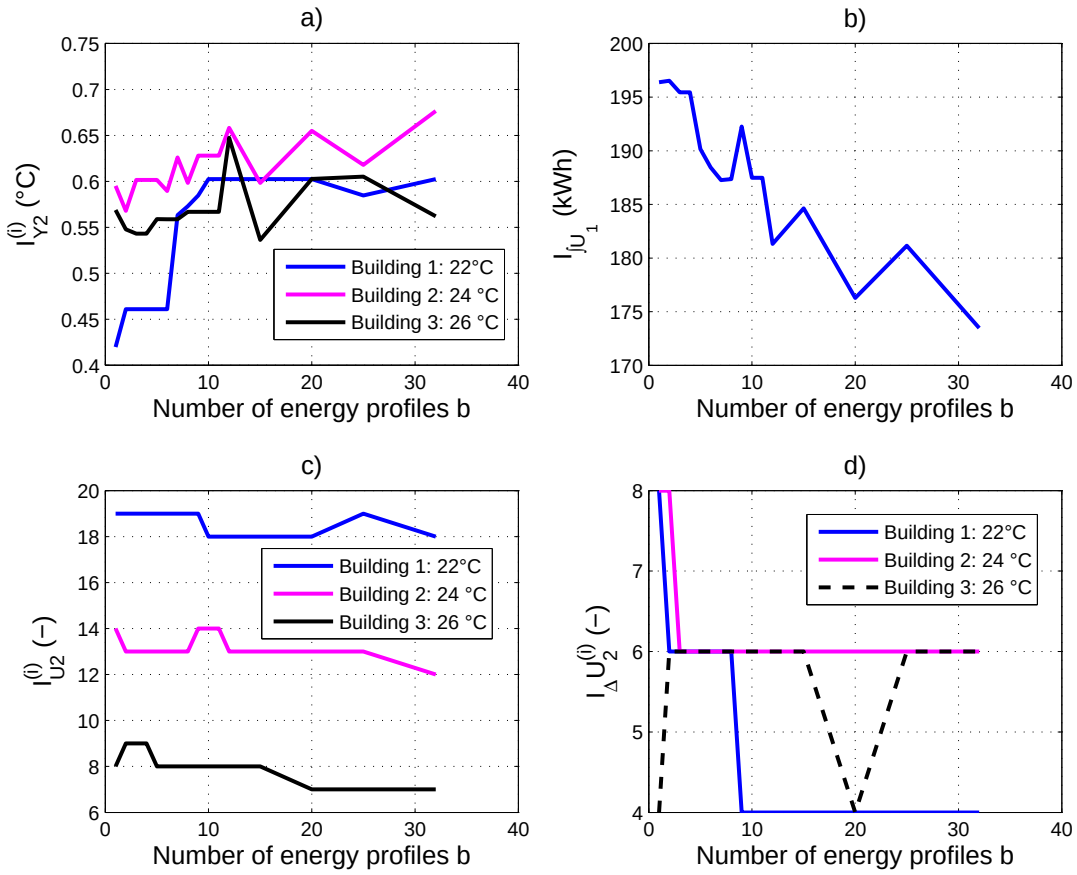

Figure 5.10: Variables behavior considering $b = 1$ up to $b = 32$.

Figure 5.10 a) shows the results of the index $I_{Y_2^{(i)}}$ previously defined in Section 5.3.3 for each of the buildings over 20 hours with a sampling time $t_k = 0.5$ hr. It is observed that this index does not drastically change as the number of profiles sent to the producer increases. Even so, the temperature deviation increasing trend for buildings $S_2^{(1)}$ and $S_2^{(2)}$ is directly related to the increasing number of energy profiles. This is evident since in the fist scenario (when $b = 1$) the i^{th} building controller sent its optimal solution, that is, the solution that better minimizes the building temperature deviation which has priority over the remaining factors of the cost function. Instead, when the number of sent profiles increases, e.g. $b = 3$, the producer controller selects the energy profile that better minimizes the global cost within these three propositions which may not correspond to the i^{th} local consumer first choice.

Figure 5.10 b) depicts the results of the index $I_{\int U_1}$ which corresponds to the auxiliary energy use. As the number of energy demand profiles increases, the electricity use decreases which is directly related to the increasing trend of the temperature deviation in buildings $S_2^{(1)}$ and

$S_2^{(2)}$. From Figure 5.10 c), the index $I_{\triangle U_2^{(i)}}$ has a decreasing tendency which is translated into a lower chiller switch on events as the number of profiles increases. Finally, the index $I_{\triangle U_2^{(i)}}$ depicted in Figure 5.10 d) decreases from buildings $S_2^{(1)}$ and $S_2^{(2)}$ and it has an arbitrary change for the building $S_2^{(3)}$.

These results imply that the bigger the number of energy consumer profiles, the bigger the temperature deviation even if this change is not significant and consequently does not compromise the building thermal comfort. In addition, the more the energy profiles, the lower the electricity use and chiller switch on events. Finally, it is not evident to observe how the number of profiles impacts on the index $I_{\triangle U_2^{(i)}}$.

Test 2: Suboptimality percentage vs number of energy profiles b

Another study has been carried out in order to quantify the difference between the results obtained using a lower number of energy demand profiles and the centralized control case. This difference is the suboptimality of the solution when the whole branch and bound tree is not explored and only a reduced number of energy profiles is sent to the producer. The suboptimality percentage is given by

$$\%_{subopt}(k) = \frac{J_g(k) - J_g^{(opt)}(k)}{J_g^{(opt)}(k)} 100\% \tag{5.3.23}$$

where,

$$J_g(k) = J_1^*(U_1^*(k), \pi_h(k)_{selected}) + J_{t_h}(k)_{selected} \tag{5.3.24}$$

The variable $J_g(k)$ is the computed optimization cost which has been obtained using a lower number of energy profiles than the centralized case (when all the branches of the tree are explored). The variable $J_g^{(opt)}(k)$ is the computed optimization cost which has been obtained considering all possible solutions of the branch and bound tree, that is, the optimal case.

The following indexes are introduced

$$\bar{x} = \frac{1}{N}\sum_{k=1}^{N} \%_{subopt}(k) \tag{5.3.25}$$

$$\sigma_{sd} = \sqrt{\frac{1}{N-1}\sum_{k=1}^{N} (\%_{subopt}(k) - \bar{x})^2} \tag{5.3.26}$$

$$\max(x) = \max_{k=1,\cdots,N} \%_{subopt}(k) \tag{5.3.27}$$

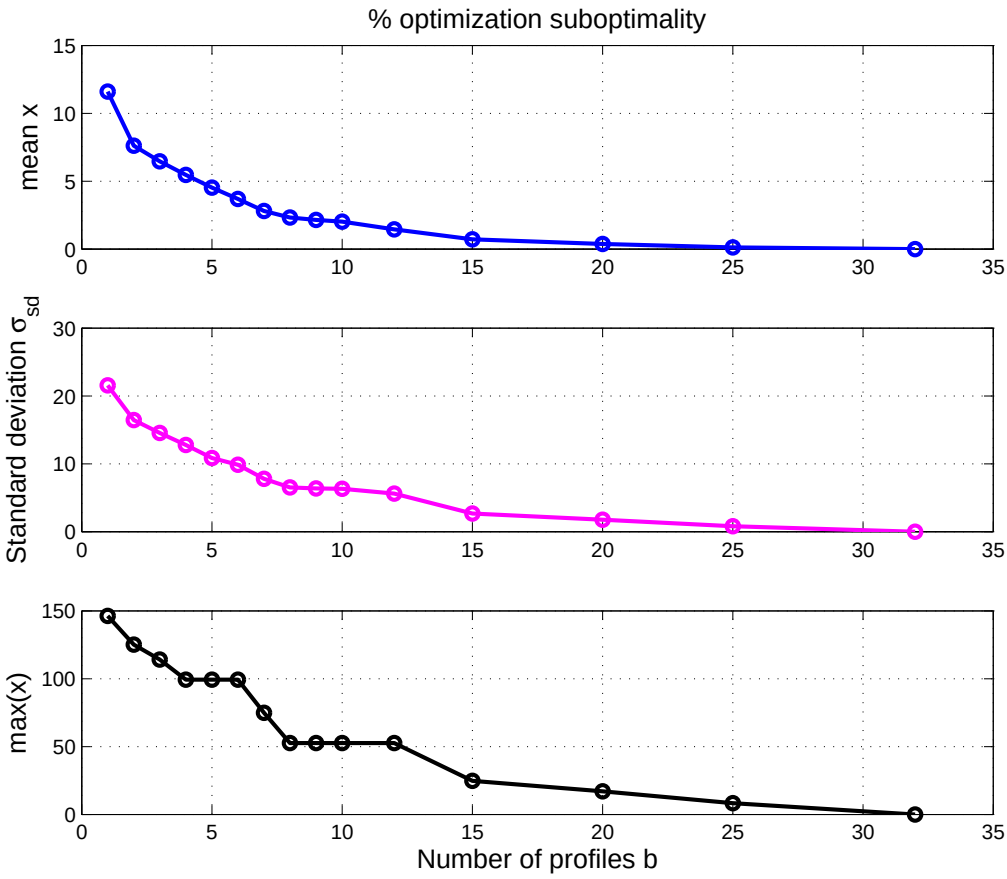

Figure 5.11: Suboptimality percentage considering $b = 1$ up to $b = 32$.

Figure 5.11 depicts the results calculated by the three indexes when the number of energy profiles varies from $b = 1$ up to $b = 32$. Each circle of the blue, magenta and black curves of Figure 5.11 represents the mean $\overline{x}$, standard deviation σ_{sd} and maximum of the suboptimality percentage $\%_{subopt}(k)$ respectively. For example, the first circle of the blue curve corresponds to the mean of the suboptimality percentage calculated from the comparison between the optimal case $b = 32$ and the simulation carried out considering $b = 1$.

Each circle of the curves corresponds to a simulation carried out during 72 hours considering a sampling time of 0.5 hours, which correspond to 145 iterations. Unlike the results depicted in Figure 5.10, the control strategy is applied in open-loop and the control inputs are the same in all the cases (from $b = 1$ up to $b = 32$). Both producer and consumers applied control inputs correspond to the optimal case which is the first element of the first energy demand profile sent to the producer controller, that is, $U_{2_{(i)}}^{(p=1)}(k)$. The objective of this experiment is to compare the optimization results within a valid scenario where the initial conditions are

the same at each iteration and correspond to the optimal case.

Figure 5.11 shows that there is a significant difference in terms of suboptimality percentage from $b = 1$ up to $b = 5$ for the mean and standard deviation. For example, the standard deviation and mean considering one energy demand profile $b = 1$ are $\overline{x} = 11.6\%$ and $\sigma_{sd} = 21.5\%$ respectively. For $b = 5$, the suboptimality percentage for the mean $\overline{x}$, standard deviation σ_{sd} and maximum value $\max(x)$ are 4.5%, 10.8% and 99.25% respectively, wich decreases as the number of energy demand profiles b increases.

Test 3: Suboptimality percentage vs optimal/random energy demand profiles b

The objective of this experiment is to observe how the energy demand profiles generated from different criteria impact on the controller performance. In the tests carried out so far, the consumer controllers compute b optimal energy demand profiles which are ranked in increasing order with respect to the value of its local optimization cost $J_2^{(i)}(k)$. That is, this set of energy profiles is the one that better minimizes its cost function. Figure 5.12 depicts the suboptimality percentage of the proposed control strategy considering $b = 5$ energy demand profiles generated according to three different criteria:

- *Optimal profiles*: This criterion of energy demand profile generation is the one that has been considered so far. The magenta lines represent the mean $\overline{x}$, standard deviation σ_{sd} and maximum value $\max(x)$ of suboptimality percentage considering that the set of b energy demand profiles sent by the i^{th} consumer controller corresponds to the optimal solutions, that is, the 5 solutions that better minimize its local cost function. These results have been already shown in Figure 5.11.

- *Partially optimal profiles*: The blue lines represent the mean $\overline{x}$, standard deviation σ_{sd} and maximum value $\max(x)$ of suboptimality percentage considering that the set of b energy demand profiles sent by the i^{th} consumer controller corresponds to a partially optimal set of energy demand profiles. This set is generated selecting 5 of the $b = 10$ optimal energy profiles calculated by the branch and bound algorithm. The first two energy profiles are the ones that have the lower optimization cost. The next three profiles are randomly selected from the eight remaining profiles of the set.

- *Random profiles*: The black lines represent the mean $\overline{x}$, standard deviation σ_{sd} and maximum value $\max(x)$ of suboptimality percentage considering that the set of b energy demand profiles sent by the i^{th} consumer controller corresponds to a random set of energy demand profiles without optimization. That is, with $N_h = 5$, the i^{th} consumer controller randomly selects $b = 5$ combinations from the $2^{N_h} = 32$ possibilities, it

calculates its corresponding optimization cost and sends these sets to the producer controller.

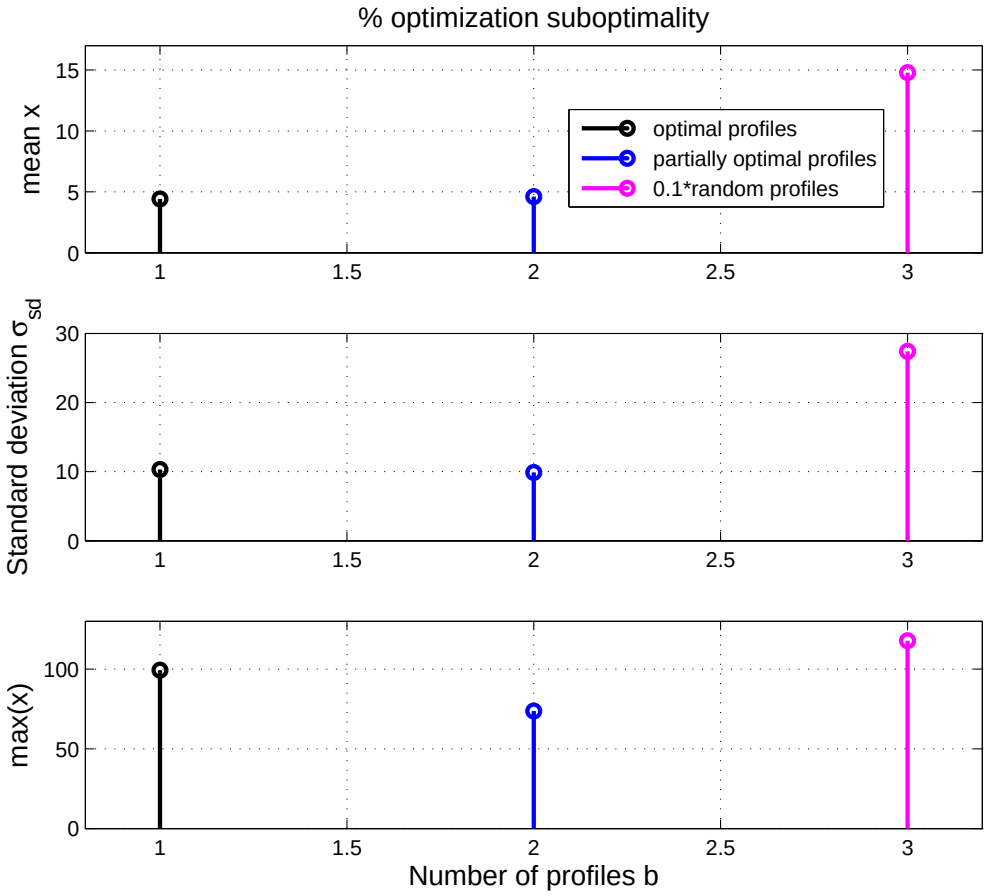

Figure 5.12: Suboptimality percentage considering $b = 5$ and different energy demand profile generation.

From Figure 5.12 it can be noticed that there is an obvious difference between the results considering optimal/partially optimal profiles and the ones obtained by considering random profiles which have a mean $\overline{x} = 147\%$, standard deviation $\sigma_{sd} = 274\%$ and maximum value $\max(x) = 1117\%$ of suboptimality. Even if there is a minimal difference compared with the optimal profiles, considering partially optimal solutions leads to a lower suboptimality percentage but computation complexity must be taken into account as the prediction horizon size increases. That is, the generation of partially optimal solutions requires the computation of a bigger number of energy demand profiles for the same number of profiles sent to the producer controller. Consequently, as the prediction horizon size increases, the optimization problem resolution becomes even more complex.

5.4 Conclusions

In this chapter, a predictive control structure for a producer-consumer system has been developed. Instead of dealing with a centralized control approach, local predictive controllers are designed for the producer and consumers. A limited number of discrete control decisions from the centralized control problem are used and sent to the producer controller which carries out its local optimization.

In order to assess the control strategy performance, the generalized model presented in Section 5.1.1 is represented by linear models. First, a logic rule-based control approach is evaluated. The simulation results showed an adequate performance in terms of building thermal comfort. However, a good temperature hysteresis controller cannot be achieved without a significant number of chiller switch on/off changes. Better results are performed by the MPC strategy which improves the building thermal comfort and significantly reduces the change in the chiller binary control input.

A study regarding the impact of the prediction horizon has been carried out. From MPC theory it is well known that the bigger the prediction horizon size, the better the minimization of the optimization criterion. This is true for the global optimization cost which is the sum of producer and consumers optimization costs. This global optimization cost is reduced as the prediction horizon increases. The increasing and decreasing behavior of the producer and consumer indexes contributes to the minimization of the global optimization cost.

In addition, the impact of the number of the energy profiles sent to the producer controller has been evaluated. The results showed that the more the energy profiles sent, the lower the auxiliary electricity use. This behavior is directly related to the buildings temperature deviation which increases as the number of energy demand profiles increases. It is worth noting that this increment of the temperature deviation does not degrade the buildings thermal comfort as the maximum average of this deviation does not go beyond 1 $^{\circ}C$.

In terms of suboptimality of the proposed control strategy, the quantitative studies showed that low percentages of suboptimality are obtained when a reduced number of energy profiles is sent to the producer controller in comparison to the centralized case, where the entire set of energy demand profiles is evaluated. Furthermore, to consider this reduced number of energy profiles becomes relevant when the prediction horizon and/or the number of consumers grow due to the required computational complexity which exponentially increases.

Another suboptimality result showed that to consider partially optimal energy profiles leads to a lower suboptimality compared with the optimal profiles generation criterion. Then, a trade-off between suboptimality minimization and computational complexity must be established.

Chapter 6

Application to a TRNSYS test case

In the previous chapter, an energy management approach based on local predictive controllers has been developed. The control proposal has been tested using simple linear models for the production-consumption system. In particular, the producer is represented by an energy storage unit that provides the energy required to maintain the buildings thermal comfort. This model allowed a quantitative analysis of the control strategy performance. The impact of the prediction horizon, number of energy profiles and energy profiles generation criterion have been studied.

The objective of this chapter is to test the control strategy developed in Chapter 5 on a more complex case. A simplified solar absorption cooling system for thermal comfort in buildings implemented in the TRNSYS simulation tool is used as case study. Then, the linear representation of the energy production-consumption system considered in the previous chapter is no longer adequate for prediction. As the producer is now represented by a solar hot water storage system composed of solar collector, heat exchanger and storage tank, the prediction model becomes nonlinear and hybrid. This entails the growth of the optimization complexity. In order not to add further complexity to the global optimization problem and according to the producer-consumer structure proposed in the previous chapter, the solar cooling installation studied here only considers one consumer composed of an absorption chiller and a building.

This chapter is organized as follows: the first part corresponds to the presentation and modeling of the solar cooling system. In a second part, a logic rule-based controller is tested on the system. Afterwards, an improved control strategy is introduced: a MPC strategy is carried out for the SHWS system while the consumer system controller remains simple. Finally, the MPC strategy developed in Chapter 5 is tested. Comparative results of the control strategies are studied.

6.1 The solar absorption cooling system

6.1.1 System description

Figure 6.1 depicts a solar absorption cooling system which is divided into two parts: the energy producer and the energy consumer. The producer corresponds to a solar hot water storage (SHWS) system and the consumer is composed of a building and an absorption chiller.

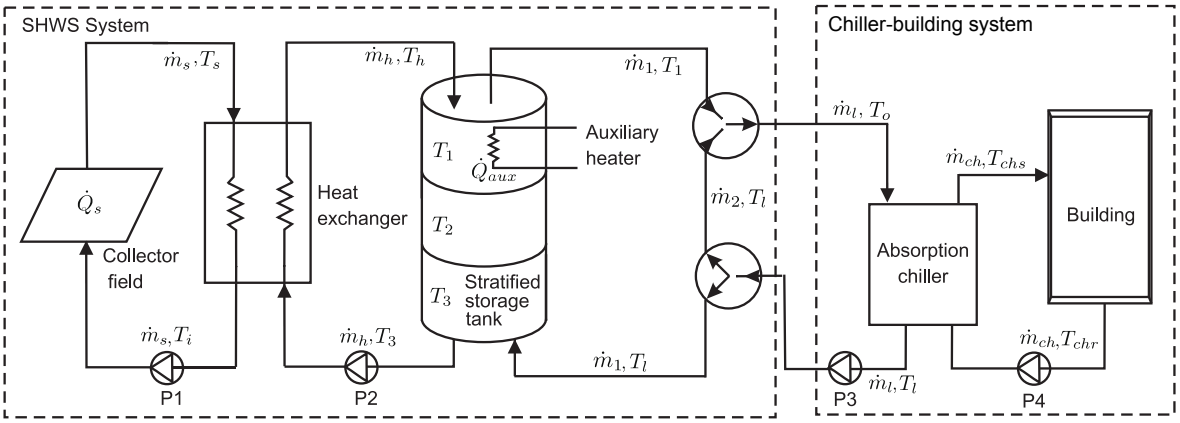

Figure 6.1: Solar cooling system

This system structure is close to the solar installation presented in Figure 3.4 of Chapter 3. The main difference with this latter is that in Figure 6.1 the cooling tower is not considered as an element of the installation. The details of the installation studied in this chapter are presented in Appendix B. The chilled water produced by the chiller is circulated to the building using a radiant ceiling. The absorption chiller is controlled by a logical signal that manipulates the water flows in the circulation pumps P3 and P4. When operating, the chiller imposes that the temperature of the inlet hot water $T_o(k)$ is constant (T_{set}) and delivers chilled water at a constant value T_{chs}. A control abstraction of the consumer composed by the building and the absorption chiller is given in Figure 6.2. The consumer is called chiller-building system from now on.

The meteorological data that influence the thermal comfort inside the building are considered as disturbances. In addition, the chiller-building system is subject to another disturbance: the hot water temperature $T_o(k)$ supplied by the SHWS system. The building thermal comfort must be guaranteed during occupancy periods.

The producer is composed of flat-plate collectors where the global area is 11.8 m^2, a constant effectiveness heat exchanger and a stratified storage tank of a 1.8 m^3 with an electric auxiliary heater at the top. A flow diverter and a mixing valve ensure that the temperature of the outgoing flow is set to the correct temperature $T_o(k)$. The flow rates of circulation pumps

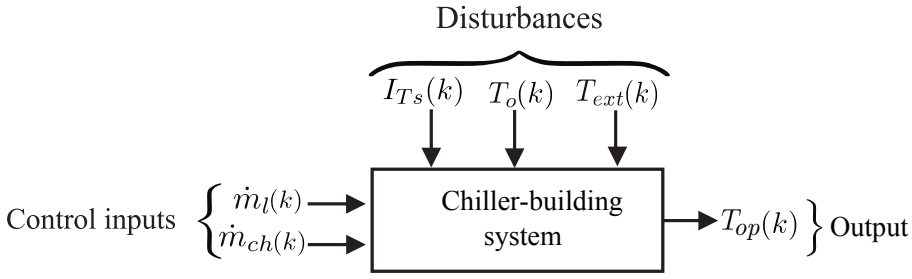

Figure 6.2: Disturbances (total radiation of building south wall $I_{Ts}(k)$, mixing valve outlet temperature $T_o(k)$ and exterior temperature $T_{ext}(k)$), control inputs (fluid mass flow rate in the chiller generator $\dot{m}_l(k)$ and evaporator $\dot{m}_{ch}(k)$) and output (building operative temperature $T_{op}(k)$) of the chiller-building system.

P1 and P2, as well as the auxiliary energy of the heater, can be controlled by continuous signals. For security reasons, the water temperatures in the various segments of the network must remain under the boiling point temperature T_{wbp}. A control abstraction of this system is given in Figure 6.3.

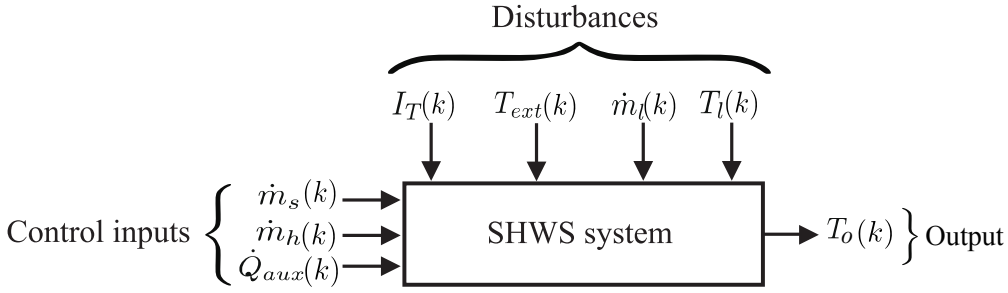

Figure 6.3: Disturbances (total radiation of building south wall $I_T(k)$, exterior temperature $T_{ext}(k)$, fluid mass flow rate in the chiller generator $\dot{m}_l(k)$ and outlet water temperature of the chiller generator $T_l(k)$), control inputs (auxiliary electric power $\dot{Q}_{aux}(k)$, fluid mass flow rate of the heat exchanger-collector loop $\dot{m}_s(k)$ and heat exchanger-tank loop $\dot{m}_h(k)$) and output (mixing valve outlet temperature $T_o(k)$) of the SHWS system.

6.1.2 Modeling

The model of the solar absorption cooling system is based on physical considerations for each subsystem and most of them are inspired by the TRNSYS documentation (TRNSYS17-Documentation, 2012). A global model is obtained from these subsystem models which are expressed in discrete time. In order to reduce the complexity of the model, the following assumptions are made:

- The specific heat of the fluid c remains constant throughout the system.

- The outlet and inlet temperatures of the circulation pumps are equal.
- The walls of the stratified storage tank are perfectly isolated.

6.1.2.1 Producer: SHWS system

As it can be seen in Figure 6.1, the SHWS system is composed of: a collector panel, a heat exchanger and a storage tank. Steady-state models for both collector panel and heat exchanger are used as the transient response of these elements is considered negligible compared to the working sampling time (0.5 hr) of the building model (which is detailed in Appendix A). Following the models of each element are presented.

Solar collector

As mentioned in Chapter 4, the collector model predicts the instantaneous performance of the component according to the collector manufacturer's data. The rate of energy change $\dot{Q}_s(k)$ transferred to the working fluid in the collector pipe is expressed as

$$\dot{Q}_s(k) = c\dot{m}_s(k)(T_s(k) - T_i(k)) = \eta A I_T(k), \tag{6.1.1}$$

where k represents each sample and the efficiency η is given by

$$\eta = a_0 - a_1\frac{(T_i(k) - T_{ext}(k))}{I_T(k)} - a_2\frac{(T_i(k) - T_{ext}(k))^2}{I_T(k)}, \tag{6.1.2}$$

where the coefficients a_0, a_1 and a_2 are the collector intercept efficiency, the efficiency slope and the efficiency curvature respectively. These coefficients are considered as provided by the collector manufacturer.

Heat exchanger

The heat exchanger is modeled considering its effectiveness ε constant. The maximum possible heat transfer is obtained with the minimum capacity rate fluid of the hot and cold side. The model is given by

$$\begin{aligned} T_i(k) &= T_s(k) - \frac{\varepsilon C_{min}(T_s(k) - T_3(k))}{c\dot{m}_s(k)} \\ T_h(k) &= T_3(k) + \frac{\varepsilon C_{min}(T_s(k) - T_3(k))}{c\dot{m}_h(k)} \end{aligned} \tag{6.1.3}$$

where

$$C_{min} = \min(c\dot{m}_s(k), c\dot{m}_h(k)) \tag{6.1.4}$$

Stratified storage tank

This component is modeled assuming that it consists of three fully-mixed equal volume segments and a perfectly thermally insulated structure. Two sets of differential equations are obtained according to the flow rate values in the cold and hot side of the tank. Thus, if the hot side flow rate $\dot{m}_h(k)$ is greater than the cold side one $\dot{m}_1(k)$, the set of differential equations (6.1.5) is used. Otherwise, the set of equations (6.1.6) describes the tank dynamics. Then, the energy balance in each segment is expressed as

If $\dot{m}_h(k) > \dot{m}_1(k)$

$$\begin{aligned} T_1(k+1) &= T_1(k) + \tfrac{\triangle t}{Vc\rho} \quad \Big(c\dot{m}_h(k)(T_h(k) - T_1(k)) + \dot{Q}_{aux}(k)\Big) \\ T_2(k+1) &= T_2(k) + \tfrac{\triangle t}{Vc\rho} \quad (c(\dot{m}_h(k) - \dot{m}_1(k))(T_1(k) - T_2(k))) \\ T_3(k+1) &= T_3(k) + \tfrac{\triangle t}{Vc\rho} \quad (c\dot{m}_h(k)(T_2(k) - T_3(k)) + c\dot{m}_1(k)(T_l(k) - T_2(k))) \end{aligned} \tag{6.1.5}$$

If $\dot{m}_1(k) \geq \dot{m}_h(k)$

$$\begin{aligned} T_1(k+1) &= T_1(k) + \frac{\triangle t}{Vc\rho} \left(c\dot{m}_1(k)(T_2(k) - T_1(k)) \right. \\ &\quad \left. + c\dot{m}_h(k)(T_h(k) - T_2(k)) + \dot{Q}_{aux}(k)\right) \\ T_2(k+1) &= T_2(k) + \frac{\triangle t}{Vc\rho} \left(c(\dot{m}_1(k) - \dot{m}_h(k))(T_3(k) - T_2(k))\right) \\ T_3(k+1) &= T_3(k) + \frac{\triangle t}{Vc\rho} \left(c\dot{m}_1(k)(T_l(k) - T_3(k))\right) \end{aligned} \tag{6.1.6}$$

where V is the volume of the storage tank, c is the specific heat of the circulating water, ρ is the water density and $\triangle t$ is the sampling period.

Flow diverter and mixing valve

These components mix the flow from the tank and the flow from the load to limit the temperature of the SHWS system outlet flow when the tank temperature $T_1(k)$ is greater than the chiller hot inlet set-point temperature T_{set}.

They are modeled by the following equations:

$$\gamma(k) = \begin{cases} (T_{set} - T_l(k))/(T_1(k) - T_l(k)) & T_1(k) > T_{set} \\ 1 & T_1(k) \leq T_{set} \end{cases} \tag{6.1.7}$$

$$\dot{m}_1(k) = \gamma(k)\dot{m}_l(k) \tag{6.1.8}$$
$$\dot{m}_2(k) = \dot{m}_l(k)(1-\gamma(k)) \tag{6.1.9}$$

Consequently, the outlet flow rate and temperature of the mixing valve are given by

$$T_o(k) = \frac{\dot{m}_1(k)T_1(k)+\dot{m}_2(k)T_l(k)}{\dot{m}_l(k)} \tag{6.1.10}$$
$$\dot{m}_l(k) = \dot{m}_1(k)+\dot{m}_2(k) \tag{6.1.11}$$

Overall SHWS system model

In order to obtain a global model of the producer, the models of each of the components are grouped. The resulting global model is a hybrid nonlinear system of the form

If $\dot{m}_h(k) > \dot{m}_1(k)$

$$T_1(k+1) = T_1(k)+\frac{\triangle t}{Vc\rho}\left(c\dot{m}_h(k)(T_3(k)-T_1(k))+\dot{Q}_s(k)+\dot{Q}_{aux}(k)\right) \tag{6.1.12}$$

$$T_2(k+1) = T_2(k)+\frac{\triangle t}{Vc\rho}\left(c(\dot{m}_h(k)-\dot{m}_1(k))(T_1(k)-T_2(k))\right)$$
$$T_3(k+1) = T_3(k)+\frac{\triangle t}{Vc\rho}\left(c\dot{m}_h(k)(T_2(k)-T_3(k))+c\dot{m}_1(T_l(k)-T_2(k))\right)$$

If $\dot{m}_1(k) \geq \dot{m}_h(k)$

$$\begin{aligned} T_1(k+1) &= T_1(k)+\frac{\triangle t}{Vc\rho}\left(c\dot{m}_1(k)(T_2(k)-T_1(k))\right. \\ &\quad \left.+c\dot{m}_h(k)(T_3(k)-T_2(k))+\dot{Q}_s(k)+\dot{Q}_{aux}(k)\right) \end{aligned} \tag{6.1.13}$$
$$T_2(k+1) = T_2(k)+\frac{\triangle t}{Vc\rho}\left(c(\dot{m}_1(k)-\dot{m}_h(k))(T_3(k)-T_2(k))\right)$$
$$T_3(k+1) = T_3(k)+\frac{\triangle t}{Vc\rho}\left(c\dot{m}_1(k)(T_l(k)-T_3(k))\right)$$

where

$$\dot{Q}_s(k) = \begin{cases} \eta A I_T(k) & \dot{m}_h(k), \dot{m}_s(k) \neq 0 \\ 0 & \dot{m}_h(k), \dot{m}_s(k) = 0 \end{cases} \tag{6.1.14}$$

The outlet temperatures of the collector, heat exchanger and mixing valve are defined as follows

$$T_h(k) = \begin{cases} \frac{\dot{Q}_s(k)}{c\dot{m}_h(k)} + T_3(k) & \dot{m}_h(k) > 0 \\ T_3(k) & \dot{m}_h(k) \leq 0 \end{cases} \tag{6.1.15}$$

$$T_s(k) = \begin{cases} \frac{\dot{Q}_s(k)}{eC_{min}} + T_3(k) & C_{min}(k) > 0 \\ T_3(k) & C_{min}(k) \leq 0 \end{cases} \tag{6.1.16}$$

$$T_i(k) = \begin{cases} T_s(k) - \frac{\dot{Q}_s(k)}{c\dot{m}_s(k)} & \dot{m}_s(k) > 0 \\ T_3(k) & \dot{m}_s(k) \leq 0 \end{cases} \tag{6.1.17}$$

$$T_o(k) = \begin{cases} \frac{\dot{m}_1(k)T_1(k)+\dot{m}_2(k)T_l(k)}{\dot{m}_1(k)+\dot{m}_2(k)} & \dot{m}_l(k) > 0 \\ T_1(k) & \dot{m}_l(k) \leq 0 \end{cases} \tag{6.1.18}$$

6.1.2.2 Consumer: chiller-building system

The building model is represented as follows

$$x(k+1) = Ax(k) + Bu(k) + Fd(k) \tag{6.1.19}$$

$$T_{op}(k) = Cx(k) \tag{6.1.20}$$

where $T_{op}(k)$ represents the operative temperature of the building. The control input $u(k)$ is the water flow rate of the absorber and evaporator circuits $\dot{m}_{ch}$ that as well as the flow rate $\dot{m}_l$ in the chiller generator circuit, depends on a binary control signal $On(k)$ as following:

$$\dot{m}_{ch}(k) = \dot{m}_{ch,nominal}On(k) \tag{6.1.21}$$

$$\dot{m}_l(k) = \dot{m}_{l,nominal}On(k) \tag{6.1.22}$$

and

$$On(k) = \epsilon \{0, 1\} \tag{6.1.23}$$

where $\dot{m}_{ch,nominal}$ and $\dot{m}_{l,nominal}$ are constants. The building is subject to disturbances as the exterior temperature T_{ext} and the solar radiation $I_{Ts}(k)$ which form the vector $d(k) = [T_{ext}(k), I_{Ts}(k)]^T$.

The temperature of the radiant ceiling outlet water $T_{chr}(k)$ is approximated by the following relation:

$$T_{chr}(k) = \kappa T_{op}(k) \tag{6.1.24}$$

This temperature is considered as a function of the building operative temperature $T_{op}(k)$ where κ is a constant. It is worth noting that this approximation is valid for the TRNSYS simulation model (detailed in Appendix B) and in practice, it may not be an adequate approximation of a radiant ceiling dynamics.

Besides, it is assumed that cooling and heating power in the absorption chiller are related by a constant effectiveness ϱ of the following form

$$\dot{Q}_{cool}(k) = \varrho \dot{Q}_{hot}(k) \tag{6.1.25}$$

where $\dot{Q}_{cool}(k)$ is the cooling power in the absorber/evaporator circuit and $\dot{Q}_{hot}(k)$ is the heating power in the generator circuit, defined as

$$\dot{Q}_{cool}(k) = c\dot{m}_{ch}(k)(T_{chr}(k) - T_{chs}) \tag{6.1.26}$$

$$\dot{Q}_{hot}(k) = c\dot{m}_{l}(k)(T_{o}(k) - T_{l}(k)) \tag{6.1.27}$$

In equation (6.1.26), it is assumed that the chilled temperature T_{chs} supplied to the building is constant and does not depend on chiller internal temperatures or pressure conditions.

From the above equations, the return hot water temperature $T_l(k)$ is defined as follows

$$T_l(k) = T_o(k) - \frac{\dot{m}_{ch}(k)}{\varrho \dot{m}_l(k)}(T_{chr}(k) - T_{chs}) \tag{6.1.28}$$

6.1.3 Operating conditions of the solar cooling system

The operating requirements of the solar cooling system can be summarized as follows

- The main objective of the solar cooling system is to guarantee the building thermal comfort maintaining the operative temperature of the building $T_{op}(k)$ as close as possible to the corresponding set-point during occupancy periods.
- During the chiller operating periods, the hot water temperature $T_1(k)$ at the top of the storage tank must remain at least at the fixed set-point temperature T_{set} in order to supply the required hot water temperature to the chiller.

- The outlet temperatures of the collector $T_s(k)$, heat exchanger $T_i(k)$, $T_h(k)$ and storage tank $T_1(k)$, $T_2(k)$, $T_3(k)$ must remain under the boiling point temperature T_{wbp} for security reasons.

These requirements can be guaranteed controlling the circulations pumps of the SHWS system and the pumps of the absorption chiller which operates at turn on/off events. It should be reminded that the solar cooling system is subject to weather conditions.

6.2 Logic rule-based control approach

The hysteresis control strategy introduced in Section 5.2 is tested on the TRNSYS model of a solar cooling system (see Appendix B). The control strategy is carried out using local hysteresis controllers included in the TRNSYS library.

The chiller-building controller manipulates the chiller flow rate of the circulation pumps in order to maintain the building temperature at a desired value during occupancy periods. It is a hysteresis controller that turns the chiller on/off according to the building operative temperature.

The producer controller manipulates the water flow rates of the SHWS system circulation pumps. It switches the circulation pumps P1 and P2 on at the maximal flow rate when the collector temperature $T_s(k)$ is greater than the temperature in the tank $T_3(k)$ with a safety condition that the temperature at the top of the tank $T_1(k)$ is below the boiling point temperature T_{wbp}.

The SHWS system controller switches the auxiliary heater on at its maximum power in order to ensure that the water temperature of the upper segment of the tank is at least T_{set} when the chiller is operating.

An example of the behavior of the system under this control is displayed in Figures 6.4 and 6.5. The tests are carried out during one week with a sampling period of $\triangle t = 0.5$ hr. In Figure 6.4, the initial temperature at the top of the tank is set at $T_1 = 82$°C and the operative temperature in the building begins at $T_{op} = 27$°C. Figure 6.5 depicts the simulation results taking into account a higher tank initial temperature $T_1 = 111$°C whereas the building operative temperature remains at $T_{op} = 27$°C.

From top to bottom of Figure 6.4, the first panel shows the storage tank temperature $T_1(k)$ evolution (blue curve), its upper and lower bounds (red curves), and the chiller water flow rate (black curves). The value of the latter curve is modified in order to fit in the figure. The second panel of the figure represents the collector outlet flow temperature (blue curve) and its upper limit (red curve). The third and fourth panel are the water flow rate $\dot{m}_h(k)$ in the

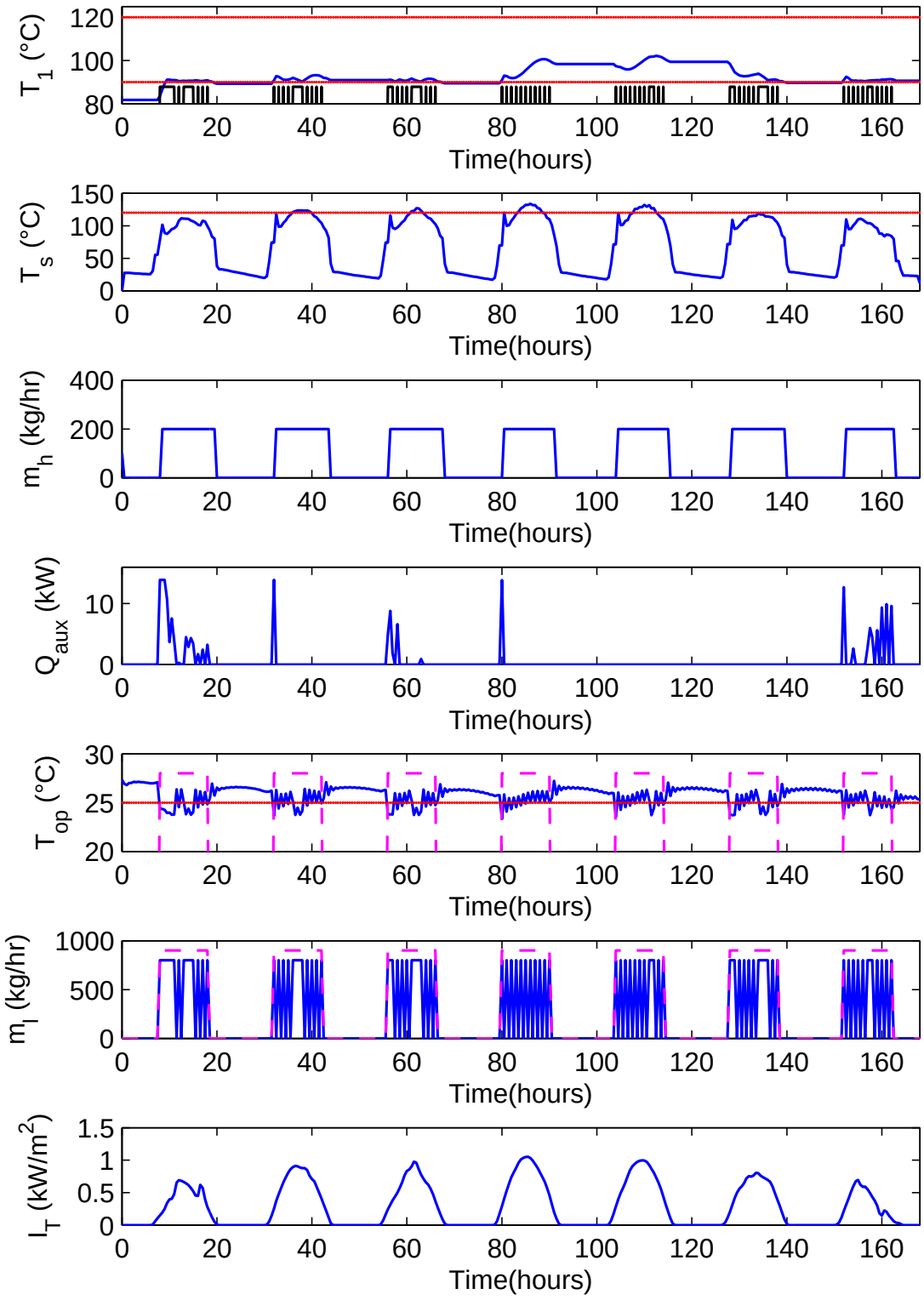

Figure 6.4: Logic rule-based controller: $T_1 = 82$ °C and $T_{op} = 27$ °C

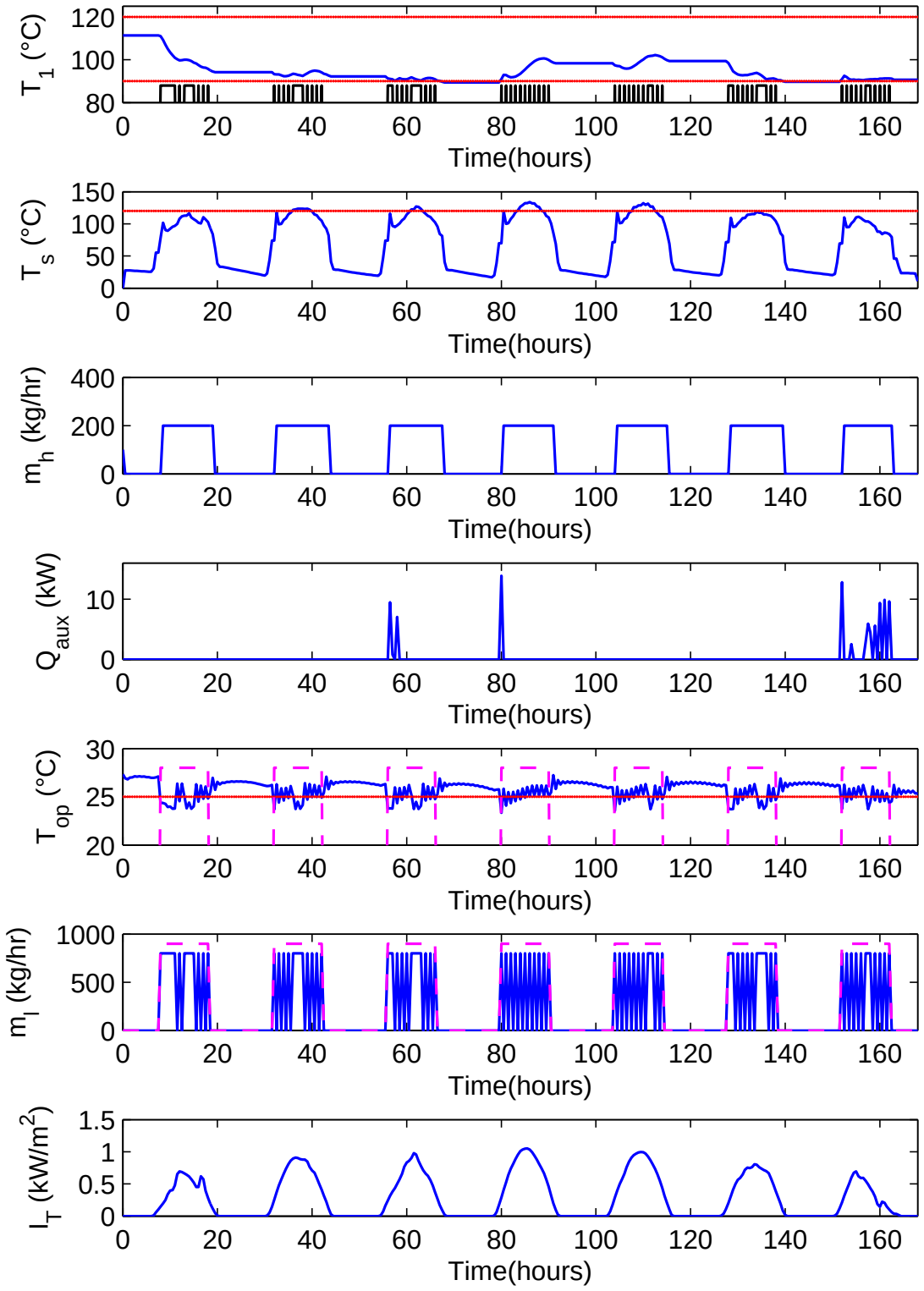

Figure 6.5: Logic rule-based controller: $T_1 = 111$ °C and $T_{op} = 27$ °C

SHWS system and the auxiliary electric energy $\dot{Q}_{aux}(k)$ respectively. The fifth panel of the figure depicts the building temperature $T_{op}(k)$ (blue curve), the occupancy periods (dashed magenta lines) and the temperature set-point (red line). Finally, the last panel shows the solar radiation $I_T(k)$.

From Figure 6.4, it can be noticed the on-off behavior of the water flow rate $\dot{m}_l(k)$. During occupancy periods (dashed magenta lines), the building hysteresis controller manipulates the water flow rate $\dot{m}_l(k)$ in order to maintain the building operative temperature as close as possible to the set-point temperature which is set at 25°C. From a practical point of view, it is desirable to avoid this on-off behavior which leads to efficiency losses in the absorption machine.

As the initial tank temperature $T_1(k)$ starts at 82°C, the SHWS hysteresis controller tries to ensure the temperature requirement by activating the electric heater $\dot{Q}_{aux}(k)$ during occupancy periods and until the temperature $T_1(k)$ reaches the desired set-point $T_{set} = 90$°C. There is no anticipation when auxiliary energy is applied, which leads to the non respect of the tank temperature condition: the temperature $T_1(k)$ reaches the set-point temperature two hours after the occupancy period has started.

It is worth noting that according to the SHWS hysteresis control structure, the hysteresis controller that manipulates the auxiliary energy $\dot{Q}_{aux}(k)$ can be activated only during occupancy periods and it does not depend on the working periods of the absorption chiller. This can lead to auxiliary energy waste or the non respect of temperature conditions for the SHWS system.

As the LRBC strategy does not take into account the upper limit condition of the collector outlet temperature $T_s(k)$, at some points this variable is above its limit T_{wbp} when solar radiation is important. This phenomenon compromises the solar cooling installation since collector stagnation temperatures must be avoided.

From 6.5 it can be noticed that even if the tank initial temperature is well above its lower limit, its decreasing trend is important when the chiller operates. This is due to the weak solar radiation. In contrast, the tank temperature behavior remains stable in the fourth and fifth day because of the higher solar radiation. In addition, from Figure 6.5 it can be seen that lower electricity is used compared to the previous experiment which is due to the higher initial tank temperature.

From these results, several control improvements are required:

- The application of auxiliary energy $\dot{Q}_{aux}(k)$ must be anticipated in order to ensure that the temperature $T_1(k)$ is above the set-point temperature T_{set} required to the correct

operation of the absorption chiller.

- The use of auxiliary energy $\dot{Q}_{aux}(k)$ must depend on the chiller working periods.
- It is necessary to minimize the on-off behavior of the chiller working periods.
- The respect of upper and limit temperatures of SHWS system components must be ensured by a better management of the water flow rates which are in function of disturbances as the weather conditions.

In the following section, an improved control strategy is presented. In order to ensure the SHWS system constraints fulfillment, a model predictive controller is developed for this subsystem whereas the chiller-building controller remains simple but with a prediction ability.

6.3 Mixed MPC-LRBC strategy for the solar cooling system

In this section, an improved control strategy for the solar cooling system is studied. The objective of this strategy is to guarantee the constraints fulfillment in the SHWS system while maintaining a straightforward control strategy in the chiller-building system. This control structure combines a model predictive control strategy for the SHWS system with a logic rule-based control (LRBC) strategy for the chiller-building system. That is, there is no on-line optimization for the consumption part but it is considered that a flow rate profile generator sends the energy demand profile to the SHWS system which calculates its local nonlinear optimization as a function of the energy demand profile received.

6.3.1 The chiller-building system controller

The structure of the consumer controller is displayed in Figure 6.6. The chiller-building model is an identified four order linear model in the state-space form whose inputs are the exterior air temperature $T_{ext}(k)$, the total tilted radiation of the surface oriented to the south $I_{Ts}(k)$ and the chiller water flow rate $\dot{m}_{ch}(k)$ as described in Section 6.1.2.2.

The hysteresis controller follows the same rules as in Section 6.2. According to the occupancy profile $\delta(\overline{k})$ over the prediction horizon N_h, the set-point temperature T_{sbg} and the current building temperature $T_{op}(k)$, it decides to switch the chiller and pumps on/off. The sequence of decision is logged to provide the flow rate profile to the SHWS system. The observer is used to initialize the state of the building model at each sampling time taking the current measure of the building operative temperature $y_m(k)$, the chiller-building disturbances $d(k)$ and control signal $u(k)$. It is a classic Luenberger observer of the form

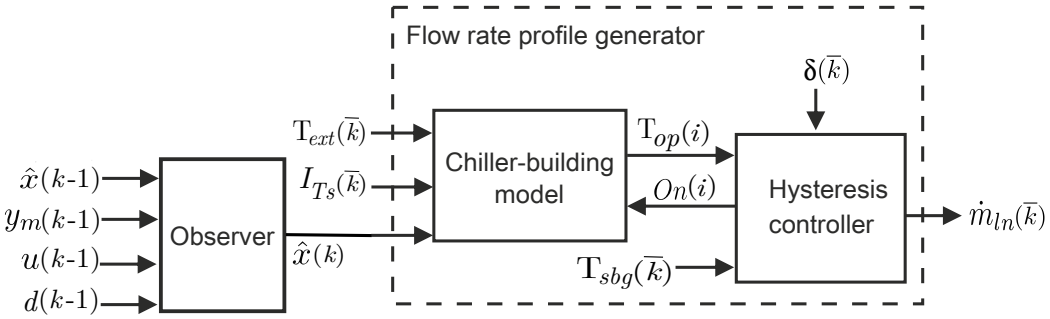

Figure 6.6: Consumer controller structure. Observer inputs: previous state vector $\hat{x}(k-1)$, measured building operative temperature $y_m(k-1)$, previous control signal $u(k-1)$ and disturbances $d(k-1)$. Chiller-building model inputs: exterior temperature $T_{ext}(\overline{k})$ over the prediction horizon, total radiation of the building south-oriented wall $I_{Ts}(\overline{k})$ over the prediction horizon, current estimated state vector $\hat{x}(k)$ and current control signal calculated by the hysteresis controller $On(i)$. Hysteresis controller inputs: occupancy profile $\delta(\overline{k})$ over the prediction horizon, current building operative temperature calculated by the model $T_{op}(k)$ and building set-point $T_{sbg}(\overline{k})$ over the prediction horizon. The output of the hysteresis controller is the generated energy demand profile $\dot{m}_{ln}(\overline{k})$ over the prediction horizon.

$$\hat{x}(k+1) = A\hat{x}(k) + Bu(k) + Fd(k) + L[y_m(k) - \hat{y}(k)] \quad (6.3.1)$$

$$\hat{y}(k) = C\hat{x}(k) \quad (6.3.2)$$

Finally, the generated flow rate profile $m_{ln}(\overline{k})$ over the prediction horizon is sent to the SHWS system controller.

6.3.2 The SHWS system controller

6.3.2.1 From the producer generalized model to the SHWS system model

According to the generalized model presented in section 5.1.1:

$$X_1(k+1) = f_{1\sigma(k)}(\overline{U}_1(k), W_{21}(k)) \quad (6.3.3)$$

The state vector, the vector of controlled variables, the disturbances vector and the vector of interacting variables for the SHWS system are defined as follows

$$X_1(k) = [T_1(k), T_2(k), T_3(k)] \tag{6.3.4}$$
$$U_1(k) = [\dot{m}_s(k), \dot{m}_h(k), \dot{Q}_{aux}(k)] \tag{6.3.5}$$
$$D_1(k) = [I_T(k), T_{ext}(k)] \tag{6.3.6}$$
$$W_{21}(k) = [\dot{m}_l(k), T_l(k)] \tag{6.3.7}$$

The interacting variable $W_{21}(k)$ is determined by the influence of the chiller-building system on the SHWS system.

The system constraints stated in Equation (5.1.7)

$$H_{1\sigma(k)}(\overline{U}_1(k), W_{21}(k)) \leq \mathbf{0} \tag{6.3.8}$$

is also a nonlinear hybrid set. The choice of the active mode influences the dynamics and also the constraints set.

The output constraints in Equation (6.3.8) according to the SHWS system model, can be expressed in an explicit way as

$$T_1(k), T_2(k), T_3(k), T_h(k), T_s(k), T_i(k) \leq T_{wbp}(k) \tag{6.3.9}$$

$$T_1(k) \geq T_{set}(k) \qquad if \quad \dot{m}_l(k) > 0 \tag{6.3.10}$$

Equation (6.3.9) represents the limit temperature constraint of the SHWS system to ensure safety performance of the system. Then, each temperature must remain below the water boiling point limit $T_{wbp}(k)$. Equation (6.3.10) refers to the minimum required operating temperature at which $T_1(k)$ must be when there is a chiller energy demand.

The vector of the SHWS system controlled variables is subject to lower and upper bounds as follows

$$U_{1\,\min} \leq U_1(k) \leq U_{1\,\max} \tag{6.3.11}$$

6.3.2.2 Prediction of disturbances

As it can be seen in Figure 6.3, the SHWS system is subjected to four disturbances. The first two of them are meteorological disturbances ($I_T(k)$, $T_{ext}(k)$).

The external temperature $T_{ext}(k)$ is necessary to calculate the collector efficiency loss (Equation (6.1.2)). Nevertheless, it has a low impact when the solar radiation is important. Moreover, in practice the solar panel is switched off when the solar radiation is low. Consequently, the knowledge of this disturbance is not crucial.

In contrast, the solar radiation $I_T(k)$ is the fundamental energy source and it has a very high impact on the behavior of the SHWS system. It is then necessary to have a good prediction of it. This is why, it is supposed that an external forecast system provides this prediction. It is reasonable to suppose that this forecast system also provides the external temperature prediction.

The two last disturbances ($\dot{m}_l(k)$, $T_l(k)$) come from the building cooling system. The hot water outlet temperature $T_l(k)$ is directly related to the internal air temperature of the building as described in Equation (6.1.28). The prediction of this temperature is obtained from this equation and taking into account the measure of the operative temperature at each sampling time.

The hot water flow rate $\dot{m}_l(k)$ has a deep impact on the global system: it is directly linked to the energy consumption, as it can cause the SHWS temperatures decrease. Besides, an operative constraint has to be fulfilled when the cooling system is operating (see Equation (6.3.10)). It is then necessary to get a good prediction of this variable. The latter is controlled by the building cooling controller which provides its prediction.

When the solar radiation is significant, the temperatures in the SHWS system can be too high. To avoid overheating while maximizing the solar energy use, the solution is to force the activation of the cooling system, even if the building does not really need it. As a consequence, the variable $\dot{m}_l(k)$ used in the prediction model is the sum of the flow rate $\dot{m}_{ln}(k)$ which is actually provided by the building cooling controller (see Section 6.3.1) and a flow rate $\triangle\dot{m}_l(k)$ which is manipulated by SHWS controller and, as the consumer flow rate $\dot{m}_{ln}(k)$, has a discrete behavior. Consequently, the controlled variables for the SHWS system in Equation (6.3.5) is rewritten as follows

$$U_1(k) = [\dot{m}_s(k), \dot{m}_h(k), \dot{Q}_{aux}(k), \triangle\dot{m}_l(k)] \tag{6.3.12}$$

6.3.2.3 Initial optimization problem

Given a prediction horizon N_h, the objective of the predictive controller is to minimize the energy use of the SHWS system, while fulfilling the constraints. The energy is consumed because of the auxiliary electrical heater $\dot{Q}_{aux}(k)$ and because of the activation of the pumps, which is linked to the flow rates $\dot{m}_s(k)$ and $\dot{m}_h(k)$.

Under these considerations, the optimization criterion is given by

$$\begin{aligned} J_1(U_1(\overline{k})) &= \sum_{j=1}^{N_h} \alpha_{\dot{Q}_{aux}} \left\| \dot{Q}_{aux}(k+j-1) \right\|_p^p + \alpha_{\dot{m}_s} \left\| \dot{m}_s(k+j-1) \right\|_p^p \\ &\quad + \alpha_{\dot{m}_h} \left\| \dot{m}_h(k+j-1) \right\|_p^p + \alpha_{\triangle \dot{m}_l} \left\| \triangle \dot{m}_l(k+j-1) \right\|_p^p \end{aligned} \tag{6.3.13}$$

In this multi-criteria objective, the variables $\alpha_{\dot{Q}_{aux}}, \alpha_{\dot{m}_s}$, $\alpha_{\triangle \dot{m}_l}$ and $\alpha_{\dot{m}_h}$ are weighting factors and $\|v\|_p^p$ is the ℓ^p-norm of vector v with exponent p. The optimization problem can be defined as follows

Problem 6.3.1 *Initial Optimization Problem. At time k, given the current state of the system $X_1(k)$ and the prediction of the disturbances $D_1(\overline{k})$, the optimization problem for the producer is formulated as follows*

$$\min_{U(\overline{k})} J_1(U_1(\overline{k})) \tag{6.3.14}$$

$s.t. \quad \forall j = 1, \ldots, N_h,$

$$\begin{aligned} X(k+j) &= f_{\sigma(\bar{U}_1(k+j-1))}(\bar{U}_1(k+j-1)) \\ H_{\sigma(\bar{U}_1(k+j-1))}(\bar{U}_1(k+j-1)) &\leq 0 \\ U_{1\min} \leq U_1(k+j-1) &\leq U_{1\max} \\ \triangle \dot{m}_l(k+j-1) \quad \epsilon \quad \{0, \dot{m}_{l,nominal}\} & \end{aligned} \tag{6.3.15}$$

Several points should be noticed:

- The first point is linked to the complexity of the optimization problem: in this current formulation, the resulting optimization problem is highly nonlinear and current available solvers fail. Some additional assumptions are made in order to simplify the optimization problem[1]. It will be simplified assuming that the two flow rates $\dot{m}_s(k)$, $\dot{m}_h(k)$ are equal. This reduces the size of the optimization variables.

- The second point is linked to the behavior of the system when the flow rate $\dot{m}_h(k)$ circulation is switched off and the solar radiation is significant, as the results obtained in the logic rule-based control strategy in Section 6.2. At this point, the collector

[1]The solver used is the MATLAB function *fmincon*, with the active-set method.

temperature considerably increases which may put at risk the security of the solar installation. To avoid this phenomenon, the lower bound of $\dot{m}_h(k)$ is increased from 0 to $\dot{m}_{h,\min}$ only when the solar radiation is significant. Consequently, the lower bound of $\dot{m}_h(k)$ is modified according to the following condition:

$$\dot{m}_h(k), \dot{m}_s(k) \text{ lower bound} = \begin{cases} 0 & \text{if} \quad I_T < I_{T_{min}} \\ \dot{m}_{h,\min} & \text{if} \quad I_T \geq I_{T_{min}} \end{cases} \tag{6.3.16}$$

where $I_{T_{min}}$ is a constant.

- The third point is related to the discrete nature of $\triangle\dot{m}_l(k)$. In order to simplify the resolution of the optimization problem, $\triangle\dot{m}_l(k)$ is considered as a continuous value with upper and lower limits set at $\dot{m}_{l,\text{nominal}}$ and 0 respectively. A post treatment of this variable is done to obtain the equivalent binary value required for the application.

- The last point is linked to the feasibility of the optimization problem. The slack variable $\lambda(k) > 0$ is added to soften the constraints. In particular, the constraint in Equation (6.3.10) is relaxed as follows

$$T_1(k) \geq T_{set}(k) - \lambda(k) \qquad if \quad \dot{m}_l(k) > 0 \tag{6.3.17}$$

The slack variable is integrated in the criterion by the term:

$$J_\lambda(\lambda\overline{k}) = \sum_{j=1}^{N_h} \alpha_\lambda \left\| \lambda(k+j-1) \right\|_p^p \tag{6.3.18}$$

Then, $\widetilde{U}_1(k) = [\dot{m}_h(k), \dot{Q}_{aux}(k), \triangle\dot{m}_l(k), \lambda(k)]$ is the vector of the new optimization variables. The optimization problem for the SHWS system controller can be formalized as

Problem 6.3.2 *Practical Optimization Problem. At time k, given the current state of the system $X_1(k)$, the prediction of the disturbances $D_1(\overline{k})$ and the energy demand profile $\dot{m}_{ln}$ controller over the prediction horizon N_h, the optimization problem for the producer is formulated as follows*

$$\min_{U(\overline{k})} J_1(U_1(\overline{k})) + J_\lambda(\lambda(\overline{k})) \tag{6.3.19}$$

$s.t. \quad \forall j = 1, \ldots, N_h,$

$$\begin{gathered} \dot{m}_s(k+j) := \dot{m}_h(k+j) \\ X(k+j) = f_{\sigma(\bar{U}_1(k+j-1))}(\bar{U}_1(k+j-1)) \\ H_{\sigma(\bar{U}_1(k+j-1))}(\bar{U}_1(k+j-1)) + H_{\sigma(\bar{U}_1(k+j-1))}(\lambda(k+j-1)) \leq 0 \\ \widetilde{U}_{1\,\min} \leq \widetilde{U}_1(k+j-1) \leq \widetilde{U}_{1\,\max} \end{gathered} \tag{6.3.20}$$

A post treatment is done before sending the control to the system. As the variable $\triangle\dot{m}_l(k)$ has been relaxed, the interpretation of its optimal value $\triangle\dot{m}_l(k)^\star$ is given by

$$\triangle\dot{m}_l(k) = \begin{cases} 0 & \text{if} \quad \triangle\dot{m}_l(k)^\star < \alpha_t \dot{m}_{l,\text{nominal}} \\ \triangle\dot{m}_l(k)^\star & \text{if} \quad \triangle\dot{m}_l(k)^\star \geq \alpha_t \dot{m}_{l,\text{nominal}} \end{cases} \tag{6.3.21}$$

Where α_t is a constant.

6.3.3 Control architecture

The global control architecture is displayed in Figure 6.7. At each sampling time, the value of the building operating temperature $y_m(k)$ is sent to the chiller-building controller. The latter uses the weather forecast and the occupancy profile to generate the chilled water profile ($\dot{m}_{ln}$, which is communicated to the SHWS system controller). Using this profile, the weather forecast and the temperature measurements ($T_l(k)$, $T_i(k)$, $T_1(k)$, $T_2(k)$ and $T_3(k)$), the SHWS system controller computes the control signal sent to the SHWS plant and the consumption request $\Delta\dot{m}_l(k)$ sent to the chiller-building controller which computes the control signal of the chiller $On(k)$.

6.3.4 Simulation results

The controller strategy has been tested using the same scenario as in Section 6.2. The model and controllers parameters are detailed in Appendix A and the results are presented in Figure 6.8 and 6.9. The prediction horizon for the SHWS predictive controller has been set at $N_h = 8$ (4 hours) and it is considered that there is no disturbances prediction error. The criterion to select the prediction horizon has been chosen taking into account a trade-off between optimization complexity and anticipation capacity. In Figure 6.8, the initial temperature at the top of the tank is set at $T_1 = 82$°C and the operative temperature in the building begins at $T_{op} = 27$°C. In Figure 6.9, the tank initial temperature is set at $T_1 = 111$°C and the building temperature remains at $T_{op} = 27$°C.

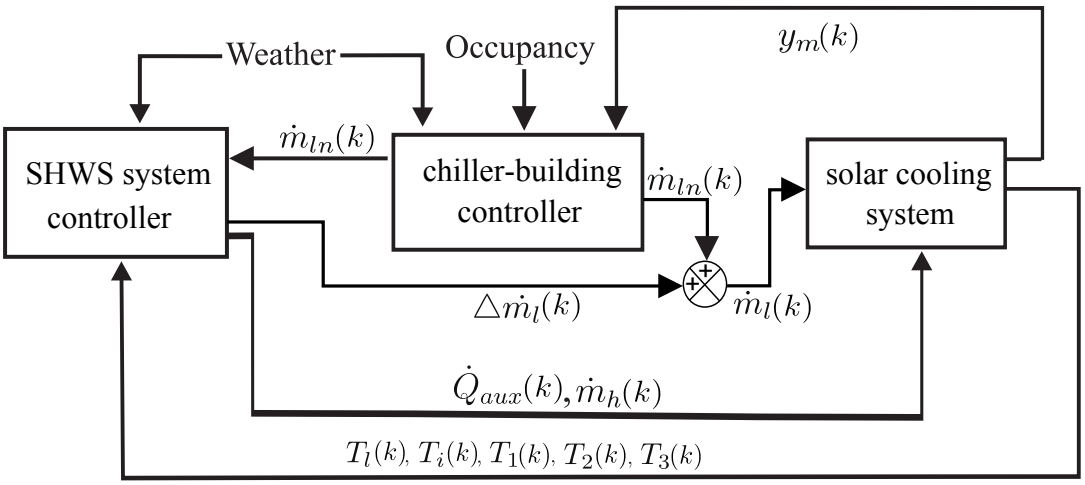

Figure 6.7: Global architecture of control

The objective of the predictive controller is to minimize the energy consumption of the system which could be translated into a linear optimization criterion. However, this has been chosen in a quadratic form in order to provide more convexity properties to the optimization problem. Furthermore, the terms included in the criterion are not only related to energy consumption but to the constraints fulfillment. According to Equation (6.3.13) and (6.3.18), $\|v\|_p^p$ has been considered as $\|v\|_2^2$.

The weighting factor values of the producer optimization cost function in Equation (6.3.13) and (6.3.18) are: $\alpha_{\dot{Q}_{aux}} = 1 \cdot 10^{-5}$, $\alpha_{\dot{m}_h} = 1 \cdot 10^{-2}$, $\alpha_{\triangle\dot{m}_l} = 1 \cdot 10^{8}$ and $\alpha_{\lambda} = 1 \cdot 10^{10}$. These values have been chosen according to the following: firstly, the variables $\triangle\dot{m}_l(k)$ and $\lambda(k)$ are highly penalized as they are not part of the initial optimization problem and they have been added to the criterion to facilitate the optimization problem resolution; and secondly, the variables $\dot{Q}_{aux}$ and $\dot{m}_h$ have the same impact on the optimization cost as they contribute to the SHWS system temperature constraint fulfillment.

From Figure 6.8 it can be noticed the on-off behavior of the chiller $\dot{m}_l(k)$ due to the predictive hysteresis controller. Unlike the logic rule-based control strategy, the predictive hysteresis controller anticipates the use of the auxiliary electric energy $\dot{Q}_{aux}(k)$ in order to ensure the correct temperature value $T_1(k)$ at the top of the tank.

The results in Figures 6.8 and 6.9 show that the fulfillment of the collector temperature constraint regarding the maximum permissible temperature T_{wbp} has been considerably improved compared with the results obtained in the logic rule-based controller of Section 6.2. Nevertheless, some minimal constraint violations occur in the first and fifth day. It has been found that this is caused by the inaccuracy of the prediction model.

From the second panel of Figure 6.8, it can be noticed in the first and last day a sudden peak

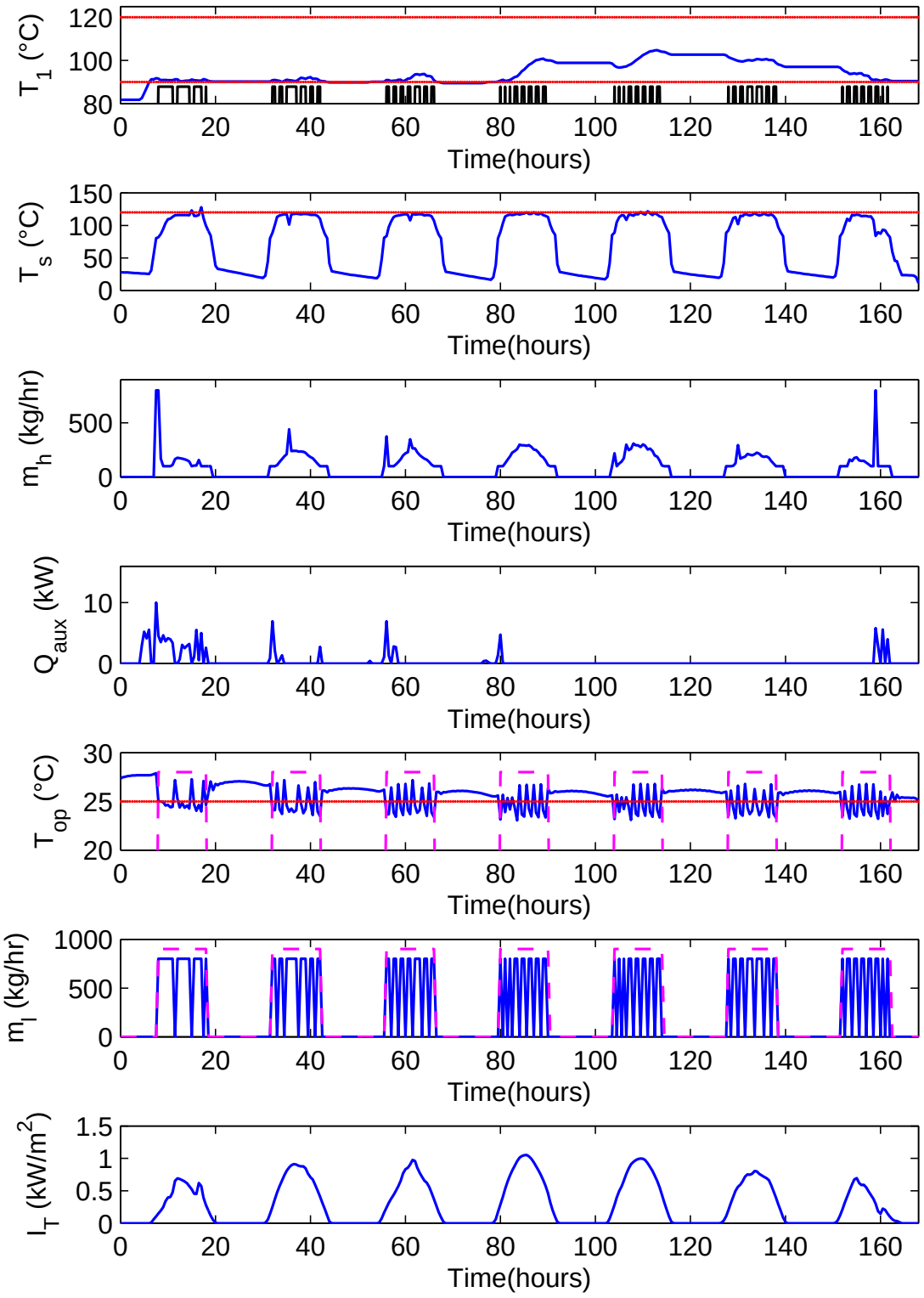

Figure 6.8: MPC-hysteresis strategy considering $T_1 = 82$ °C and $T_{op} = 27$ °C

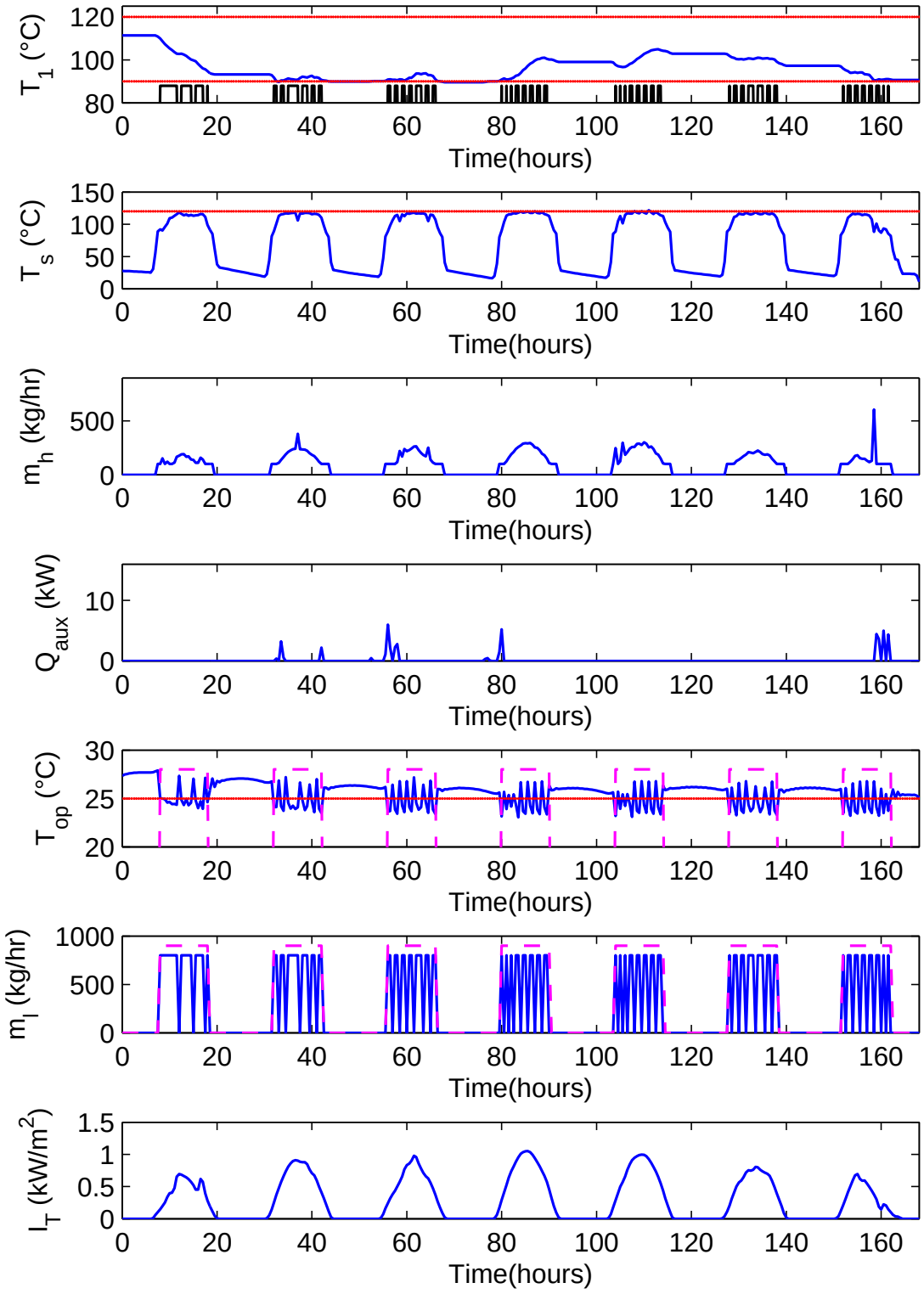

Figure 6.9: MPC-hysteresis strategy considering $T_1 = 111$ °C and $T_{op} = 27$ °C

in the flow rate $\dot{m}_h$. At this point, the electric heater power is also high. Even if the solver found a feasible solution, this behavior is not desirable from a practical point of view. At this point, the solar radiation and the tank temperature $T_1(k)$ are weak. Consequently, it is expected that the water flow from the collector to the tank remains low in order to allow the heating of the tank water using the auxiliary heater. In contrast, this phenomenon is not presented in the first day of Figure 6.9 as the tank initial temperature is well above its lower limit. Also, it can be noticed that lower auxiliary energy is required compared with the results in Figure 6.8.

Compared with the logic rule-based control strategy, it is noticeable that the operative temperature deviation from the set-point is higher which is due to the building prediction model inaccuracy. Even so, the building thermal comfort is still guaranteed as, on average, the operative temperature deviation is around 1 °C.

In summary, the Mixed-LRBC strategy improves the logic rule-based control strategy results according to the following: the lower and upper temperature conditions are respected (except for some minimal exceeding values in the temperature T_s due to prediction model errors) and the auxiliary energy has been minimized.

Following the application of the MPC strategy developed in Chapter 5 to the TRNSYS model is carried out. It is expected that better results can be obtained compared with the others. The sudden peaks presented in the water flow can be avoided by sending more than one energy profile to the producer controller. Also, the on/off changes may be minimized.

6.4 Model Predictive Control approach

In previous sections, two control strategies have been investigated. The first one, the logic rule-based control approach, has shown that temperature constraints in the SHWS system cannot be satisfied. On the other hand, the Mixed MPC-LRBC approach has improved these results but still some issues remain related to the solver computed solutions. In this section, the MPC strategy developed in Section 5.3 is tested on the TRNSYS solar cooling system.

In this strategy, one energy producer (the SHWS system) and one energy consumer (chiller-building system) are involved. First, the chiller-building system controller computes a number b of energy demand profiles. As only one consumer is involved ($m = 1$), the set $\Pi(\overline{k})$ is composed of b energy demand profiles. In addition, the set $J_t(\overline{k})$ is the set of optimization costs associated to each energy demand profile and $J_{t_h}(\overline{k})_{h=1,\ldots,b}$ is one element of this set associated to the energy demand profile $\pi_h(\overline{k})_{h=1,\ldots,b}$.

The sets $\Pi(\overline{k})$ and $J_t(\overline{k})$ are sent to the energy producer controller which afterwards calculates b optimizations. Once the b optimizations are computed, the producer controller selects the

solution that better minimizes the global optimization cost. This decision is sent to the consumer controller which applies the corresponding control signal.

Following the consumer and producer optimization problems are defined. Later, the control architecture is detailed. In order to assess the performance of the control strategy, simulation results are presented.

6.4.1 Consumer optimization problem

The objective of the chiller-building controller is to minimize the energy use of the system and, at the same time, to minimize the change of the control input $On(k)$ (in order to avoid the absorption chiller damage or malfunction) while maintaining the building operative temperature $T_{op}(k)$ as close as possible to the set-point T_{sbg}. The optimization cost function is given by

$$\begin{aligned} J_2(On(\overline{k})) = \sum_{j=1}^{N_h} \Big[& \alpha_{On} \left\| On(k+j-1) \right\|_p^p + \alpha_{\triangle On} \left\| \Delta On(k+j-1) \right\|_p^p \\ & + \alpha_{T_{op}} \delta(k+j) \left\| T_{op}(k+j) - T_{sbg}(k+j) \right\|_p^p \Big] \end{aligned} \tag{6.4.1}$$

In this criterion α_{On}, $\alpha_{\triangle On}$ and $\alpha_{T_{op}}$ are weighting factors.

The interacting variable $W_{21}(k)$ between producer and consumer is composed of the chiller flow rate $\dot{m}_l(k)$ over the horizon N_h and of the chiller water temperature $T_l(k)$. This latter temperature is obtained from Equation (6.1.28) which depends on the building operative temperature $T_{op}(k)$.

Then, the optimization problem can be formalized as follows:

Optimization problem. At a time k and given the prediction horizon N_h, the current state of the system $X_2(k)$, the precedent control input $On(k-1)$ and the prediction of the uncontrolled variables $d(\overline{k})$, the optimization problem for the energy consumer predictive controller can be defined as

$$\min_{On^{(p)}(\overline{k})} J_2^{(p)}(On^{(p)}(\overline{k})) \tag{6.4.2}$$

s.t. $\quad \forall j = 1, \ldots, N_h, \quad \forall p = 1, \ldots, b$

$$On^{(p)}(k+j-1)\, \epsilon\, \{0,1\} \tag{6.4.3}$$

which is a discrete optimization problem. The energy consumer controller computes b optimal control sequences which compose the set $ON(\overline{k})$ of the form

$$ON(\overline{k}) = \begin{bmatrix} On^{(1)}(\overline{k}) \\ \vdots \\ On^{(p)}(\overline{k}) \\ \vdots \\ On^{(b)}(\overline{k}) \end{bmatrix} \tag{6.4.4}$$

The associated optimization cost of each of these control sequences form the set $J_t(\overline{k})$ as follows

$$J_t(\overline{k}) = \begin{bmatrix} J_2^{(1)}(\overline{k}) \\ \vdots \\ J_2^{(p)}(\overline{k}) \\ \vdots \\ J_2^{(b)}(\overline{k}) \end{bmatrix} \tag{6.4.5}$$

where $J_2^{(1)}$ is the optimization cost with the lower value and $J_2^{(b)}$ is the one with the higher cost value. The set $\Pi(\overline{k})$ is built as

$$\Pi(\overline{k}) = \begin{bmatrix} \dot{m}_l^{p=1}(\overline{k}), & T_l^{p=1}(\overline{k}) \\ \vdots & \vdots \\ \dot{m}_l^{p=b}(\overline{k}), & T_l^{p=b}(\overline{k}) \end{bmatrix} \tag{6.4.6}$$

where

$$\dot{m}_l^{(p)}(\overline{k}) = \dot{m}_{l,nominal} On^{(p)}(\overline{k}) \tag{6.4.7}$$

Finally, the sets $\Pi(\overline{k})$ and $J_t(\overline{k})$ are sent to the producer controller.

6.4.1.1 Consumer controller structure

Figure 6.10 displays the structure of the chiller-building controller. According to the occupancy profile $\delta(k)$, the set-point temperature T_{sbg} and the building operative temperature $T_{op}(k)$, the hybrid predictive controller decides to turn the chiller and pumps on/off. The sequence of decision is obtained solving an integer optimization problem based on the branch and bound optimization method detailed in Section 5.3.4.2. This optimization generates a set of energy demand profiles $\Pi(\overline{k})$ associated with its optimization cost $J_t(\overline{k})$ over the control horizon N_h which are sent to the SHWS system controller.

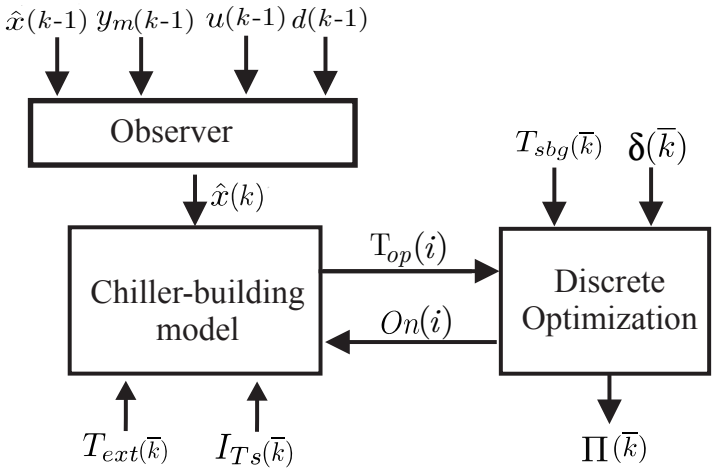

Figure 6.10: Structure of the energy consumption controller.

6.4.2 Producer optimization problem

Section 6.3.2.3 introduced the formulation of the optimization problem for the SHWS system. In order to decrease the complexity of the problem, some relaxations have been done and a practical optimization problem has been obtained. In this section, the previous problem formulation is used but considering a reduction in the number of controlled variables. That is, the optimization variable $\triangle\dot{m}_l(k)$ is not introduced since it is expected that the chiller working periods remain with lower turn on/off changes. This behavior demands more energy to the SHWS system and may avoid the significant raising of the collector outlet temperature. Consequently, the new vector of controlled variables is reduced as follows

$$\breve{U}_1(k) = [\dot{m}_h(k), \dot{Q}_{aux}(k), \lambda(k)] \tag{6.4.8}$$

The optimization problem can then be formalized as

Problem 6.4.1 *Optimization Problem. At time k, given the current state of the system $X_1(k)$, the prediction of the disturbances $D_1(\overline{k})$ and the sets $\Pi(\overline{k})$ and $J_t(\overline{k})$ of the b energy demand profiles computed by the consumer controller over the prediction horizon N_h, the optimization problem for the producer is formulated as follows*

$$\min_{U_1(\overline{k}),\pi_h(\overline{k})} J_1(U_1(\overline{k}), \pi_h(\overline{k})) + J_{t_h}(\overline{k}) + J_\lambda(\lambda(\overline{k})) \tag{6.4.9}$$

$$s.t. \quad \forall j = 1, \ldots, N_h, \quad \forall h = 1, \ldots, b$$

$$\begin{aligned} \dot{m}_s(k+j) &:= \dot{m}_h(k+j) \\ X(k+j) &= f_{\sigma(\bar{U}_1(k+j-1),\pi_h(k+j-1))}(\bar{U}_1(k+j-1), \pi_h(k+j-1)) \\ & H_{\sigma(\bar{U}_1(k+j-1),\pi_h(k+j-1))}(\bar{U}_1(k+j-1), \pi_h(k+j-1)) \\ & + H_{\sigma(\bar{U}_1(k+j-1),\pi_h(k+j-1))}(\lambda(k+j-1)) \leq 0 \\ & \breve{U}_{1\,\min} \leq \breve{U}_1(k+j-1) \leq \breve{U}_{1\,\max} \end{aligned} \tag{6.4.10}$$

6.4.3 Proposed MPC architecture for the solar cooling system

Figure 6.11 represents the MPC structure applied to the solar cooling system. The SHWS system controller refers to the nonlinear predictive controller which solves the optimization problem stated in the previous section. First, the chiller-building controller calculates the sets $\Pi(\overline{k})$ and $J_t(\overline{k})$ which are sent to the SHWS system controller.

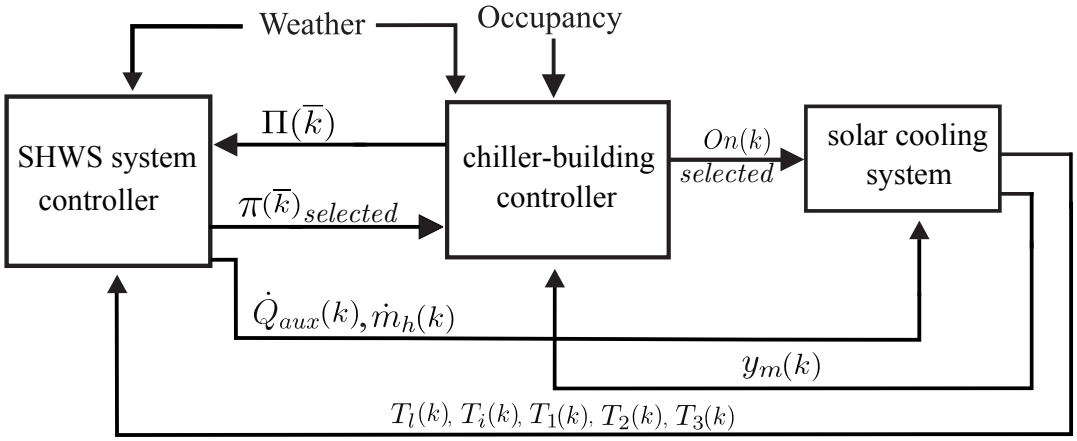

Figure 6.11: Global architecture of control

Then, the SHWS system controller computes b optimizations and selects the one that better minimizes the global optimization cost. The selected energy demand profile $\pi(\overline{k})_{selected}$ is sent to the chiller-building controller which sends the corresponding control signal $On(k)$ to the absorption chiller.

6.4.4 Simulation results

For these experiments, the parameters of the models and controllers are detailed in Appendix A. In addition, the ℓ^2-norm and weighting factors values of the producer cost function have been chosen as in the MPC-LRBC strategy (see Section 6.3.4). As for the consumer optimization cost, the criterion to select the weighting factors is the one that it has been applied

in Chapter 5 (see Section 5.3.4). Consequently, according to Equation (6.4.1): $\alpha_{On} = 5 \cdot 10^2$, $\alpha_{\triangle On} = 4 \cdot 10^3$ and $\alpha_{T_{op}} = 5 \cdot 10^3$.

Figure 6.12 and 6.13 depict the simulation results using a prediction horizon $N_h = 8$ (4 hours) and a sampling time of $\triangle t = 0.5$ hr. In order to exemplify the strategy, the number of energy demand profiles has been arbitrarily set to $b = 3$. In Figure 6.12, the initial temperature at the top of the tank is set at $T_1 = 82$°C and the operative temperature in the building begins at $T_{op} = 27$°C. In Figure 6.13, the tank initial temperature is $T_1 = 111$°C and the building temperature remains at $T_{op} = 27$°C.

Figure 6.12 displays the time evolution of the tank temperature $T_1(k)$ and its upper and lower limits $T_{wbp} = 120$°C and $T_{set} = 90$°C respectively. In order to ensure that the temperature $T_1(k)$ is greater or equal to T_{set} when the chiller operates, the SHWS controller anticipates the use of the auxiliary energy $\dot{Q}_{aux}(k)$. Due to the energy minimization criterion, it can be noticed that when the use of $\dot{Q}_{aux}(k)$ is necessary, the optimization maintains the temperature $T_1(k)$ equal to the lower limit T_{set}. It can be seen that the safety constraints of temperatures $T_1(k)$ and $T_s(k)$ are respected (imperceptible violations occur due to model prediction errors).

The priority of the building predictive controller is to maintain as small as possible the difference between the building operative temperature and the set-point T_{sbg} which is set at 25 °C. The secondary objectives are the minimization of the chiller switch on/off changes and the use of chilled water. Compared to the results obtained in the Mixed MPC-LRBC strategy, the building thermal comfort is guaranteed but with lower switch on/off changes. These changes cannot be significantly reduced as a further minimization may degrade the building thermal comfort.

From the previous section it has been observed that some sudden peaks occur in the collector flow rate $\dot{m}_h$. This behavior has been minimized as it is shown in the second panel of Figures 6.12 and 6.13. In addition, the use of the auxiliary heater is minimized compared to the Mixed MPC-LRBC strategy.

In summary, compared to the Mixed MPC-LRBC, the MPC strategy has minimized chiller switch on/off changes, use of the electric heater and collector sudden peaks. Furthermore, the temperature constraints are fulfilled and the building thermal comfort is guaranteed.

Figure 6.14 depicts the same experiment carried out in Figure 6.12. The only difference is the number of energy profiles generated. Instead of sending $b = 3$ profiles as in Figure 6.12, the consumer controller only sends one profile. Two undesirable events occur. The first one, the lower limit tank temperature constraint is not fulfilled. When the consumer controller request for consumption, the producer controller cannot properly quantify the amount of electricity. Consequently, the resulting tank temperature is not high enough. The second one is the

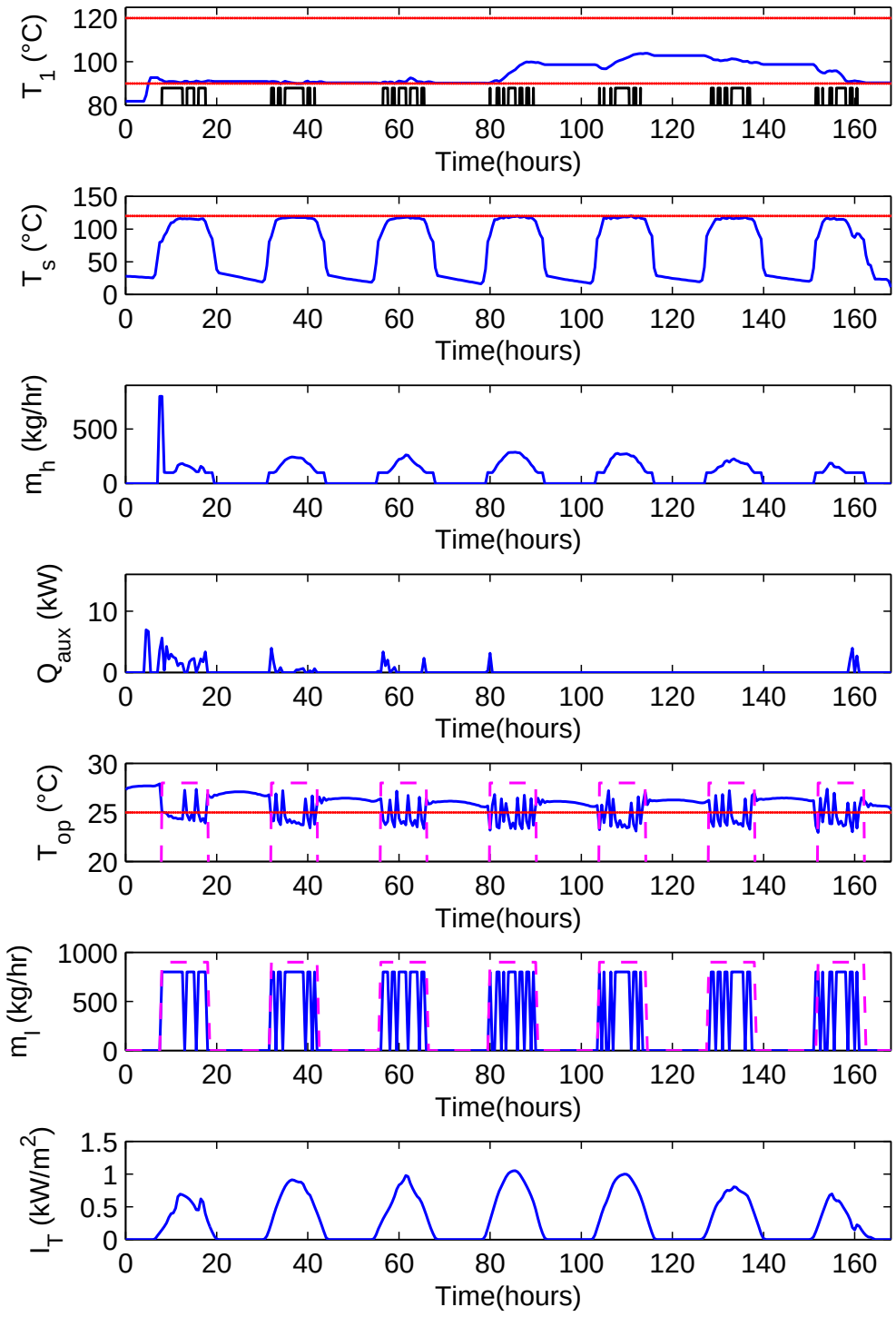

Figure 6.12: MPC strategy considering $T_1 = 82$ °C, $T_{op} = 27$ °C and $b = 3$.

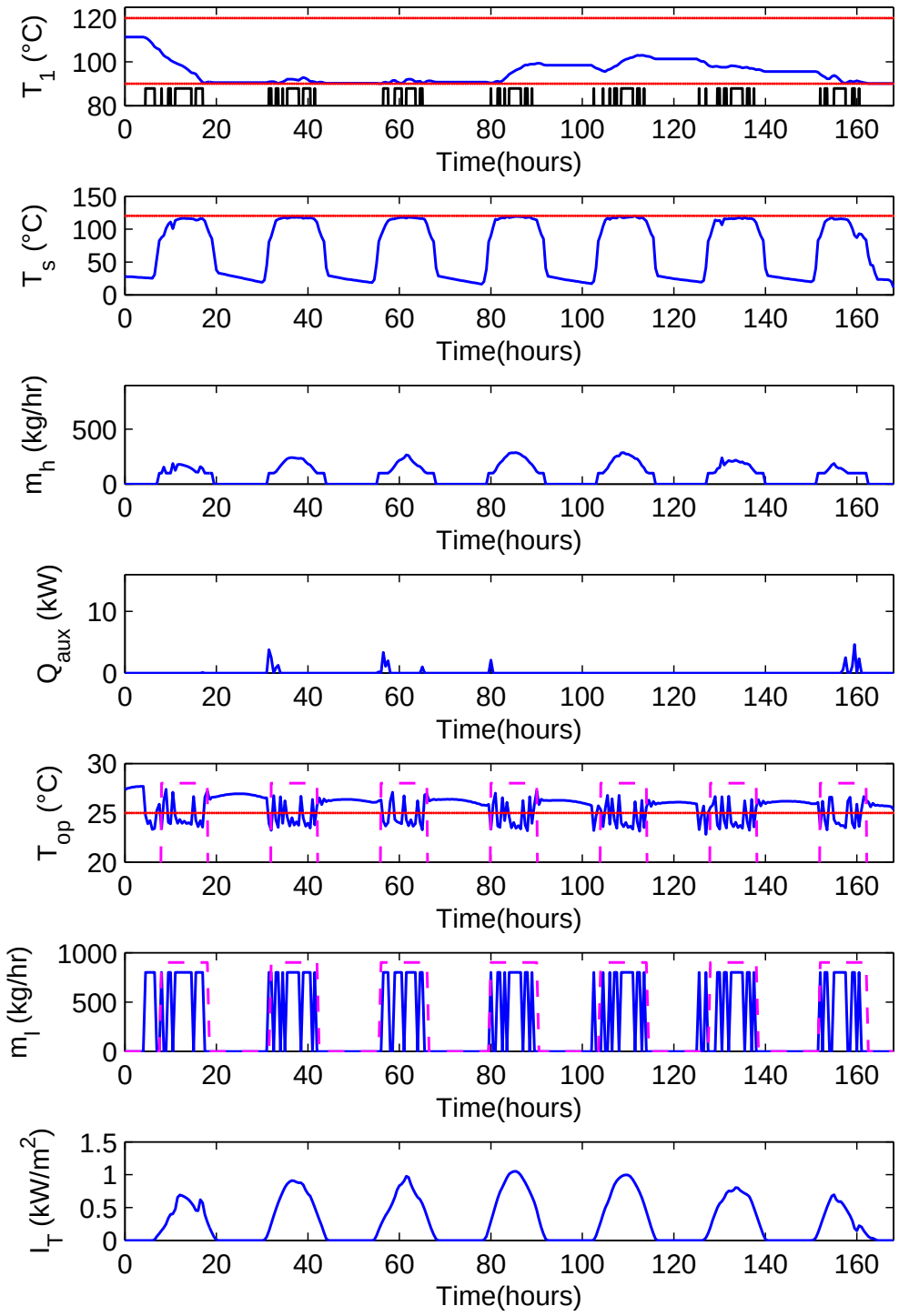

Figure 6.13: MPC strategy considering $T_1 = 111$ °C, $T_{op} = 27$ °C and $b = 3$.

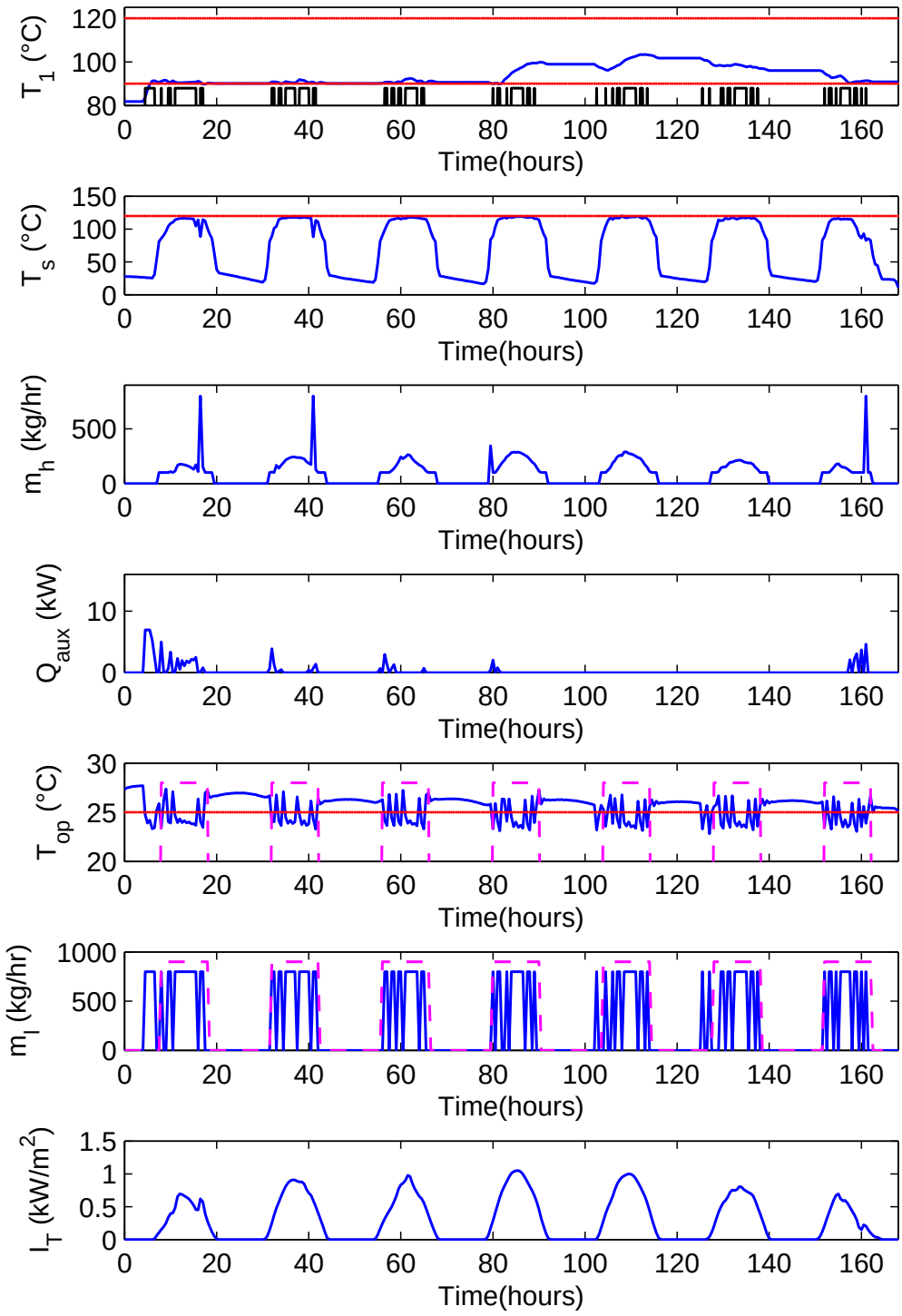

Figure 6.14: MPC strategy considering $T_1 = 82$ °C, $T_{op} = 27$ °C and $b = 1$.

Table 6.1: Profiles generated and selected when $b = 3$

	Profiles generated	Profile selected
$k = 9$	$ON(\overline{k}) = \begin{bmatrix} 0 & 0 & 0 & 0 & 0 & 0 & 0 & 0 \\ 0 & 0 & 0 & 0 & 0 & 0 & 0 & 1 \\ 0 & 0 & 0 & 0 & 0 & 0 & 1 & 1 \end{bmatrix}$	$On^{(1)}(\overline{k})$
$k = 10$	$ON(\overline{k}) = \begin{bmatrix} 1 & 1 & 1 & 1 & 1 & 1 & 1 & 1 \\ 0 & 1 & 1 & 1 & 1 & 1 & 1 & 1 \\ 0 & 0 & 1 & 1 & 1 & 1 & 1 & 1 \end{bmatrix}$	$On^{(3)}(\overline{k})$

increase of the collector flow rate sudden peaks which are related to the solver solutions.

To clearly observe how the experiment in Figure 6.12 overcomes the lower limit temperature violation in Figure 6.14, Table 6.1 shows the vector of energy profiles generated by the consumer controller when $b = 3$ at the time instants $k = 9$ and $k = 10$ respectively. Obviously, when $b = 1$ only the first element $On^{(1)}$ is generated. When $b = 3$, at $k = 9$ the producer controller selected the fist energy profile $On^{(1)}$ while at $k = 10$, it selected the third one $On^{(3)}$. This choice delays the chiller activation and may facilitate the optimization problem resolution. Consequently the chiller control signal applied to the system is zero and therefore the lower limit temperature violation does not occur.

From this experiment it can be concluded that by sending more than one energy demand profile, the producer controller finds a better solution to its optimization problem. At the same time, the bigger the number of energy demand profiles, the more the possibilities to find the optimal solution of the global control problem.

6.5 Quantitative analysis and conclusions of the proposed control strategies

Table 6.2 summarizes the assessment of the different control strategies applied to the solar cooling system by using the controllers performances indexes defined in Section 5.3.3. Two indexes have been aggregated: the index $I_{\triangle T_s}$ (measured in °C) quantifies the upper limit constraint violation of the collector outlet temperature $T_s(k)$ and $I_{\triangle T_1}$ (measured in °C) quantifies the lower limit constraint violation of the tank temperature $T_1(k)$. Table 6.2 shows the performance indexes of the simulation results presented in Sections 6.2, 6.3 and 6.4.

Table 6.2: Control strategies comparison

	LRBC strategy		Mixed MPC-LRBC strategy		MPC strategy	
	$T_1 = 82$°C $T_{op} = 27$°C	$T_1 = 111$°C $T_{op} = 27$°C	$T_1 = 82$°C $T_{op} = 27$°C	$T_1 = 111$°C $T_{op} = 27°C$	$T_1 = 82$°C $T_{op} = 27$°C	$T_1 = 111$°C $T_{op} = 27$°C
$I_{\triangle U_2}$	124	124	96	96	74	80
I_{U_2}	92	92	103	103	63.5	65
I_{Y_2}	0.76	0.76	1.16	1.15	1.18	1.25
$I_{\int P_{csm}}$	369.73	369.73	397.75	397.7	392.76	396.04
$I_{\int U_1}$	102.14	47.16	68.91	23.04	43.76	14.69
$I_{\triangle T_s}$	211.74	213.32	13.33	2.71	0.46	0
$I_{\triangle T_1}$	17.16	0	0	0	0.29	0

It can be noticed that the MPC strategy developed in Section 6.4 has the lower switch on/off changes $I_{\triangle U_2}$ and the lower use of the chiller I_{U_2}. This is natural since it is the only strategy that focuses on the minimization of the chiller use and switch on/off changes.

It can be noticed that the LRBC strategy has the lower I_{Y_2} value. This result is not surprising as both the controller and simulation model are developed in TRNSYS and because the controller is not based on prediction models which lead to estimation errors (this claim is demonstrated observing the results obtained in Chapter 5 where the MPC strategy improves the LRBC results in terms of building temperature control). Nevertheless, the building thermal comfort remains acceptable. On average, the maximum temperature deviation is 1.25°C.

In addition, the index $I_{\int U_1}$ shows that the MPC strategy has the lower electricity consumption and the lower temperature constraint violations. It is worth noting that the constraints violations of the MPC-LRBC and MPC strategies are related to the difference found between the TRNSYS simulation model and the prediction model.

Another improvement of the MPC strategy is that by sending more than one energy consumers, the producer controller can better solve its optimization problem. This have been reflected in the minimization of the sudden peaks in the collector flow rate.

From these results it can be concluded that the MPC strategy outperforms the others in terms of producer and controller energy use, minimization of switch on/off changes and temperature constraint fulfillment. In addition, the building thermal comfort remains acceptable despite the minimal increase of the temperature deviation.

Chapter 7

Conclusions and perspectives

7.1 Conclusions

The present study is dedicated to the development of a solar cooling system management for thermal comfort control in buildings. The first part of this thesis addressed the understanding of this system. Two main subsystems have been identified: the hot water storage system seen as the energy production part and the chiller-building system which is the energy consumption part. The hot water storage system is responsible for providing the heat to drive the absorption chiller for the cooling of the building. The main control challenge is to achieve an energy balance between production and consumption parts while maintaining the operating conditions within the desired reference values.

The study of absorption cooling systems for temperature control in buildings has demonstrated that advanced control strategies are needed in order to achieve an adequate coordination between energy production and consumption taking into account the nonlinear and hybrid nature of the installation. In order to provide modularity and simplicity to the control structure, the management of the energy production-consumption system is developed using a partitioning system approach which allows the design of a decentralized control structure with minimal information exchange.

In this partitioning approach, the producer is seen as a heat central that provides hot water to various consumers connected to the grid. Both producer and consumers control design are independent and in order to minimize the degradation of the optimal solution, interaction mechanisms are established.

In a first part, the proposed control strategy is applied to a simplified model where both producer and consumers are represented by linear models. The producer is an abstraction of the solar hot water storage system and it represents a solar and electric energy storage unit connected to the chiller-building systems. The main characteristic of this simplified model lies on its hybrid and bilinear dynamics. The interacting variable which relates the producer

and consumers is the total energy consumption. In a second part, the producer is composed of a collector panel, heat exchanger and a stratified storage tank.

The coordination between the local controllers is achieved by a non-iterative information exchange between producer and consumer controllers. A number of energy demand profiles generated by the local consumer controllers (which solve an integer optimization based on the branch and bound method) is sent to the producer controller which solves a local optimization according to this information. The producer controller decides which of these profiles is applied to each of the consumers according to the global optimization cost. Instead of solving a centralized control approach by exploring the entire branch and bound tree in the consumers control structure, the proposed control strategy only considers a limited number of branches which reduces significantly the computational burden. Even if this consideration may lead to a suboptimal solution, quantitative simulation results have demonstrated that, by considering a reduced number of branches, the percentage of suboptimality is not significant and an important computational time is saved.

In the proposed control strategy, the set of energy demand profiles sent by each of the consumers corresponds, in a first stage, to its optimal solutions. That is, the ones that have the lower optimization cost value. Other quantitative studies to assess the control strategy performance have been done considering different criteria to generate the set. The results have shown that a minimal suboptimality reduction is achieved by composing the set of energy profiles randomly chosen from a bigger number of optimal solutions. This leads to a higher computational complexity. Table 7.1 summarizes the main characteristics of the logic rule-based control (LRBC) strategy and the proposed MPC strategy considering the different criteria to generate the set of energy profiles.

Table 7.2 summarizes the main characteristics of the control strategies applied to the TRNSYS solar absorption cooling system. The LRBC strategy results showed that an advanced control strategy is required in order to respect the SHWS system temperature conditions. Moreover, the chiller switch on/off changes and auxiliary energy use are significant.

An improved control strategy has been studied which involves a model predictive controller for the production part whereas the chiller-building system remains controlled by a LRBC approach. An energy profile generator sends the predicted energy demand profile to the producer controller. The nonlinear and hybrid dynamics of the production part has been relaxed by reducing the number of optimization variables and considering a discrete optimization variable as continuous. Simulation results have demonstrated that temperature conditions in the production part can be mostly respected. Model prediction errors occur in both producer and consumer systems which lead to producer temperature constraint violations and an increased

Table 7.1: Comparative table of control strategies for the simplified model

Energy production-consumption system: Simplified model			
Characteristics		Difficulties	
One producer and several consumers structure. Linear models in both producer and consumers.		Bilinear dependency between consumers and producer. Consumers hybrid dynamics.	
Control strategies			
	Characteristics	Advantages	Drawbacks
LRBC strategy	Hysteresis controllers in both producer and consumers.	Optimization not required. Easy implementation in real plants.	Significant consumers switch on/off changes. High auxiliary energy consumption due to on/off control behavior.
MPC strategy	Linear and hybrid MPC approach.	Consumers switch on/off changes minimized. Auxiliary energy use adapted to load consumption.	Computational complexity exponentially increases with consumers number. Time consuming. Information exchange required.
MPC: Optimal profiles	Set of energy consumer profiles that have the lower optimization cost.	Both producer and consumers constraints fulfillment are satisfied.	A reduced number of possibilities offered to the producer controller. Suboptimal resolution compared to the centralized case.
MPC: Partially optimal profiles	Set of profiles have higher optimization values than optimal profiles.	Suboptimality indexes are better than considering optimal profiles.	Higher computational complexity.
MPC: Random profiles	Optimization not involved in the generation of the profiles.	Fast resolution.	Constraints in both producer and consumers are not respected.

building temperature deviation from the corresponding set-point. Even so, these violations are not significantly high and the building thermal comfort is still guaranteed.

Table 7.2: Comparative table of control strategies for the TRNSYS solar absorption cooling system

Energy production-consumption system: TRNSYS solar absorption cooling system			
Characteristics		Difficulties	
One producer and one consumer structure.		Nonlinear hybrid dynamics in the producer. Consumer hybrid dynamics.	
Control strategies			
	Characteristics	Advantages	Drawbacks
LRBC strategy	Hysteresis controllers in both producer and consumer.	Optimization not required. Easy implementation in real plants.	Significant consumer switch on/off changes. High auxiliary energy consumption due to on/off control behavior.
Mixed MPC-LRBC strategy	Hysteresis predictive controller in consumer. Nonlinear MPC in producer.	Optimization not required in consumer control strategy. Lower number of nonlinear optimizations performed.	Prediction model errors cause temperature constraint violations.
MPC strategy: Optimal profiles sent to the producer	Integer optimization in consumer. Nonlinear MPC in producer.	Auxiliary energy use, chiller switch on events and switch on/off changes are minimized.	Computational complexity exponentially increases with consumers number. Time consuming.

A relevant enhancement has been done by implementing the proposed MPC strategy to the solar cooling system. The simulations results showed that by sending more than one energy demand profile to the producer controller, the solver can find better solutions which may avoid undesirable behaviors as the sudden peaks in the collector flow rate. In general, the proposed MPC strategy has a better performance compared with the others.

7.2 Perspectives

Concerning the proposed MPC strategy, the following improvements are suggested:

- Suboptimality percentages may be minimized if further studies are done regarding the generation of the set of energy demand profiles. In addition, another decision-making mechanism may be considered in order to reduce the number of optimizations in the producer control strategy which exponentially grows as the number of consumers increases.
- Distributed or hierarchical MPC strategies may be taken into account in order to guarantee the optimality of the solution and to improve the balance between producer and consumer constraints fulfillment.

Concerning the modeling and control of solar cooling systems in buildings:

- The building thermal comfort results may be improved by considering a supervisory MPC strategy controlling the TRNSYS building model at a local level.
- Other modeling techniques may be interesting for the building. The TRNSYS building model is influenced by several weather variables, internal gains and wall losses which are not taken into account in the prediction model.
- Better TRNSYS control results can be obtained by improving the prediction model of the solar hot water storage system.
- A prediction model that estimates the radiant ceiling water outflow temperature may be developed in order to better predict the consumers energy demand.
- A chilled water storage may be included in the installation. This may improve the building thermal comfort as the chiller operation will be indirectly connected to the building.
- A more detailed modeling is suitable for the absorption chiller. Pressure and weather conditions are determinant factors in the chiller efficiency. Also, the cooling tower as heat rejection component may be included in the installation.
- The suggested prediction model improvements can better characterize the chiller, radiant ceiling and other components inertia which may offer a higher degree of freedom to the control structure.

Appendix A

Model and control parameters

A.1 Model parameters

A.1.1 Consumer model parameters

In Chapters 5 and 6, the building represented by a linear model of the form

$$x(k+1) = Ax(k) + Bu(k) + Fd(k) \tag{A.1.1}$$

$$T_{op}(k) = Cx(k) \tag{A.1.2}$$

has been studied. The corresponding parameters are defined as

$$A = \begin{bmatrix} 0.9907 & 0.01801 & 0.050276 & 0.010807 \\ 0.015113 & 0.70914 & -0.28662 & -0.21723 \\ 0.10674 & -0.50807 & -0.34083 & -0.025452 \\ -0.033633 & 0.088119 & 0.36012 & 0.87395 \end{bmatrix} \tag{A.1.3}$$

$$B = \begin{bmatrix} -3.1104e-05 \\ 0.00031401 \\ 0.00057885 \\ -5.3283e-05 \end{bmatrix} \tag{A.1.4}$$

$$F = \begin{bmatrix} 0.00010533 & 1.9279e-05 \\ -0.0013994 & -0.00015231 \\ 0.00031583 & -0.00043977 \\ -0.00085981 & 8.1885e-05 \end{bmatrix} \tag{A.1.5}$$

$$C = \begin{bmatrix} 104.86 & -1.9237 & 2.5191 & -0.49427 \end{bmatrix} \tag{A.1.6}$$

This linear model has been obtained from identification (see Appendix C) and therefore the parameters of the matrices have no physical meaning.

In addition, the gain vector L of the Luenberger observer that estimates the building operative temperature has been calculated using the MATLAB function *dlqr* which solves the discrete algebraic Ricatti equation for linear quadratic regulators. The matrix obtained is

$$L = \begin{bmatrix} 0.0013 \\ 0.4616 \\ -0.0967 \\ -0.0588 \end{bmatrix} \tag{A.1.7}$$

Concerning the chiller steady-state equations described in Chapter 5 (see Equations (5.1.13)-(5.1.18)), the following parameters are used

Table A.1: Consumer model parameters

φ_1	700	kg/hr
φ_2	0.98	$-$
ς	0.8	$-$
T_{chs}	12	°C

A.1.2 Producer model parameters

The parameters of the SHWS system model developed in Chapter 6 are presented in Table A.2.

Table A.2: SHWS model parameters

A	11.8	m^2
a_0	0.799	$-$
a_1	3.97	$kJ/hr \cdot m^2 \cdot K$
a_2	0.016	$kJ/hr \cdot m^2 \cdot K^2$
V	1.8	m^3
c	4.19	$kJ/Kg \cdot K$
ρ	1000	kg/m^3
ε	0.7	$-$
$\dot{m}_{ch,nominal}$	500	kg/hr
$\dot{m}_{l,nominal}$	800	kg/hr

A.2 Controllers parameters

A.2.1 Control parameters in Chapter 5

The control parameters for the system developed in Chapter 5 are specified in Tables A.3 and A.4. The first one details the control parameters of the LRBC strategy and the second one describes the parameters of the MPC strategy.

Table A.3: LRBC parameters

$Y^{(1)}_{2\,\max}(k) = Y^{(1)}_{2\,\min}(k)$	22	°C
$Y^{(2)}_{2\,\max}(k) = Y^{(2)}_{2\,\min}(k)$	24	°C
$Y^{(3)}_{2\,\max}(k) = Y^{(3)}_{2\,\min}(k)$	26	°C
$E_{\min}$	0	kWh
$P_{elc,\max}$	30	kW
$P_{elc,\min}$	0	kW
$\dot{m}^{(i)}_{ch}(k)$	700	kg/hr
t_k	0.5	hr

Table A.4: MPC parameters

$Q^{(i)}_1(k)$	2	–
$Q^{(i)}_2(k)$	0.5	–
$Q^{(i)}_3(k)$	5	–
$Y^{(1)}_r(k)$	22	°C
$Y^{(2)}_r(k)$	24	°C
$Y^{(3)}_r(k)$	26	°C
$E_{\min}$	0	kWh
$P_{elc,\max}$	30	kW
$P_{elc,\min}$	0	kW
$\dot{m}^{(i)}_{ch}(k)$	700	kg/hr
t_k	0.5	hr
c	4.19	$kJ/Kg \cdot K$
ς	0.8	–
p	1	–

A.2.2 Control parameters in Chapter 6

The control parameters for the system developed in Chapter 6 are specified in Tables A.5, A.6 and A.7 for the LRBC, Mixed MPC-LRBC and MPC strategy respectively.

Table A.5: LRBC parameters

T_{sbg}	25	°C
T_{set}	90	°C
$\dot{Q}_{aux,max}$	14	kW
T_{wbp}	120	°C
$\dot{m}_{h,max}$	200	kg/hr
$\dot{m}_l$	800	kg/hr
$\dot{m}_{ch}^{(i)}(k)$	500	kg/hr
$\triangle t$	0.5	hr

Table A.6: Mixed MPC-LRBC parameters

$\alpha_{\dot{Q}_{aux}}$	$1 \cdot 10^{-5}$	–
$\alpha_{\dot{m}_h}$	$1 \cdot 10^{-2}$	–
$\alpha_{\triangle \dot{m}_l}$	$1 \cdot 10^{8}$	–
α_λ	$1 \cdot 10^{10}$	–
α_t	0.75	–
N_h	8	–
T_{sbg}	25	°C
T_{set}	90	°C
$\triangle t$	0.5	hr
$\dot{m}_{h,min}$	100	kg/hr
$\dot{I}_{Tmin}$	300	kg/m^2hr
$\dot{m}_{h,max}$	800	kg/hr
$\dot{Q}_{aux,max}$	14	kW
$\triangle \dot{m}_{l,max}$	1	–
p	2	–

Table A.7: MPC parameters

α_{On}	$5 \cdot 10^2$	–
$\alpha_{\triangle On}$	$4 \cdot 10^3$	–
$\alpha_{T_{op}}$	$5 \cdot 10^3$	–
$\alpha_{\dot{Q}_{aux}}$	$1 \cdot 10^{-5}$	–
$\alpha_{\dot{m}_h}$	$1 \cdot 10^{-2}$	–
α_λ	$1 \cdot 10^{10}$	–
N_h	8	–
T_{sbg}	25	°C
T_{set}	90	°C
$\triangle t$	0.5	hr
$\dot{m}_{h,min}$	100	kg/hr
$\dot{I}_{Tmin}$	300	kg/m^2hr
$\dot{m}_{h,max}$	800	kg/hr
$\dot{Q}_{aux,max}$	14	kW
p (consumer optimization)	1	–
p (producer optimization)	2	–

Appendix B

TRNSYS simulation model

The assessment of the proposed control structures has been carried out using the TRNSYS software which is a powerful tool to assess the performance of thermal systems and to model other dynamical systems. The consumers prediction model used in Chapter 5 and 6 is obtained from the TRNSYS building model.

The TRNSYS software is composed of two subprograms: the TRNSYS simulation studio which is the main visual interface containing an extensive library components and the building visual interface called TRNBuild which is the visual tool used to configure the building characteristics. Table B.1 details the components used for the solar cooling systems and its controllers. Each of these model components can be configured by the user. As it has been said in previous chapters, the MPC and Mixed-MPC controllers have been designed in MATLAB and they have been linked with TRNSYS in order to apply the computed control signals to the thermal system. This process is achieved by using the TRNSYS component Type 155.

Table B.2 details the building description. The characteristics of the walls are inspired by BESTEST Case 960 which simulates a two-zone building with a glazed sun space facing south and an opaque back zone behind it. The sun zone is the one to be conditioned using a chilled ceiling with 0.2 m of pipe spacing and 0.02 m of pipe inside diameter. Besides, the external south wall of the sun zone has a 20 m^2 window. The internal gains have been set constant during occupancy periods and considering 5 persons with low activity (each one adds 100 W) and 5 personal computers (50 W each one). As for the back zone, the internal gains have been set constant throughout the simulation and with a radiative and convective power of 432 kJ/hr and 288 kJ/hr respectively.

Figures B.1 and B.2 depict the TRNSYS simulation models used in the three control strategies. The first one corresponds to the LRBC strategy which is carried out using the TRNSYS differential controller and pump components. Instead of using the mentioned components, in the second figure the controller is implemented using the MATLAB link component (Type 155).

Table B.1: TRNSYS components used for the solar cooling system and controllers

Component	Symbol	Description
Type 155: TRNSYS-MATLAB link		A Fortran routine communicates with Matlab using a Component Object Model (COM). This component is used to sent the control signals of the MPC and Mixed MPC-LRBC strategies to the TRNSYS thermal model.
Type 2: On/off differential controller		It generates a binary control signal which takes values 1 or 0. The hysteresis controller generates the output as a function of a temperature difference taking into account dead bands values.
Type 56: Multi-zone building		It models the thermal behavior of a building. The building characteristics are defined from the TRNSYS preprocessor program TRNBuild. The building can contain up to 25 zones.
Type 1: Flat-plate collector		This component represents an experimental validated model of a flat-plate collector. The incidence angle modifier is determined by a second order quadratic function.
Type 91: Heat exchanger		This component is independent of the system configuration and it is described as a constant effectiveness device.
Type 4: Storage tank		This component is composed of fully-mixed equal volume segments. The degree of stratification is defined by the user. It contains two electric heaters which can be activated according to the user's specifications.
Type 109: Weather data		It reads a standard weather file in the TMY2 format. The data used for the experiments are from Chihuahua, Mexico.
Type 93: Input value recall		This component logs the value of the inputs for a preceding time step number. This component is used to save the previous outputs and input signals.
Type 14: Forcing Function		This time dependent function is a set of discrete points defined by the user. This component is used to define the building occupancy periods.
Type 3: Pump		This component computes a mass flow rate from a binary control signal. The outlet temperature and mass flow rate can be calculated from user defined linear functions.
Equation builder		With this component the user can define static equations from external components output signals.
Type 65: Plotter		This online graphical plotter with output file is used to display the system variables. The generated data can be saved in different formats.

Table B.2: Characteristics of the TRNSYS building (Type 56)

	Wall	Area (m^2)	Layer	Thickness (m)	Conductivity ($kJ\,h^{-1}m^{-1}K^{-1}$)	Density ($kg\,m^{-3}$)	Capacity ($kJ\,kg^{-1}K^{-1}$)
Sun zone	Adjacent back zone	32.4	Concrete	0.2	1.83	1	1400
	External south	32.4	Concrete Foam insulation Wood siding	0.1 .061 0.009	1.83 0.14 0.5	1 1.4 0.9	1400 10 530
	External east, west	27	Concrete Foam insulation Wood siding	0.1 .061 0.009	1.83 0.14 0.5	1 1.4 0.9	1400 10 530
	Roof (chilled ceiling)	120	Plaster board Fiberglass Roof deck	0.010 0.112 0.019	0.57 0.14 0.5	0.84 0.84 0.9	950 12 530
	Floor	120	Concrete slab	0.08	4.068	1	1400
Back zone	Adjacent sun zone	32.4	Concrete	0.2	1.836	1	1400
	External north	32.4	Plaster board Fiberglass Wood siding	0.012 0.066 0.006	0.576 0.144 0.504	0.84 0.84 0.9	950 12 530
	External east, west	16.2	Plaster board Fiberglass Wood siding	0.012 0.066 0.006	0.57 0.14 0.5	0.84 0.84 0.9	950 12 530
	Roof	72	Plaster board Fiberglass Roof deck	0.010 0.112 0.019	0.57 0.14 0.5	0.84 0.84 0.9	950 12 530
	Floor	72	Timber flooring	0.025	0.504	1.2	650

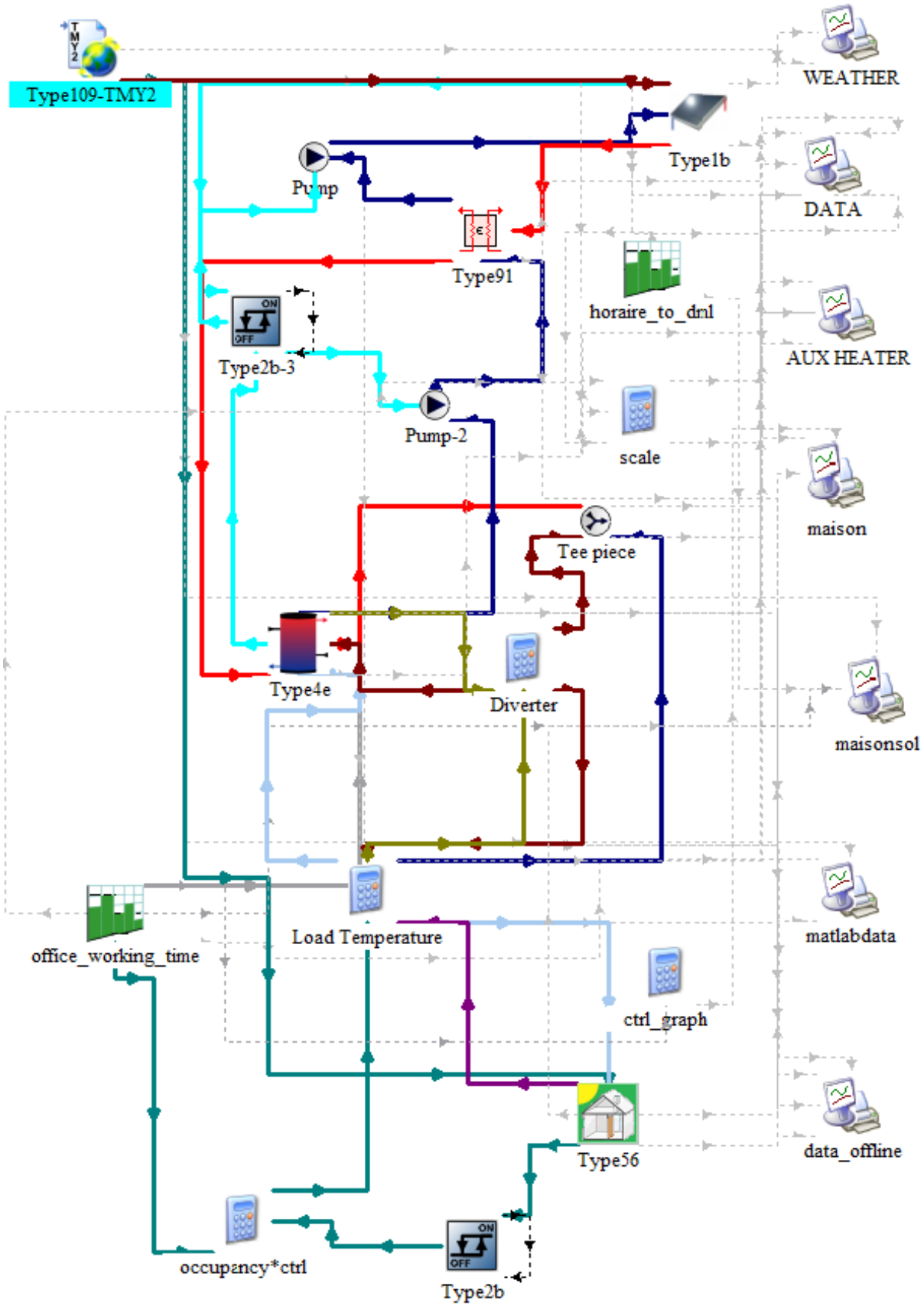

Figure B.1: TRNSYS diagram of the LRBC strategy.

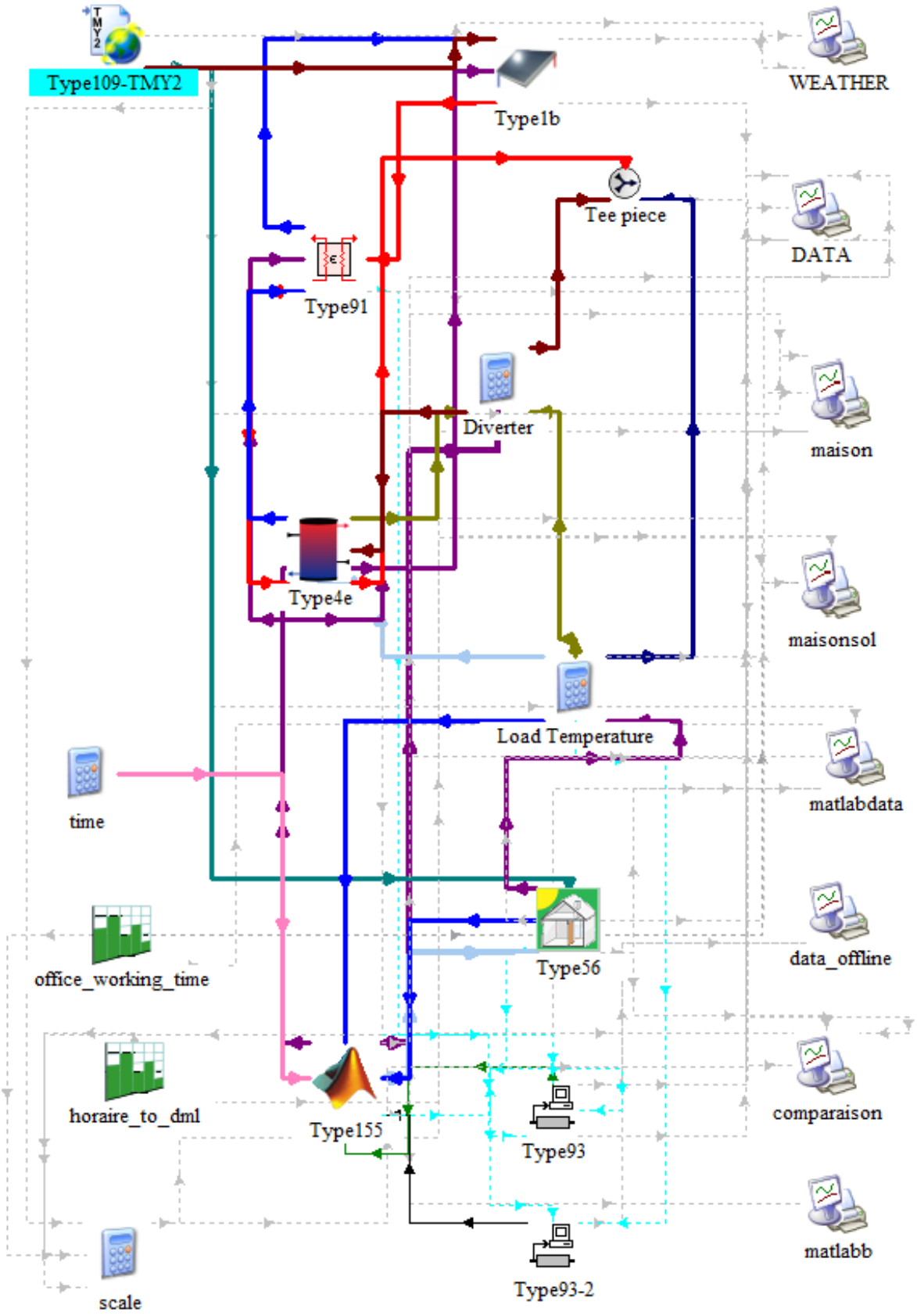

Figure B.2: TRNSYS diagram of the MPC and Mixed MPC-LRBC strategy.

Appendix C

Building model identification

A linear state-space model of the TRNSYS building has been obtained using the MATLAB system identification toolbox. The output variable of interest is the operative temperature of the building sun zone. Each wall of the TRNSYS building model represented by the Type 56 is subject to weather conditions (beam radiation, total tilted surface radiation, total horizontal radiation, etc.). In order to obtain a simple model, the disturbances taken into account for the identification process are the total tilted radiation of the wall oriented to the south and the exterior temperature as it is considered that these variables have a strong impact on the building behavior. As the internal gains are constant during the occupancy profiles, they are not considered as part of the disturbances for identification. The control input of the building is the water flow circulated to the radiant ceiling.

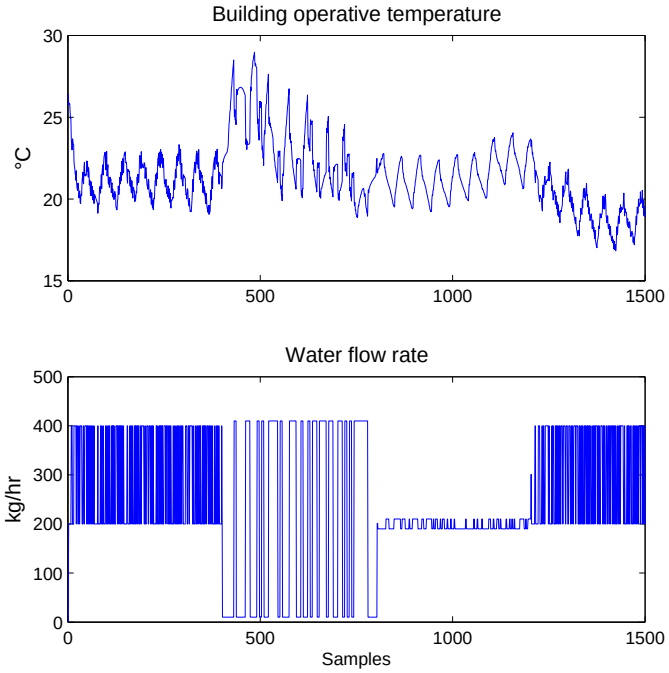

Figure C.1: Output and input signal for identification.

Figure C.1 depicts the building operative temperature and water flow rate considered for the identification process. The other two inputs are the exterior temperature and the total tilted radiation of the wall oriented to the south. The water flow rate is built from pseudo-random binary sequences (PRBS) with different frequencies and amplitudes. System identification techniques require excitation of the plant over the frequency range of interest, where typically random input signals such as pseudo-random binary sequences (PRBS) are used to excite the plant to be identified (Ma et al., 2014). The PRBS signals have been generated using the PRBS generator function proposed by (Landau and Zito, 2006). The data used for the identification is generated during 31 days.

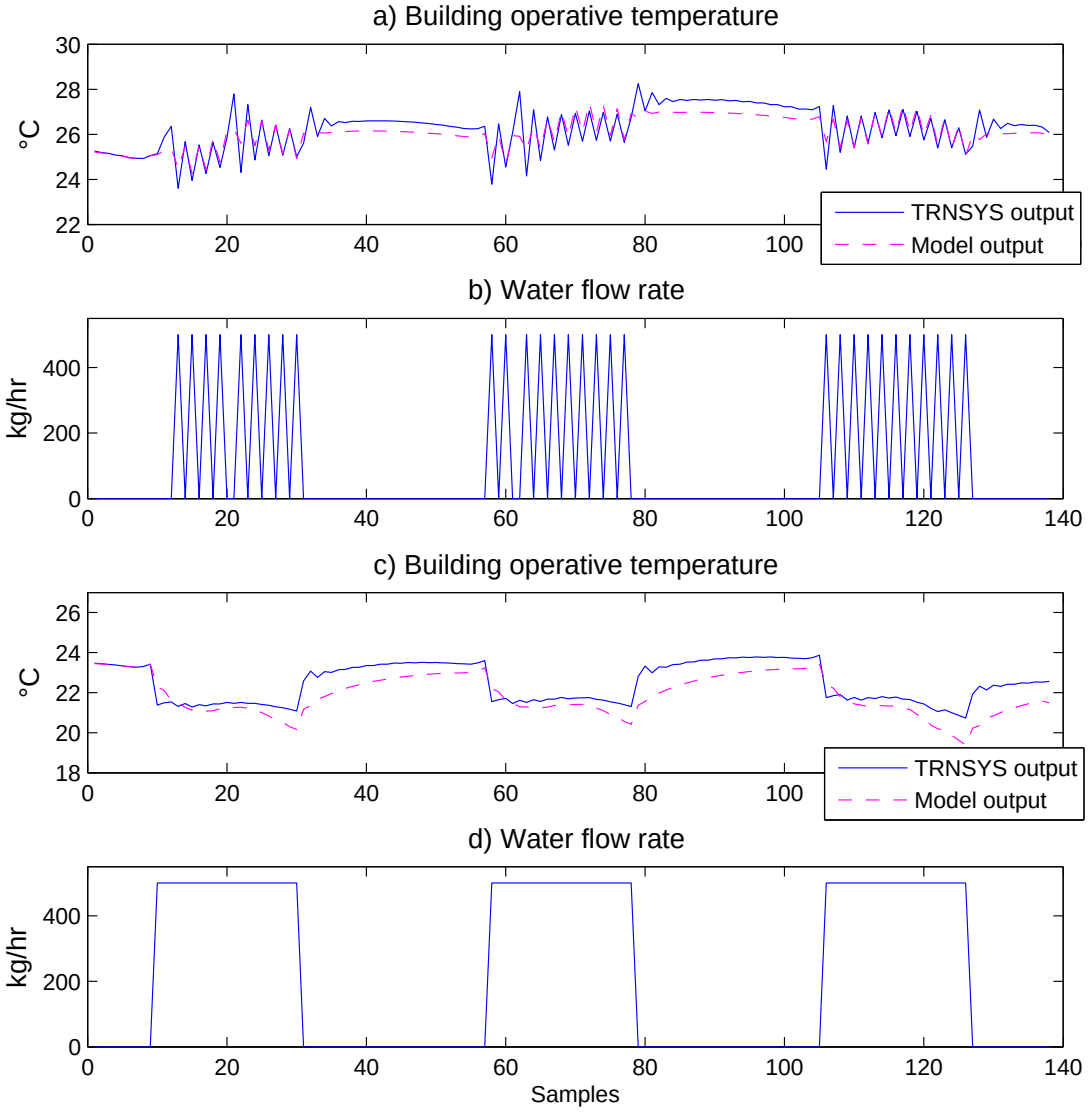

Figure C.2: Model comparison.

The TRNSYS identification data is used to obtain a black-box model using the MATLAB function *pem*. This function estimates the parameters of a linear state-space model structure. The input parameters required by the function are the generated identification data and the desired order of the model.

The model sampling time has been set at $t_k = 0.5$ hr in order to obtain an adequate balance between prediction model performance and controller complexity. Indeed, the prediction model is used for optimization and therefore a lower value may increase the controller complexity.

Figure C.2 shows the performance of the identified model in two cases: constant and intermittent flow rate behavior during occupancy periods. Figure C.2 a) shows the temperature response of the TRNSYS and identified model subject to the intermittent behavior of the water flow rate depicted in Figure C.2 b). Figure C.2 c) depicts the temperature response of the TRNSYS and identified model subject to constant water flow rate as shown in Figure C.2 d).

It can be seen that the model has an adequate prediction of the TRNSYS building temperature. An improved model may be obtained taking into account all the disturbances that influences the building dynamics.

List of Figures

List of Tables

Bibliography

Al-Alili, A., Hwang, Y., Radermacher, R., and Kubo, I. (2010). Optimization of a solar powered absorption cycle under abu dhabi's weather conditions. *Solar Energy*, 84(12):2034 – 2040.

Ali, A. H. H., Noeres, P., and Pollerberg, C. (2008). Performance assessment of an integrated free cooling and solar powered single-effect lithium bromide-water absorption chiller. *Solar Energy*, 82(11):1021 – 1030.

Alvarez, J. D., Redondo, J. L., Camponogara, E., Normey-Rico, J., Berenguel, M., and Ortigosa, P. M. (2013). Optimizing building comfort temperature regulation via model predictive control. *Energy and Buildings*, 57:361–372.

Ameen, A. (2006). *Refrigeration and air conditioning*. Prentice-Hall of India.

Anies, G. (2011). *Modélisation, simulation dynamique, validation expérimentale et optimisation énergétique d'une unité de rafraîchissement solaire par absorption*. Université de Pau et des Pays de l'Adour.

ASHRAE (2007). *ASHRAE Handbook. HVAC Applications (SI)*. American Society of Heating Refrigerating and Air-Conditioning Engineers, Atlanta.

ASHRAE (2008). *ASHRAE Handbook. HVAC systems and Equipment (SI)*. American Society of Heating Refrigerating and Air-Conditioning Engineers, Atlanta.

Assilzadeh, F., Kalogirou, S. A., Ali, Y., and Sopian, K. (2005). Simulation and optimization of a LiBr solar absorption cooling system with evacuated tube collectors. *Renewable Energy*, 30(8):1143 – 1159.

Bahnfleth, W. P. and Song, J. (2005). Constant flow rate charging characteristics of a full-scale stratified chilled water storage tank with double-ring slotted pipe diffusers. *Applied Thermal Energy*, 25:3067–3082.

Balghouthi, M., Chahbani, M. H., and Guizani, A. (2012). Investigation of a solar cooling installation in Tunisia. *Applied Energy*, 98(0):138 – 148.

Beghi, A., Cecchinato, L., Rampazzo, M., and Simmini, F. (2014). Energy efficient control of {HVAC} systems with ice cold thermal energy storage. *Journal of Process Control*, 24(6):773 – 781. Energy Efficient Buildings Special Issue.

Bemporad, A., Heemels, M., and Johansson, M. (2010). *Networked Control Systems*. Springer-Verlag, Berlin, Heidelberg.

Bermejo, P., Pino, F. J., and Rosa, F. (2010). Solar absorption cooling plant in seville. *Solar Energy*, 84(8):1503 – 1512.

Binggeli, C. and Greichen, P. (2011). *Interior graphic standards*. John Wiley and Sons, Inc., New Jersey, second edition.

Boehm, R. (2012). An approach to decreasing the peak electrical demand in residences. *Energy Procedia*, 14(0):337 – 342. 2011 2nd International Conference on Advances in Energy Engineering (ICAEE).

Bujedo, L. A., Rodríguez, J., and Martínez, P. J. (2011). Experimental results of different control strategies in a solar air-conditioning system at part load. *Solar Energy*, 85(7):1302 – 1315.

Calise, F. (2010). Thermoeconomic analysis and optimization of high efficiency solar heating and cooling systems for different italian school buildings and climates. *Energy and Buildings*, 42(7):992 – 1003.

Calise, F., d'Accadia, M. D., and Palombo, A. (2010). Transient analysis and energy optimization of solar heating and cooling systems in various configurations. *Solar Energy*, 84(3):432 – 449.

Calise, F., d'Accadia, M. D., and Vanoli, L. (2011). Thermoeconomic optimization of solar heating and cooling systems. *Energy Conversion and Management*, 52(2):1562 – 1573.

Camacho, E. F. and Bordons, C. (2004). *Model predictive control*. Springer.

Castilla, M., Álvarez, J. D., Berenguel, M., Rodríguez, F., Guzman, J. L., and Perez, M. (2011). A comparison of thermal comfort predictive control strategies. *Energy and Buildings*, 43:2737 – 2746.

Castilla, M., Álvarez, J. D., Normey-Rico, J. E., and Rodríguez, F. (2014). Thermal comfort control using a non-linear {MPC} strategy: A real case of study in a bioclimatic building. *Journal of Process Control*, 24(6):703 – 713. Energy Efficient Buildings Special Issue.

Chandan, V. and Alleyne, A. G. (2014). Decentralized predictive thermal control for buildings. *Journal of Process Control*, 24(6):820 – 835. Energy Efficient Buildings Special Issue.

de Guadalfajara, M., Lozano, M. A., and Serra, L. M. (2012). Evaluation of the potential of large solar heating plants in Spain. *Energy Procedia*, 30(0):839 – 848. 1st International Conference on Solar Heating and Coolingfor Buildings and Industry (SHC 2012).

Domahidi, A., Ullmann, F., Morari, M., and Jones, C. N. (2014). Learning decision rules for energy efficient building control. *Journal of Process Control*, 24(6):763 – 772. Energy Efficient Buildings Special Issue.

Duffie, J. and Beckman, W. A. (1974). *Solar Engineering of Thermal Processes*. Wiley, New York.

Eicker, U. and Pietruschka, D. (2009). Design and performance of solar powered absorption cooling systems in office buildings. *Energy and Buildings*, 41:81–91.

Evola, G., Pierrès, N. L., Boudehenn, F., and Papillon, P. (2013). Proposal and validation of a model for the dynamic simulation of a solar-assisted single-stage libr/water absorption chiller. *International Journal of Refrigeration*, 36(3):1015 – 1028.

Eynard, J., Grieu, S., and Polit, M. (2012). Predictive control and thermal energy storage for optimizing a multi-energy district boiler. *Journal of Process Control*, 22(7):1246 – 1255.

Florides, G. A., Kalogirou, S. A., Tassou, S. A., and Wrobel, L. C. (2002). Modelling, simulation and warming impact assessment of a domestic-size absorption solar cooling system. *Applied Thermal Engineering*, 22(12):1313 – 1325.

Freire, R. Z., Oliveira, G. H. C., and Mendes, N. (2008). Predictive controllers for thermal comfort optimization and energy savings. *Energy and Buildings*, 40:1353 – 1365.

Garcia-Gabin, W., Zambrano, D., and Camacho, E. F. (2009). Sliding mode predictive control of a solar air conditioning plant. *Control Engineering Practice*, 17(6):652 – 663.

Garnier, A., Eynard, J., Caussanel, M., and Grieu, S. (2014). Low computational cost technique for predictive management of thermal comfort in non-residential buildings. *Journal of Process Control*, 24(6):750 – 762. Energy Efficient Buildings Special Issue.

González-Gil, A., Izquierdo, M., Marcos, J. D., and Palacios, E. (2011). Experimental evaluation of a direct air-cooled lithium bromide-water absorption prototype for solar air conditioning. *Applied Thermal Engineering*, 31(16):3358 – 3368.

Hall, M. (2010). *Materials for Energy Efficiency and Thermal Comfort in Buildings*. Woodhead Publishing Limited, Cambridge.

Halvgaard, R., Bacher, P., Perers, B., Andersen, E., Furbo, S., Jørgensen, J. B., Poulsen, N. K., and Madsen, H. (2012). Model predictive control for a smart solar tank based on weather and consumption forecasts. *Energy Procedia*, 30(0):270 – 278. 1st International Conference on Solar Heating and Cooling for Buildings and Industry (SHC 2012).

Hang, Y., Du, L., Qu, M., and Peeta, S. (2013). Multi-objective optimization of integrated solar absorption cooling and heating systems for medium-sized office buildings. *Renewable Energy*, 52(0):67 – 78.

Hang, Y., Qu, M., and Zhao, F. (2011). Economical and environmental assessment of an optimized solar cooling system for a medium-sized benchmark office building in Los Angeles, california. *Renewable Energy*, 36(2):648 – 658.

Hazyuk, I., Ghiaus, C., and Penhouet, D. (2012). Optimal temperature control of intermittently heated buildings using model predictive control: Part II: Control algorithm. *Building and Environment*, 51(0):388 – 394.

Hazyuk, I., Ghiaus, C., and Penhouet, D. (2014). Model predictive control of thermal comfort as a benchmark for controller performance. *Automation in Construction*, 43(0):98 – 109.

Hu, J. and Karava, P. (2014). A state-space modeling approach and multi-level optimization algorithm for predictive control of multi-zone buildings with mixed-mode cooling. *Building and Environment*, 80(0):259 – 273. Energy Efficient Buildings Special Issue.

Jabbour, N. (2011). *Intégration des systèmes à absorption solaire de petites puissances aux bâtiments - approche multifonction solaire : chauffage, ECS et rafraîchissement*. INSA de Lyon, <NNT : 2011ISAL0085>. <tel-00708518>.

Kalogirou, S. (2004). Solar thermal collectors and applications. *Progress in Energy and Combustion Science*, 30(3):231 – 295.

Kreith, F. and West, R. (1997). *CRC Handbook of Energy Efficiency*. CRC Press, United States of America.

Kreuzinger, T., Bitzer, M., and Marquardt, W. (2008). State estimation of a stratified storage tank. *Control Engineering Practice*, 16(3):308 – 320.

Kulkarni, G. N., Kedare, S. B., and Bandyopadhyay, S. (2007). Determination of design space and optimization of solar water heating systems. *Solar Energy*, 81:958–968.

Labinaz, G. and Guay, M. (2011). *Viability of Hybrid Systems: A Controllability Operator Approach*. Springer Science & Business Media, Ontario.

Labus, J. (2011). *Modelling of small capacity absorption chillers driven by solar thermal energy or waste heat*. Rovira i Virgily University.

Labus, J., Korolija, I., Marjanovic-Halburd, L., Zhang, Y., and Coronas, A. (2012). Ann application to modelling and control of small absorption chillers. In *First Building Simulation and Optimization Conference Loughborough, UK*.

Landau, I. and Zito, G. (2006). *Digital control systems*. Springer-Verlag, London.

Lecuona, A., Ventas, R., Venegas, M., Zacarías, A., and Salgado, R. (2009). Optimum hot water temperature for absorption solar cooling. *Solar Energy*, 83(10):1806 – 1814.

Li, H. and Shi, Y. (2013). Output feedback predictive control for constrained linear systems with intermittent measurements. *Systems & Control Letters*, 62(4):345 – 354.

Li, X., Li, L., Yu, J., Liu, J., and Wu, Y. (2013). Investigation of the dynamic characteristics of a storage tank discharging process for use in conventional air-conditioning system. *Solar Energy*, 96(0):300 – 310.

Li, Z. F. and Sumathy, K. (2001). Experimental studies on a solar powered air conditioning system with partitioned hot water storage tank. *Solar Energy*, 71:285–297.

Lunze, J. (2014). *Control Theory of Digitally Networked Dynamic Systems*. Springer International Publishing Switzerland, Cham.

Ma, J., Qin, S. J., and Salsbury, T. (2014). Application of economic {MPC} to the energy and demand minimization of a commercial building. *Journal of Process Control*, 24(8):1282 – 1291.

Ma, Y., Kelman, A., Daly, A., and Borrelli, F. (2012). Predictive control for energy efficient building with thermal storage. *IEEE Control Systems Magazine*, 32:44–64.

Maestre, J. M. and Negenborn, R. R. (2014). *Distributed Model Predictive Control Made Easy*, volume Vol. 69. Science and Engineering.

Mahmoud, M. (2011). *Decentralized Systems with Design Constrains*. Springer-Verlag, London.

Marc, O., Lucas, F., Sinama, F., and Monceyron, E. (2010). Experimental investigation of a solar cooling absorption system operating without any backup system under tropical climate. *Energy and Buildings*, 42(6):774 – 782.

Martínez, P. J., Martínez, J. C., and Lucas, M. (2012). Design and test results of a low-capacity solar cooling system in Alicante (Spain). *Solar Energy*, 86:2950–2960.

MATLAB (2012). *version 7.14.0.739 (R2012a)*. The MathWorks Inc., Natick, Massachusetts.

Menchinelli, P. and Bemporad, A. (2008). Hybrid model predictive control of a solar air conditioning plant. *European Journal of Control*, 14(6):501 – 515.

Molle, D. and Patry, P. (2013). *RT 2012 et RT existant: Réglementation thermique et efficacité énergétique*. Editions Eyrolles, Paris, second edition.

Monné, C., Alonso, S., Palacín, F., and Serra, L. (2011). Monitoring and simulation of an existing solar powered absorption cooling system in Zaragoza (Spain). *Applied Thermal Engineering*, 31:28–35.

Moreno, A. G., Peláez, P. J. C., Garrido, F. A. D., Carnicero, J. M. P., García, R. L., and Peragón, F. C. (2010). Results of an experimental study of a solar cooling system in Jaén using single effect lithium bromide absorption chiller. In *International Conference on Renewable Energies and Power Quality (ICREPQ10), Granada, Spain.*

Morosan, P. D., Bourdais, R., Dumur, D., and Buisson, J. (2010). Building temperature regulation using a distributed model predictive control. *Energy and Buildings*, 42:1445 – 1452.

Morosan, P. D., Bourdais, R., Dumur, D., and Buisson, J. (2011). A distributed mpc strategy based on benders' decomposition applied to multi-source multi-zone temperature regulation. *Journal of Process Control*, 21(5):729–737.

Núñez-Reyes, A., Normey-Rico, J. E., Bordons, C., and Camacho, E. F. (2005). A smith predictive based MPC in a solar air conditioning plant. *Journal of Process Control*, 15(1):1 – 10.

OECD (2014). *OECD Factbook 2014: Economic, Environmental and Social Statistics*. Organization for Economic Cooperation and Development, 2014, ISBN-13: 978-92-64-20415-7.

Oldewurtel, F., Parisio, A., Jones, C. N., Gyalistras, D., Gwerder, M., Stauch, V., Lehmann, B., and Morari, M. (2012). Use of model predictive control and weather forecasts for energy efficient building climate control. *Energy and Buildings*, 45:15–27.

Ortiz, M., Barsun, H., He, H., Vorobieff, P., and Mammoli, A. (2010). Modeling of a solar-assisted {HVAC} system with thermal storage. *Energy and Buildings*, 42(4):500 – 509.

Palacín, F., Monné, C., and Alonso, S. (2011). Improvement of an existing solar powered absorption cooling system by means of dynamic simulation and experimental diagnosis. *Energy*, 36(7):4109 – 4118.

Piper, J. E. (1999). *Operations and Maintenance Manual for Energy Management*. M. E. Sharpe, Armonk, New York.

Praene, J. P., Marc, O., Lucas, F., and Miranville, F. (2011). Simulation and experimental investigation of solar absorption cooling system in reunion island. *Applied Energy*, 88(3):831 – 839.

Prud'homme, T. and Gillet, D. (2001). Advanced control strategy of a solar domestic hot water system with a segmented auxiliary heater. *Energy and Buildings*, 33:463–475.

Rodríguez, M., Prada, C. D., Capraro, F., and Cristea, S. (2008). Logic embedded {NMPC} of a solar air conditioning plant. *European Journal of Control*, 14(6):484 – 500.

Rodríguez-Hidalgo, M., Rodríguez-Aumente, P., Lecuona, A., and Nogueira, J. (2012). Instantaneous performance of solar collectors for domestic hot water, heating and cooling applications. *Energy and Buildings*, 45(0):152 – 160.

Rosiek, S. and Batlles, F. J. (2009). Integration of the solar thermal energy in the construction: Analysis of the solar-assisted air-conditioning system installed in {CIESOL} building. *Renewable Energy*, 34(6):1423 – 1431.

Rosiek, S. and Batlles, F. J. (2012). Performance evaluation of solar-assisted air-conditioning system with chilled water storage (ciesol building). *Energy Conversion and Management*, 55(0):81 – 92.

Salazar, J., Castillo, M., Rodríguez, F., and Tadeo, F. (2013). Minimization of the operation costs of a solar/gas airconditioning system using duration-based predictive control. *Energy Procedia*, 42(0):784 – 793. Mediterranean Green Energy Forum 2013: Proceedings of an International Conference MGEF-13.

Sayadi, Z., Thameur, N. B., Bourouis, M., and Bellagi, A. (2013). Performance optimization of solar driven small-cooled absorption-diffusion chiller working with light hydrocarbons. *Energy Conversion and Management*, 74(0):299 – 307.

Scattolini, R. (2009). Architectures for distributed and hierarchical model predictive control a review. *Journal of Process Control*, 19:723 – 731.

Scherer, H. F., Pasamontes, M., Guzmán, J. L., Álvarez, J. D., Camponogara, E., and Normey-Rico, J. E. (2014). Efficient building energy management using distributed model predictive control. *Journal of Process Control*, 24(6):740 – 749. Energy Efficient Buildings Special Issue.

Scholz, D. (2012). *Deterministic Global Optimization*. Springer Optimization and Its Applications.

Shah, S. and MacGregor, J. (2005). *Dynamics and control of process systems 2004*. Elsevier IFAC publications, Oxford, first edition.

Steinert, P., Goppert, S., and Platzer, B. (2013). Transient calculation of charge and discharge cycles in thermally stratified energy storages. *Solar Energy*, 97(0):505 – 516.

Tagliafico, L. A., Scarpa, F., and Rosa, M. D. (2014). Dynamic thermal models and CFD analysis for flat-plate thermal solar collectors - a review. *Renewable and Sustainable Energy Reviews*, 30(0):526 – 537.

Taylor, P., Fuller, R., and Luther, M. (2008). Energy use and thermal comfort in a rammed earth office building. *Energy and Buildings*, 40(5):793 – 800.

Tran, T., Ling, K.-V., and Maciejowski, J. (2014). Economic model predictive control. A review. In *Proceedings of International Symposium on Automation and Robotics in Construction. Sydney, Australia, 9-11 July 2014, 35-42.*

TRNSYS17-Documentation (2012). *A Transient Simulation Program*. Solar Energy Laboratory, University of Wisconsin, Madison.

Tsoutsos, T., Aloumpi, E., Gkouskos, Z., and Karagiorgas, M. (2010). Design of a solar absorption cooling system in a greek hospital. *Energy and Buildings*, 42(2):265 – 272.

Vana, Z., Cigler, J., Siroky, J., Zacekova, E., and Ferkl, L. (2014). Model-based energy efficient control applied to an office building. *Journal of Process Control*, 24(6):790 – 797. Energy Efficient Buildings Special Issue.

Wallace, M., McBride, R., Aumi, S., Mhaskar, P., House, J., and Salsbury, T. (2012). Energy efficient model predictive building temperature control. *Chemical Engineering Science*, 69:45 – 58.

Yin, Y. L., Song, Z. P., Li, Y., Wang, R. Z., and Zhai, X. Q. (2012). Experimental investigation of a mini-type solar absorption cooling system under different cooling modes. *Energy and Buildings*, 47:131–138.

Yoon, J., Bladick, R., and Novoselac, A. (2014). Demand response for residential buildings based on dynamic price of electricity. *Energy and Buildings*, 80(0):531 – 541.

Zambrano, D. and Garcia-Gabin, W. (2008). Hierarchical control of a hybrid solar air conditioning plant. *European Journal of Control*, 14(6):464 – 483.

Zhai, X. Q., Qu, M., Li, Y., and Wang, R. Z. (2011). A review for research and new design options of solar absorption cooling systems. *Renewable and Sustainable Energy Reviews*, 15(9):4416 – 4423.

Zhao, D. L., Li, Y., Dai, Y. J., and Wang, R. Z. (2011). Optimal study of a solar air heating system with pebble bed energy storage. *Energy Conversion and Management*, 52:2392 – 2400.